SEISMIC VULNERABILITY OF MASONRY STRUCTURES IN TURKEY

A THESIS SUBMITTED TO
THE GRADUATE SCHOOL OF NATURAL AND APPLIED SCIENCES
OF
MIDDLE EAST TECHNICAL UNIVERSITY

BY

H. BURAK CERAN

IN PARTIAL FULFILLMENT OF THE REQUIREMENTS
FOR
THE DEGREE OF MASTER OF SCIENCE
IN
CIVIL ENGINEERING

DECEMBER 2010

Approval of the thesis:

SEISMIC VULNERABILITY OF MASONRY STRUCTURES IN TURKEY

submitted by **H. BURAK CERAN** in partial fulfillment of the requirements for the degree of **Master of Science in Civil Engineering Department, Middle East Technical University** by,

Prof. Dr. Canan Özgen _____
Dean, Graduate School of **Natural and Applied Sciences**

Prof. Dr. Güney Özcebe _____
Head of Department, **Civil Engineering**

Assoc. Prof. Dr. Murat Altuğ Erberik _____
Supervisor, **Civil Engineering Dept., METU**

Examining Committee Members:

Prof. Dr. Haluk Sucuoğlu _____
Civil Engineering Dept., METU

Assoc. Prof. Dr. Murat Altuğ Erberik _____
Civil Engineering Dept., METU

Assoc. Prof. Dr. Barış Binici _____
Civil Engineering Dept., METU

Assoc. Prof. Dr. Erdem Canbay _____
Civil Engineering Dept., METU

Asst. Prof. Dr. Tolga Yılmaz _____
Engineering Science Dept., METU

Date: _____

I hereby declare that all information in this document has been obtained and presented in accordance with academic rules and ethical conduct. I also declare that, as required by these rules and conduct, I have fully cited and referenced all material and results that are not original to this work.

Name, Last name: H. Burak Ceran

Signature:

ABSTRACT

SEISMIC VULNERABILITY OF MASONRY STRUCTURES IN TURKEY

Ceran, H. Burak

M.Sc., Department of Civil Engineering

Supervisor: Assoc. Prof. Dr. Murat Altuğ Erberik

December 2010, 152 pages

This study focuses on the evaluation of seismic safety of masonry buildings in Turkey by using fragility curves. Fragility curves for masonry buildings are generated by two behavior modes for load bearing walls: in-plane and out-of-plane. By considering the previous research and site investigations, four major parameters have been used in order to classify masonry buildings with in-plane behavior mode. These are number of stories, strength of load-bearing wall material, regularity in plan and the arrangement of walls (required length, openings in walls, etc.). In addition to these four parameters, floor type is also taken into account for the generation of fragility curves by considering out-of-plane behavior mode. During generation of fragility curves, a force-based approach has been used. In this study there exist two limit states, or in other words three damage states, in terms of base shear strength for in-plane behavior mode and flexural strength for out-of-plane behavior mode. To assess the seismic vulnerability of unreinforced masonry buildings in Turkey, generated fragility curves in terms of in-plane behavior, which is verified by damage statistics obtained during the 1995 Dinar earthquake, and out-of-plane behavior,

which is verified by damage statistics obtained during the 2010 Elazığ earthquake, is combined. Throughout the analysis, ground motion uncertainty, material variability and modeling uncertainty have also been considered. In the final part of the study, a single-valued parameter, called as ‘vulnerability score”, has been proposed in order to compare the seismic safety of unreinforced masonry buildings in Fatih sub province of Istanbul and to assess the influence of out-of-plane behavior together with the in-plane behavior of these existing masonry buildings.

Keywords: Unreinforced masonry buildings, in-plane behavior, out-of-plane behavior, fragility curve, vulnerability score.

ÖZ

TÜRKİYE'DEKİ YIĞMA YAPILARIN SİSMİK AÇIDAN HASAR GÖREBİLİRLİLİĞİ

Ceran, H. Burak

Yüksek Lisans, İnşaat Mühendisliği Bölümü

Tez Yöneticisi: Doç. Dr. Murat Altuğ Erberik

Aralık 2010, 152 sayfa

Bu çalışma Türkiye'deki yığma binaların deprem güvenirliliğinin hasar potansiyel eğrileri aracılığıyla belirlenmesini esas almaktadır. Yığma binaların hasar potansiyel eğrileri taşıyıcı duvarların iki ayrı davranış biçimi düşünülerek oluşturulmuştur. Bunlar düzlem içi ve düzlem dışı davranış biçimleri. Daha önce yapılmış olan çalışmalar ve saha gözlemleri de göz önüne alınarak yığma binaların düzlem içi davranış biçimine göre sınıflandırılması için dört ana parametre kullanılmıştır. Bu parametreler kat adedi, taşıyıcı duvar malzeme dayanımı, plan geometrisi ve taşıyıcı duvar boşluk oranı ve düzensizliğidir. Bu dört parametreye ek olarak, döşeme tipi hasar potansiyel eğrilerinin düzlem dışı davranış biçimi düşünülerek oluşturulmasında dikkate alınmıştır. Hasar potansiyel eğrilerinin belirlenmesinde kuvvete dayalı bir hesap yöntemi kullanılmıştır. Bu çalışmada düzlem içi davranış biçimi için temel kesme dayanımı, düzlem dışı davranış biçimi için eğilme dayanımı cinsinden ifade edilen iki değişik sınır durum, başka bir deyişle üç farklı hasar bölgesi kabul edilmiştir. Türkiye'deki donatısız yığma binaların depremsel hasar görebilirliliklerinin değerlendirmesi için, 1995 Dinar depreminde elde edilen

istatistiksel bilgilerle doğruluğu kanıtlanan, düzlem içi davranış biçimine göre üretilen hasar potansiyel eğrileri ile 2010 Elazığ depreminde elde edilen istatistiksel bilgilerle doğruluğu kanıtlanan, düzlem dışı davranış biçimine göre üretilen hasar potansiyel eğrileri birleştirilmiştir. Araştırma boyunca hasar potansiyeli eğrilerinin elde edilmesi aşamasında yer hareketi kayıtlarından, malzemeden ve kullanılan analitik modelden kaynaklanan belirsizlikler de göz önüne alınmıştır. Çalışmanın son aşamasında, İstanbul'un Fatih ilçesindeki donatısız yığma binaların deprem güvenirliliğinin karşılaştırılabilmesi ve mevcut binalarda düzlem dışı davranış biçiminin düzlem içi davranış biçimiyle birlikte etkisinin değerlendirilebilmesi için tek değerli bir parametre olan "hasar görebilirlik puanı" adıyla bir parametre önerilmiştir.

Anahtar Kelimeler: Donatısız yığma binalar, düzlem içi davranış, düzlem dışı davranış, hasar potansiyeli, hasar görebilirlik puanı.

To My Family

ACKNOWLEDGMENTS

I would like to express my full indebtedness to my supervisor *Assoc. Prof. Dr. Murat Altuğ ERBERİK*, who chose me as his MSc student and introduced me the exciting world of masonry. Without his care regarding every aspect of my MSc studentship, the conversations that clarified my thinking, his friendship and professional collaboration as well as his kind encouragement, which meant a great deal to me, this thesis would not have been possible.

I would like to thank to my family, *Saadet Ceran, Ümran Ceran and Dr. Murat Ceran*, for their support, encouragement and endless love.

I also would like to thank to my colleagues for their invaluable friendship, tolerance and moral support during the study. I am particularly grateful to *Serhat Melik, Mehmet Ünal and Alper Aldemir* for their invaluable help and contributions.

I wish to thank specially my dear friend *Dr. Volkan Esat* gratefully for his never-ending cross border support and fellowship.

The financial support of *The Scientific and Technological Research Council of Turkey (TÜBİTAK)* within the context of Programme 2228 (The Fellowship for Senior Students for the Domestic Studies) is gratefully acknowledged.

TABLE OF CONTENTS

LIST OF TABLES

TABLES

LIST OF FIGURES

FIGURES

LIST OF SYMBOLS

a: depth of the stress block

a_g: peak ground acceleration

a_i: storey acceleration at the i^{th} storey

a_{wall}: acceleration on the wall

a(t): acceleration time history

A: gross area

c: ratio of ultimate shear stress to elastic shear stress limit

e_x: eccentricities between center of mass and center of rigidity as a ratio of total plan length in x-direction

e_y: eccentricities between center of mass and center of rigidity as a ratio of total plan length in y-direction

E: elasticity modulus

f_{cr}: cracking strength

f_m: compressive strength of masonry

$f_t^{'}$: tensile strength

F_c: combined fragility

F_i: fragility curve for the i^{th} structural type

g: acceleration of gravity

G: shear modulus

$G^{'}$: viscous counterpart of shear modulus

$\bar{G}$: elastic shear modulus

$\bar{G}'$: viscous damping coefficient in the linear range

$\overset{*}{G}'$: viscous damping coefficient after shear strain exceeds shear strain at ultimate shear stress

h_e: equivalent height

h_i: height of the i^{th} floor level

h_{st}: story height

I: building importance factor

I_m: moment of inertia

I_a: Arias Intensity

l: unit length of the stress block

l_{bi}: maximum length of openings

l_n: unsupported length of the wall

L_{b1}: plan length of each window opening

L_{b2}: plan length of each door opening

L_d: total length of masonry load bearing walls in any of the orthogonal directions in plan

L_{max}: maximum unsupported wall length

L_{w1}: plan length of the wall segment between the corner of a building and the nearest window or door opening

L_{w2}: plan lengths of load-bearing walls between window or door openings

m: mass per unit length

m_e: equivalent mass

m_i: concentrated mass at the i^{th} floor level

$M_{C,cr}$: cracking moment capacity at the onset of cracking

M_d: maximum moment demand in wall element

M_D : median moment demand

$M_{LS,1}$: moment capacity at LS-I

$M_{LS,2}$: ultimate moment capacity ay LS-II

$M_{LS,i}$: median moment capacity at the i^{th} limit state

n: number of stories

N: resulting gravity load due to loads on floors and self weight of the wall per 1m length

N_t: total number of buildings

N_i: number of buildings for the i^{th} structural type.

P_i: damage state probability for the assigned PGA value

$P(LS_i / PGA)$: probability of exceeding the i^{th} limit state for a given PGA level

q: out of plane loading of a masonry wall due to inertia

s: standard error

$S_{a,e}$: elastic spectral acceleration at the fundamental period of the building subjected to a specific ground motion

t: thickness of the wall

T: fundamental period of unreinforced masonry building

T_n : natural period of the masonry building for the corresponding n^{th} mode

V_D : median base shear demand

$V_{LS,i}$: median base shear capacity of the i^{th} limit state

VS: vulnerability score

w_i: damage state constant for the corresponding damage state

β_C: uncertainty in capacity

β_D: uncertainty related with demand

β_M: uncertainty related with analytical modeling

γ_c : shear strain at ultimate shear stress

γ_m : unit weight of masonry wall material

$\bar{\gamma}$: elastic shear strain limit

μ: mean

ξ_n : damping ratio of the masonry building

σ: standard deviation

σ_y : vertical stress on the wall element

τ_c : ultimate shear stress

$\bar{\tau}$: elastic shear stress

$\varphi_{C,cr}$: curvature capacity at the onset of cracking

ϕ_i: first mode displacement at the i^{th} floor level normalized such that the first mode displacement at the top storey $\phi_n=1$

Φ: standard normal cumulative distribution function

CHAPTER 1

INTRODUCTION

1.1. SEISMIC VULNERABILITY ASSESSMENT OF MASONRY STRUCTURES IN GENERAL

Masonry is one of the oldest known building materials still in use for the construction of modern building systems, although modern masonry has evolved considerably from its ancient origins. It is a well proven building material possessing excellent properties not only in terms of appearance, durability, thermal and acoustic insulation as well as fire and weather protection but also provision of subdivision of space and cost in comparison with alternatives. In spite of all these advantages, masonry is a complex composite material and its mechanical behavior, which is influenced by a large number of factors, is not generally well understood. In addition to these, the design and construction of especially unreinforced masonry buildings are carried out in a traditional manner based on experience but without using any scientific methods and engineering tools. That is why a significant percentage of physical losses in past earthquakes were due to insufficient performance of non-engineered masonry buildings with low construction quality. Considering this fact and with the continuing search for economy and new forms in the built environment, traditional masonry has been replaced by the modern times materials such as steel and concrete. Unfortunately our knowledge about masonry has not improved very much due to this replacement. This leads to lack of knowledge about masonry which causes negative attitude towards the use of this structural type.

Although the design of new masonry buildings seems marginal when compared to wide spread use of reinforced concrete and steel construction, it is an undeniable fact that there exist a huge building stock of existing masonry structures all over theworld, especially in earthquake prone regions like the North and South America (including the United States of America, Mexico and Peru), South and East Europe (including Italy, Greece and Turkey) and Asia (including Iran, Armenia, India, Pakistan, China and Japan). Most of this building stock is composed of unreinforced and non-engineered masonry buildings that are used for residential purposes. Hence it is not surprising that nowadays research has been dedicated on the seismic performance of existing residential unreinforced masonry structures and the issues related to assessment and mitigation of their seismic vulnerability. The details of the research efforts are presented in the next section. Of course, in countries that possess a long history of civilization like Turkey, there exists the problem of protecting cultural heritage, or in other words, the historical masonry construction. However, this issue is out of the scope of the thesis study.

1.2. LITERATURE SURVEY

Seismic vulnerability assessment of existing masonry structures is a very complex issue since construction practices, structural forms and material properties differ from country to country to a great extent. Hence it is not possible to develop standard engineering procedures for such widely varying construction practices. The problem is case sensitive to each country or region and has to be solved in a specific manner. That is why there exist different approaches to determine the seismic vulnerability of existing masonry structures based on the level of accuracy required and the computational effort provided. In general these approaches can be listed as follows in the order of decreasing computational effort and accuracy (Lang 2002):

- Detailed analysis procedures

- Score assignment
- Simple analytical methods
- Expert opinion
- Observed vulnerability

Detailed analysis procedures can be used for an individual building or for a limited number of buildings since using sophisticated analysis methods and developing refined models are time consuming tasks. Different analytical procedures can be employed depending on the level of sophistication: linear static, linear dynamic, nonlinear static and nonlinear dynamic. Type of modeling also differs from the elaborate finite element meshing to equivalent frame and macro-element modeling. As Lourenço (1996) stated, computational strategies differ due to the level of complexity required and afforded. In the most detailed micro-modeling, masonry unit, mortar and the interface between the unit and the mortar are modeled separately. On the other hand, in macro-modeling, the masonry wall is considered as a continuum in which the properties of the constituents (unit, mortar and interface) are smeared. In between these two modeling strategies, there exits simplified micro modeling, in which the mortar and the interface are modeled together as a "joint" in addition to brick units. There are many research efforts that have used one of these modeling strategies to assess the performance of masonry structures.

There are numerous masonry models in the literature that were developed and widely used by researchers who investigate the damage mechanics of these structures or aim to provide a research environment for the masonry buildings. In the early attempts, Brencich et al. (1998) developed a two-node macro element to take into account the overturning, damage and frictional shear mechanisms experimentally observed in shear panels. The rapid enhancement in powerful computers accelerated the development and comparison of different masonry models. In one of these studies, Kappos et al (2002) compared different models for the seismic analysis of

unreinforced masonry buildings; and tried to figure out under which conditions a simple equivalent frame model can be used for assessment purposes. They concluded that it is possible to obtain reasonably accurate results by using simple equivalent frame model in comparison with the complex finite element modeling. The kinematics of the masonry buildings can be easily simulated by discrete parameter models since the geometry of these models are less complicated then the finite element models. A different perspective is provided by Formica (2004). A discrete brick masonry model was developed in which the masonry wall is characterized as an assemblage of rigid bricks linked to each another by 6 interface elements or in other words mortar joints. The development of powerful computers paved the way to perform nonlinear analysis which requires less demand on computational power for analyzing the linear models. Some computer programs devoted to the nonlinear analysis of masonry structures have been developed. Three of the most commonly used ones can be listed as MAS (Mengi et al. 1992), TREMURI (Galasco et al 2004) and FaMIVE (D'Ayala, 2005).

Score assignment methods can be applied to a population of buildings in order to rank them in terms of vulnerability by comparing their structural deficiencies. These deficiencies are determined by observing the actual damage of the buildings experienced in past earthquakes. In one of the earliest comprehensive methods, ATC-14 (1987), which was developed by Applied Technology Council (ATC), the existing buildings were evaluated by identifying deficiency and weakness which cause structural failure. Whereas ATC-14 (1987) made a good point on the idea of score assignment, the procedures developed for ATC-14 project was employed in FEMA 178, entitled as "the handbook for the seismic evaluation of existing buildings" (NEHRP 1992). Later on, the enhancement of the procedure continued with FEMA 310 (1998), a prestandard for the seismic evaluation of buildings. Finally FEMA 310 was replaced by SEI/ASCE 31 (2003). The procedures given in the above documents require detailed information about the inspected buildings and some destructive tests to examine the material properties. Therefore they are not very suitable to assess the seismic vulnerability of a large population of buildings. In that

case, more practical procedures reported in FEMA 154 and 155 (1988) reports can be applied.

Besides the score assessment method, another method (called as GNDT method) was proposed by Benedetti et al (1988). By this method, Vulnerability Index concept, which is assigned for each building based on visual observations through field surveys, is offered in order to identify the response of existing buildings under earthquake excitations.

If a large number of buildings are to be assessed in a short period of time, then it is suitable to use rather simple methods with few input parameters. Hence it should be realized that the results obtained from such a simplified analysis can lack a certain level of accuracy and should be interpreted with caution. A very good example for this approach is the study conducted by D'Ayala et al. (1997) in order to estimate the seismic loss for historic town centers in Europe. The structural type under concern was unreinforced masonry and the procedure was applied to a case study in the Alfama District in Lisbon. In this study, masonry buildings were investigated in terms of structural features and condition. The masonry buildings, which were mapped with a GIS system, were then analyzed in terms of principal collapse mechanisms to define static collapse loads under horizontal forces for each building. The results were used for the development of vulnerability functions. Generated functions were validated by the comparison with functions derived from statistical analysis of world-wide damage reports and with damage reports of the 1755 Lisbon earthquake. The same approach was used for the earthquake loss estimation after the 1997 Umbria-Marche (Italy) earthquakes (Spence and D'Ayala 1999) as well.

Calvi (1999) developed a simple method which represents global loss estimate prediction based on an evaluation of the displacement limit states and energy dissipation of existing buildings in city of Catania. Based on the results of Calvi (1999) , Faccioli et al (1999) states that results of the method developed by Calvi

(1999) about the damage scenario in the city of Catania are complied with the empirical approach based on statistical score assignment.

Another simple method for the seismic vulnerability assessment of unreinforced masonry buildings in Switzerland was proposed by Lang (2002) considering both in-plane and out-of-plane behavior. According to the deformation oriented method, five different damage grades are established for the generated fragility curves and the probability of a building class of reaching or exceeding a particular damage grade given a deterministic estimate of the spectral displacement.

A different perspective is provided by rigid body dynamic model developed by Valluzzi et al (2004) in order to assess the vulnerability of historical masonry buildings in Italy. The method, which Valluzzi et al (2004) proposed, is for the limit analysis of existing buildings regarding the application of single or combined kinematic models involving the equilibrium of structural macro elements. The developed procedure can be used both for assessment of buildings and for prediction of the vulnerability or for simulation of proper interventions

Expert opinion is a subjective approach of assessing the seismic vulnerability of buildings since it possesses a high degree of uncertainty due to subjective opinions of the experts. One of the first attempts to assess the vulnerability of buildings systematically is summarized in a report, ATC-13 (1985), established by ATC and funded by the Federal Emergency Management Agency (FEMA). The report is constructed by asking fifty eight experts such as noted structural engineers and builders to estimate the expected percentage of damage for a specific structural type subjected to a given intensity based on their personal knowledge and experience. Due to this subjectivity, inherent uncertainties in building performance, calibration difficulties of expert opinions and nonconformity to apply in other building types, ATC-13 is always disputed until the mid 1990's. As the years passed, the expert opinion methodology became more reputable. In 1997, another FEMA funded vulnerability assessment methodology is published: HAZUS (1999), interactive

software for risk assessment. Although it is still relies on expert opinion to estimate the state of damage, the intensities are replaced by spectral displacements and spectral accelerations as a measure of the seismic input. With the 1999 updated version, structural and non-structural damages are also considered separately and sub-level seismic design levels are provided.

Observed vulnerability can be used as a suitable method if there exists building damage data obtained from past earthquakes. It is a challenging task to collect building damage data after an earthquake; therefore such databases are very valuable for earthquake engineering research. The drawback of this method is that it is only valid for the region that the data has been collected and can only be used in areas of similar building inventory. In one of these studies, Swiss Reinsurance Company gathered two building databases obtained after 1978 Albstadt (Germany) and 1985 Chile earthquakes. These databases were applied to estimate the losses for the historical Basel earthquake of 1356 (Porro and Schaft, 1989). The authors preferred the mean damage ratio of the affected buildings to express the extent of the damage. The mean damage ratio is defined as the amount of loss of all affected buildings as a ratio of their values. The relationship between the damage and type of construction, building height, the mean damage ratio of the affected buildings and the earthquake intensity is investigated in this study with the help of data gathered from Chilean earthquake. On the other hand, Albstadt earthquake data provide enough information to investigate the correlation between the damage ratio and the subsoil.

Coburn and Spence (1992) used damage data collected after different earthquakes in different countries in order to develop vulnerability functions for various structural types including unreinforced masonry. In the study, the scatter of intensity at which each structure passes a given damage threshold is assumed to be normally distributed and the damage distribution is expressed graphically by the probability of exceedance of a certain damage grade given the seismic input defined by a parameterless scale of intensity (PSI). With the help of this approach, Orsini(1999) proposed a model for buildings' vulnerability assessment using the Parameterless

Scale of Seismic Intensity (PSI) noting that the values of PSI are in good correlation with the values of the Medvedev-Sponheuer-Karnik Scale (MSK-Scale), which has been replaced by the European Macroseismic Scale (EMS) afterwards.

There exist also studies in which observed damage and expert opinion are used together in order to assess the seismic vulnerability of buildings. A very good example of this is the European Macroseismic Scale developed by Grünthal (1998). Grünthal (1998) proposed o vulnerability function which is the use of vulnerability of the buildings implied in the macroseismic scale. Macroseismic intensities use building damage to measure the strength of the ground motion in a certain region. The deductions are gathered from the vulnerability functions according to the description of the building damages.

Another method to describe the vulnerability of building structures by using one or more of the aforementioned approaches is the generation of fragility curves. This tool has also been used before for masonry structures. HAZUS (1999) includes fragility curves of many different masonry subclasses in terms of structural type, occupancy class, building height and construction year. Belmouden and Lestuzzi (2007) derived fragility functions of masonry buildings in Switzerland by using simple and complex analytical methods.

1.3. OBJECTIVE AND SCOPE

The scope of this research is focused on the development of a seismic vulnerability assessment procedure for populations of unreinforced masonry structures in Turkey. The procedure is mainly based on score assignment and it employs rigorous (for the in-plane behavior) and simple (for the out-of-plane behavior) analytical techniques together in order to estimate the overall seismic vulnerability of building populations. It may be misleading to apply the procedure to individual masonry buildings since it possesses many simplifications and assumptions to provide a quick estimation for a

large number of buildings. The aim of the procedure is to compare and rank masonry buildings in accordance with their existing vulnerabilities. The assumptions and simplifications are based on previous analytical and experimental research results and some engineering rules of thumb and will be stated wherever necessary.

The masonry structures are classified according to some basic structural parameters and for each class a set of fragility curves are generated for in-plane and out-of-plane directions separately. Structural parameters are obtained after a statistical study based on rural (Dinar, Afyon) and urban (Zeytinburnu and Fatih, Istanbul) masonry building databases. Then the results are combined together to yield the overall vulnerability of the buildings under consideration. This is achieved by assigning a vulnerability score to each building as a function of its fragility characteristics and the level of seismic hazard. While obtaining the fragility characteristics, ground motion variability, material and geometrical uncertainties and modeling uncertainty have also been taken into account. Identification of seismic hazard is out of the scope of this study and the values regarding seismic hazard are obtained from other studies.

The proposed methodology is then used in Fatih, Istanbul, which is a study region for Istanbul Masterplan Project, as the first (preliminary) stage of a two-stage seismic risk evaluation methodology. The purpose in this first stage evaluation is to obtain a priority list of buildings in terms of potential seismic risk. Then the obtained data is used in order to distinguish the buildings with high risk and examine them in detail in the second stage. Hence by using the proposed procedure, it becomes possible to address the masonry buildings under high seismic risk among a large population of buildings. The obtained results are valuable since they can be used as a guide during the development of strategies for pre-earthquake planning and risk mitigation for earthquake prone regions in Turkey.

The study is composed of six chapters. First chapter provides brief information on seismic vulnerability assessment of masonry buildings and the literature survey on the approaches to determine the seismic vulnerability of existing masonry structures

in terms of on the level of accuracy required and the computational effort provided. The objective and scope of the thesis study are presented in this chapter.

Chapter 2 presents the information about unreinforced masonry practice in Turkey. The major parameters that affect the vulnerability of the unreinforced masonry buildings are investigated with the comparison of Turkish Earthquake Code and Eurocode Standards. Then the characteristics of Turkish masonry buildings and their conformity to the current seismic regulations are discussed in terms of these major parameters by utilizing the statistics obtained from building databases, Dinar, Zeytinburnu and Fatih.

Chapter 3 explains the generation of fragility curves of Turkish masonry buildings by considering in-plane failure modes. First, general outline of the method used for the generation of fragility curves is described comprehensively. Second, the masonry building models produced by considering the major parameters that affect the seismic performance are introduced in detail. Then, how the load bearing wall material properties are determined is explained before general properties of the analysis program, MAS, which used to identify the demand and capacity of the masonry buildings is described in a comprehensive manner. Next, determination of capacity and demand procedures are presented respectively. Finally, the generation of fragility curves and the verification of these generated curves by comparison of the estimated and observed damages in Dinar earthquake is explained in depth.

Chapter 4 represents the generation of fragility curves of Turkish masonry buildings by considering out-of-plane failure modes. The chapter starts with the introduction of the methods to evaluate the out of plane action in a comparative manner and describes the developed procedure briefly. Then calculation of seismic demand and capacity of the masonry is expressed in detail. After that, the procedure developed for the assessment of masonry structures considering only by out-of-plane is introduced clearly. In the final part of this chapter, the results of the procedure are verified by comparison of the estimated and observed damages in Elazığ earthquake.

Chapter 5 includes the case study of seismic damage estimation of unreinforced masonry buildings in Fatih region by considering a scenario earthquake which is simulated within the context of Earthquake Master Plan of Istanbul. The results are compared with the study, which is based on only in-plane failure modes, conducted by METU.

Chapter 6 is devoted to summary and conclusion of the study. The procedure followed throughout the study is summarized and conclusions are drawn. The future recommendations are made concerning the improvement of this proposed model.

CHAPTER 2

UNREINFORCED MASONRY CONSTRUCTION PRACTICE IN TURKEY

2.1. GENERAL

In terms of geological position, Turkey is one of the most frequent destructive earthquakes occurring country in the world. In the last 20 years, it is clearly observed that about every four or five years, Turkey was subjected to serious damaging earthquakes (Erzincan 1992, Dinar 1995, Marmara 1999, Düzce 1999, Bingöl 2003, Elazığ 2010). If the building types that have been damaged or totally collapsed after these earthquakes are considered, it can immediately be revealed that the performance of unreinforced masonry buildings under seismic action has been rather unsatisfactory. This means that most of the people living in these structures, which constitute a significant percentage of the building stock in Turkey, are exposed to severe risk.

The most effective way of reducing possible similar losses in the future earthquakes is to take lessons from past experiences. With the aim of determining structural parameters that affect the seismic performance of masonry structures, studies on damaged masonry buildings point out that some of the structural parameters have a pronounced effect on the seismic behavior of Turkish unreinforced masonry buildings. Therefore, priority should be given to these major structural parameters in order to evaluate the seismic vulnerability of masonry structures in Turkey.

2.2. MAJOR PARAMETERS THAT AFFECT SEISMIC VULNERABILITY OF UNREINFORCED MASONRY BUILDINGS IN TURKEY

Unreinforced masonry buildings in Turkey have been exposed to many major earthquakes and the seismic performances of these buildings have been examined after each earthquake. The discussions in this section are all based on the field observations regarding the seismic behavior, and in turn the seismic vulnerability of masonry buildings.

Among the major structural parameters that affect the seismic behavior of Turkish masonry buildings, the most important one may be considered as the number of stories. The experiences gained by the past earthquakes has revealed that the buildings less than three stories generally exhibited adequate resistance while the ones with more than two stories suffered serious damage under seismic action. With the addition of each story, the weight of the structure increases and this results in additional seismic lateral loads on the load bearing walls which are vulnerable to even small lateral forces. Moreover, if the additional story is constructed with another masonry material which has not been used in the construction of the original structure, the probability of experiencing damage increases significantly. In order to prevent these unfavorable situations, the maximum number of stories of the masonry buildings has been limited according to the earthquake zones since 1975 earthquake regulations in Turkey (Turkish Ministry of Public Works and Settlement 1975, 1998, 2007). Accordingly, the criteria regarding the permitted number of stories (with a single basement) in the last three versions of the Turkish earthquake code is presented in Table 2.1. Adobe masonry buildings are excluded since they can only be constructed with a single story regardless of the seismic zone due to the low shear strength provided by the adobe units in general. Furthermore, a penthouse with a gross area exceeding 25% of the building area at foundation level is accepted as a full story according to the regulations.

Limitations of this type is unlikely to come across in the regulations in force in European countries or in the United States because in developed countries the materials used in masonry buildings exceed a standard quality and also reinforced or confined masonry building construction is much more common. There is only one exception to this case such that a limitation is proposed in Eurocode 8 (European Committee for Standardization, 2003) for a special class of masonry structures called as "simple buildings". These simple buildings are very similar to masonry buildings which have been constructed in relation to the empirical rules of Turkish earthquake code. Table 2.2 shows that the numbers given for the maximum number of stories in Eurocode for "simple buildings" are slightly more conservative than the ones given in Turkish seismic regulations. In Table 2.2, a_g stands for the peak ground acceleration of the corresponding seismic zone.

Table 2. 1. Maximum number of stories permitted in Turkish seismic regulations

Seismic Zone	Maximum number of stories
1	2
2	3
3	3
4	4

Table 2. 2. Maximum permitted number of stories for "simple buildings" according to Eurocode 8

Seismic Zone	Maximum number of stories
Zone 1 ($a_g \geq 0.4g$)	1
Zone 2 ($0.3g \leq a_g < 0.4g$)	1
Zone 3 ($0.2g \leq a_g < 0.3g$)	2
Zone 4 ($0.1g \leq a_g < 0.2g$)	3

Another important parameter that triggers the damage of masonry buildings is the plan geometry. Masonry buildings which have irregular plan geometry are exposed to torsional effects due to shifting of center of rigidity apart from the center of mass. This eccentricity enforces load bearing walls much more by torsion which may cause partial or complete collapse of buildings. The field observations especially after Dinar earthquake are that masonry buildings with irregular plan geometries were damaged seriously (METU-EERC 1996). Similar cases have also been considered after other major earthquakes.

In order to identify irregular buildings, the related clause in the last two versions of the Turkish earthquake code (TEC-98 and TEC-07) can be used. According to this rule, the buildings, in which projections beyond the re-entrant corners in both of the two principal directions in plan exceed the total plan dimensions of the building in the respective directions by more than 20%, are considered as irregular in plan (see Figure 2.1). In the code this is called as the "type A3 irregularity".

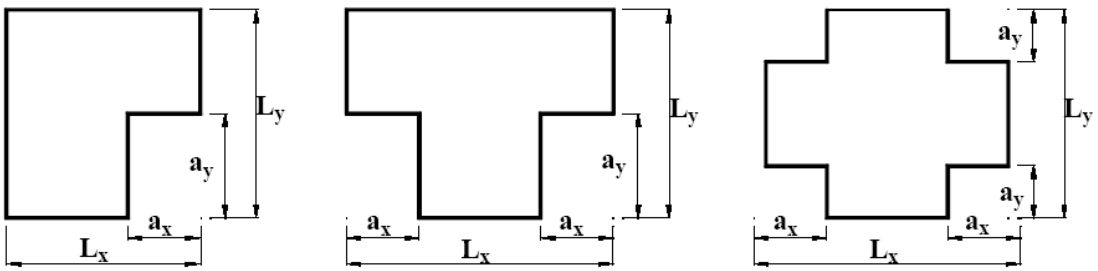

Type **A3** *irregularity :*

$a_x > 0.2\ L_x$ *and at the same time* $a_y > 0.2\ L_y$

Figure 2. 1. Type A3 irregularity stated by TEC-98 and TEC-07

There should exist adequate length of load bearing walls for a masonry building in order to resist the horizontal forces during earthquake motion. For this purpose,

Turkish earthquake code proposes a criterion above a certain limit regarding the ratio of minimum total length of masonry load bearing walls in any of the orthogonal directions in plan, L_d (shaded parts in Figure 2.2 by excluding door and window openings) to the gross area, A , being above a certain limit.

$$L_d / A \geq 0.20\, I \,(m/m^2) \qquad (2.1)$$

In Equation 2.1, *I* represents Building Importance Factor, which is equal to unity for residential buildings. This criterion, not defined in TEC-75, is first published in TEC-98 where the constant was 0.25 instead of 0.20. It is revised in the latest form of the code.

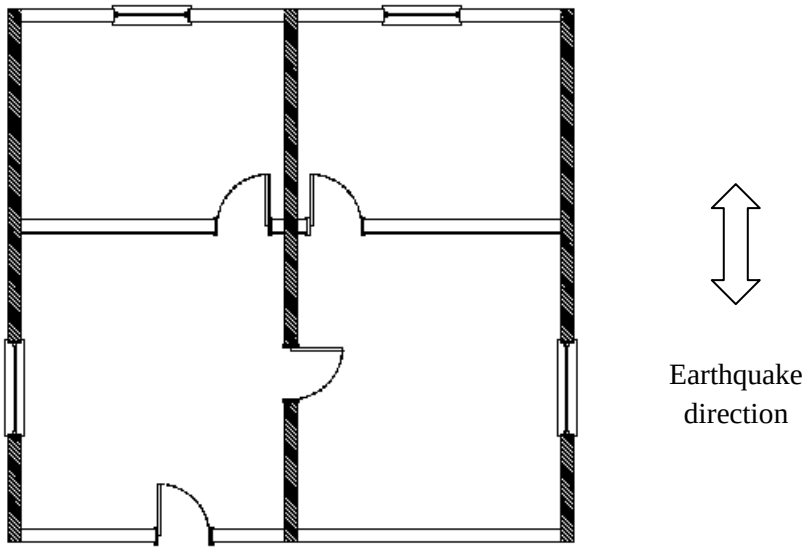

Figure 2. 2. Illustration from the Turkish code (1998 and 2007) regarding L_d/A criterion

Although this ratio seems to be a very simple parameter, it has been observed to be correlated with observed earthquake damage (Bayülke 1992, METU-EERC 1996). Since shear stresses per unit wall area become very high during seismic action for

masonry buildings having less wall ratio, the limited shear capacity is generally exceeded easily which leads to cracking of masonry walls. After cracking, load bearing capacity of masonry walls reduce suddenly which results in partial or complete collapse of the structure.

In Eurocode 8 (2003), in contrast to the definition of minimum total length of load bearing walls in each orthogonal direction as percentage of the total area, minimum sum of cross sectional areas of horizontal shear walls in each direction as percentage of the total area per story is employed. When the criterion given in Eurocode is compared with the one given in Turkish code, it is seen that both versions (i.e. TEC-98 and TEC-07) yield safer values than Eurocode 8 (Erberik et al, 2008).

Number and location of window and door openings in masonry buildings is another parameter that has affected the performance of masonry buildings during previous earthquakes. When load bearing walls of masonry buildings have larger openings than it should be, they can not resist the shear forces during seismic motion. As a result of this, masonry buildings are seriously damaged or completely collapsed. Masonry buildings, which have openings that are close to each other or close to corner of the buildings or placed irregularly, can sustain serious damage due to critical regions where stress concentrations take place. It has been clearly identified that the size and position of wall openings have strong effect on the earthquake resistance after the observations of past earthquake damages. As a result, new clauses were added to the seismic code related to openings in load bearing walls.

According to TEC-75, in the case where the building height is less than 7.5 m, plan length of the load-bearing wall segment between the corner of a building and the nearest window or door opening to the corner may be reduced to 1.0 m in Seismic Zones 1 and 2 whereas this width can be reduced to 0.80 m in Seismic Zones 3 and 4. Excluding the corners of buildings, plan lengths of the load-bearing wall segments between the window or door openings shall not be less than 25% of the width of the

larger opening on either side, nor less than 0.80 m in Seismic Zones 1 and 2 and 0.60 m in Seismic Zones 3 and 4.

There are similar but more detailed rules in the last two versions of the code, namely TEC-98 and TEC-07, related to the length and placement of openings in masonry buildings as illustrated in Figure 2.3. The rules define minimum lengths between opening and corner of the building, between two openings, between an opening and the next wall in the perpendicular direction. The criteria are given separately for Seismic Zones 1-2 and 3-4. Furthermore the maximum length of openings, l_{bi}, and the ratio of total opening length to the unsupported length of the wall, l_n, are also considered.

$$L_{bi} \leq 3.0\,\text{m} \tag{2.2}$$

$$\sum L_{bi} \leq 0.4 l_n \tag{2.3}$$

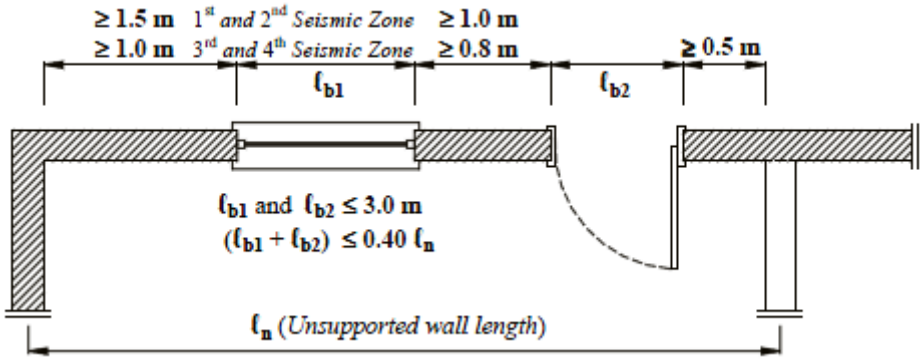

Figure 2. 3. Rules related to length and placement of openings in load bearing walls in the last two versions of the Turkish code

According to TEC-75, the unsupported length of load-bearing masonry walls between the centers of two consecutive perpendicularly connecting walls providing stability shall not exceed 5.5 m in Seismic Zone 1 and 7.0 m in other seismic zones.

TEC-98 agrees with TEC-75 in terms of maximum unsupported length of bearing walls. According to TEC-07, unsupported length of a load-bearing wall between the connecting wall axes in the perpendicular direction shall not exceed 5.5 m. in the first seismic zone and 7.5 m in other seismic zones. The unsupported length is important for out-of-plane stability of masonry walls in general.

Another important factor that affects the vulnerability of masonry buildings is the lack of material strength. According to the code, masonry materials to be used in the construction of load-bearing walls are defined as natural stone, solid brick, bricks with vertical holes satisfying the maximum void ratios defined in the relevant Turkish standards (TS-2510 and TS-705), solid concrete blocks and other similar blocks. However in practice different types of materials that should not be used in load-bearing wall construction are used, which impairs the strength capacity of existing masonry buildings.

The choice of construction material may vary in rural and urban regions. This will be discussed in detail in the next section. This choice mainly depends on the availability of material, environmental conditions and economical reasons. But the most important thing is that the improper choice of masonry construction material increases the seismic vulnerability of masonry buildings.

Except the above mentioned parameters, there are other factors that affect the earthquake performance of masonry buildings such as whether masonry buildings have horizontal beams and lintels or not, adequacy of wall-to-wall and wall-to-floor connections, slenderness ratio of load bearing walls, pattern of masonry units that compose the load bearing walls and type of floor diaphragm (rigid or flexible) in masonry buildings.

2.3. CHARACTERISTICS OF TURKISH MASONRY BUILDINGS BY CONSIDERING BUILDING DATABASES

In this study, three different masonry building databases; Dinar (Afyon), Zeytinburnu (Istanbul) and Fatih (Istanbul), are employed in order to assess the inherent characteristics of unreinforced masonry buildings in Turkey. These databases are the main resources utilized to form the basis of the seismic vulnerability assessment procedure proposed in this study. A variety of information about the masonry buildings can be gathered from these databases which were collected by different engineering teams with specific objectives.

The Dinar building database was constituted after the 1995 Dinar Earthquake which caused extensive damage to building structures. It was an earthquake of magnitude 5.9 on the Richter scale. About 14,000 dwellings and offices suffered various degrees of damage. Teams of engineers from the Middle East Technical University Earthquake Engineering Research Center (METU-EERC) played a significant role in the structural assessment of masonry and reinforced concrete buildings classified as "moderately damaged" by the General Directorate of Disaster Affairs. As a part of this study, 152 masonry buildings were examined for structural assessment of damage and feasibility of rehabilitation by the METU-EERC. The appraisal consisted of site investigation, studies of re-constituted architectural plans, classification using a Damage Evaluation Form, laboratory tests on materials and a simplified lateral load analysis. All these knowledge acquired from 152 masonry buildings, which comprises the Dinar Database. The details can be found elsewhere (METU-EERC, 1996).

The other two building databases are rather new. One year after the 1999 Marmara Earthquake, the Japanese International Cooperation Agency (JICA) and Istanbul Metropolitan Municipality, launched the study of "Earthquake Loss Estimation" in order to predict the damage of a scenario earthquake that will affect Istanbul. The results of this study were presented in a report (JICA 2002). According to the results

of JICA project, unacceptable level of losses caused by an upcoming earthquake is expected to occur in Istanbul. “Istanbul Master Plan” was the first measures of Istanbul Metropolitan Municipality which started in 2003. In the Master plan, in relation to the outputs of the JICA project, gradual and alternative implementation methods were developed in order to mitigate the existing seismic risks, especially in the districts of maximum possible damages estimated. In this context, the core part of the Master plan was the assessment of the existing buildings for earthquake safety and strengthening. For the implementation of the proposed methods, Zeytinburnu was selected as a pilot area. Seismic safety of 69 urban masonry buildings in Zeytinburnu was assessed first. In the light of information obtained from pilot study region, the seismic assessments of 9.457 masonry buildings in Fatih district in Istanbul were inspected.

The characteristics of Turkish masonry buildings and their conformity to the current seismic regulations are discussed in the following paragraphs by utilizing the statistics obtained from building databases. The discussion is based on the major structural parameters introduced in the previous section.

It was previously stated that number of stories is one of the most important parameters for the evaluation of seismic vulnerability of masonry buildings in Turkey. Figure 2.4 presents the distribution of the database buildings with respect to the number of stories. All databases are located in Seismic Zone 1 according to the Turkish Seismic Zone Map. Therefore TEC-07, the allowable numbers of stories for masonry and adobe buildings are limited by 2 and 1 in TEC-07, respectively. As it is seen from Figure 2.5, the conformity of the database buildings to code values in terms of number of stories in Dinar is much higher than in Zeytinburnu and Fatih. In Dinar, about 92% of the buildings obey the code enforcements about maximum number of stories whereas in Fatih this rate drops down to almost 50%. Figure 2.5 also shows the case when all databases are taken into account.

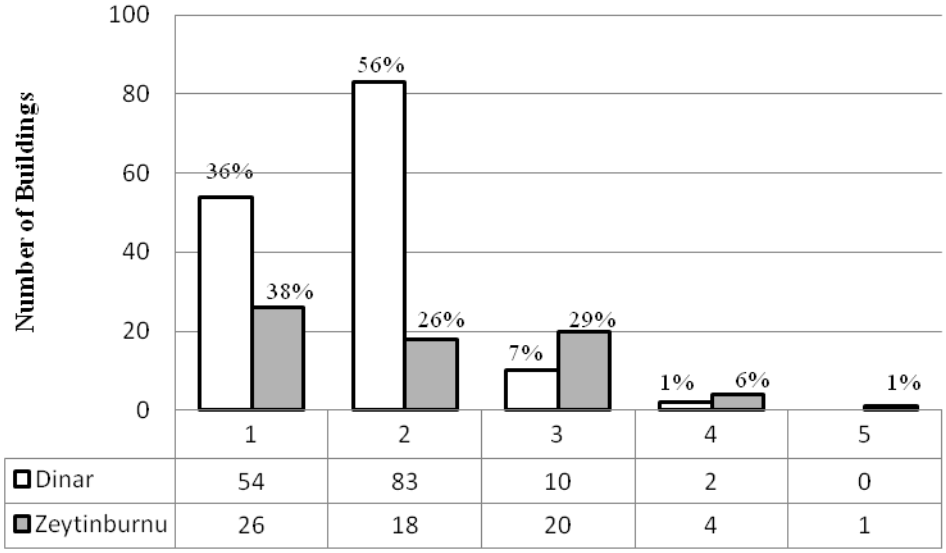

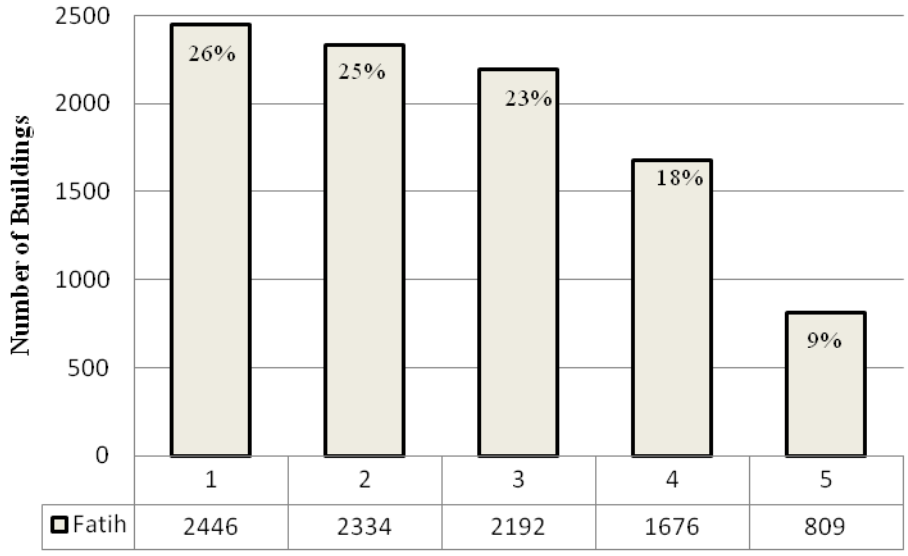

Figure 2. 4. Distribution of buildings according to the number of stories a) in Dinar and Zeytinburnu databases, b) in Fatih database

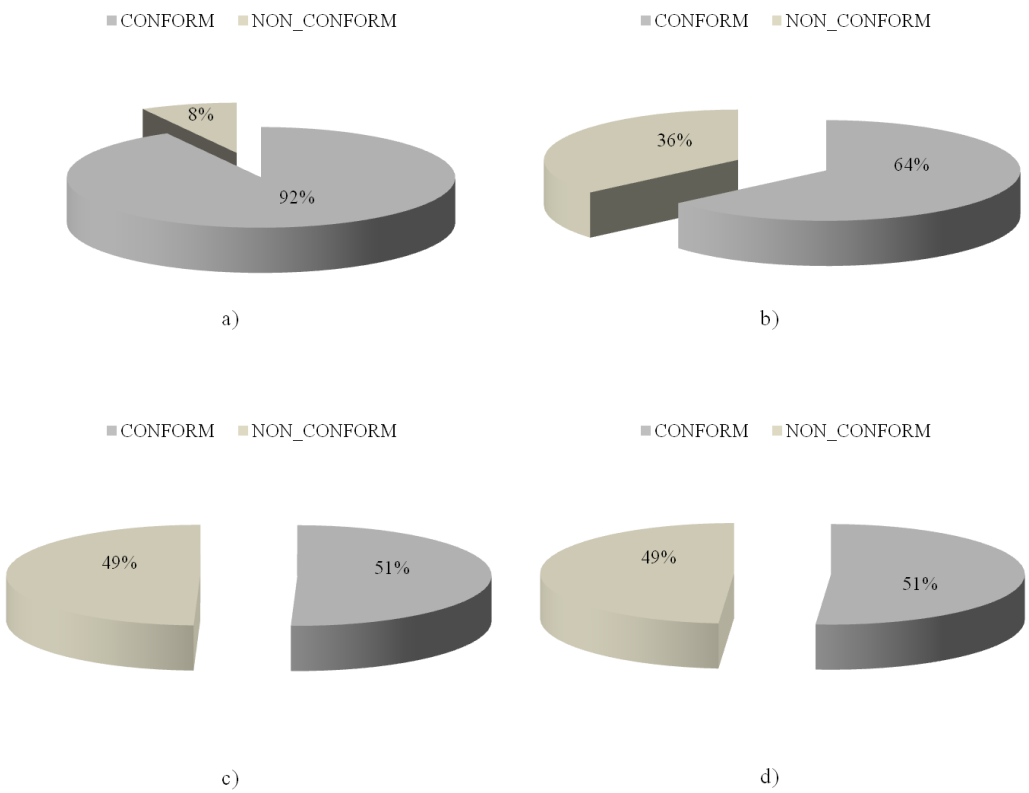

Figure 2. 5. Conformity of the database buildings to current code in terms of number of stories for a) Dinar database, b)Zeytinburnu database, c) Fatih database, d) all databases.

From the results, it can be concluded that, with the increase of the population due to migration from rural to urban regions in Turkey, demand on dwellings for shelter raises rapidly which obliges the people to build multi-storey masonry buildings or to add a new storey on the existing structures because of economy and material availability. When this situation combines with inadequate structural control which should be done by municipality administratives, almost 50% of the masonry buildings in the center of Istanbul do not fulfill the code requirements in terms of maximum number of stories permitted. It is possible to encounter five story unreinforced masonry buildings in Fatih as seen in Figure 2.6.

Figure 2. 6. Examples of masonry buildings which do not obey the code regulations in terms of number of stories in Fatih, Istanbul.

In rural regions, there is a different case since most of the dwellings are either one or two story. In two story buildings, the ground story is generally used as animal barn whereas people live in the second story. Therefore the violations regarding number of stories are not frequently encountered in these regions.

Regarding the plan geometry of the masonry buildings located in the databases, the statistics are shown in Figure 2.7. The "regular" buildings are accepted as the ones which have rectangular or nearly rectangular plan layouts that do not possess A3 type of irregularity as stated in TEC. On the other hand, the "irregular" buildings are the ones which do not match to the definition of "regular" buildings, or the ones with large projections (A3 type of irregularity), non-parallel axes of structural elements, or L-, U-, T-shaped buildings. Typical plan layouts of actual masonry buildings in Fatih (Istanbul) are given in Figure 2.8.

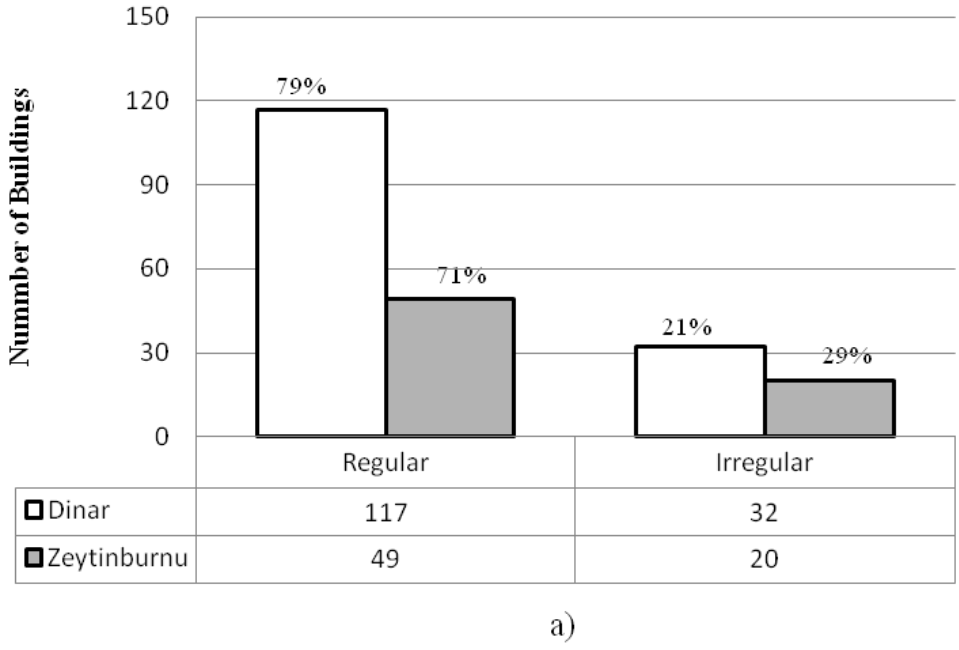

a)

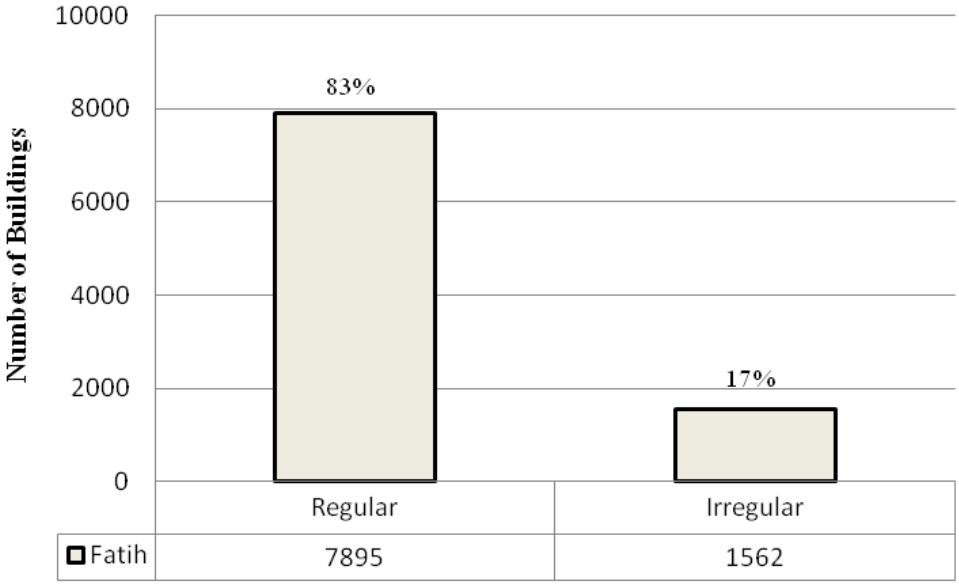

b)

Figure 2. 7. Distribution of buildings according to their plan geometry. a) in Dinar and Zeytinburnu databases, b) in Fatih database

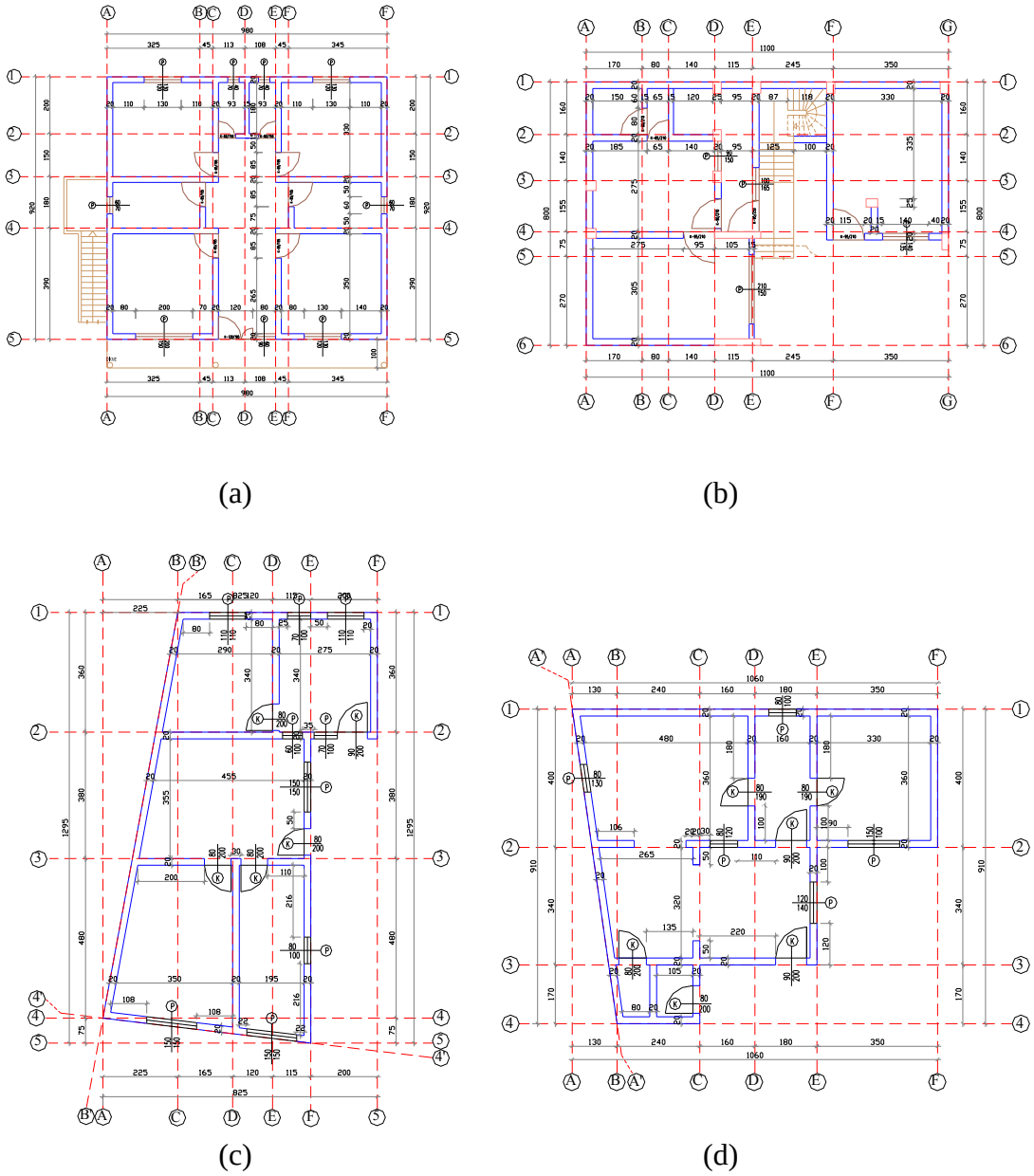

Figure 2. 8. Typical plan layouts of existing masonry buildings in Fatih, Istanbul. a) regular, b) L-shaped, c) with non-parallel axes of structural elements, d) very irregular.

According to Figure 2.7, 79% of the masonry buildings satisfy the criteria regarding regularity in plan in Dinar (rural) database. It is common to encounter small box-like buildings in rural regions like Dinar. This number is 71 % for the buildings in Zeytinburnu (urban) database and 83 % for the buildings in Fatih (urban) database. This means that 29% of the buildings in Zeytinburnu database can be considered as irregular. This is not a surprising outcome since generally large apartments with many projections (or wings) are preferred due to urban residential housing demands.

The compliance of Dinar and Zeytinburnu database buildings with the code in terms of minimum wall length requirement in two orthogonal directions is examined and the results are presented in Figure 2.9. Unfortunately there is no available information for Fatih database related to wall length of the buildings.

The results in Figure 2.9 are obtained by the calculation of the length of the existing load-bearing walls of the buildings in the database according to Equation 2.1 as defined in TEC-07. The code conformity of the buildings with respect to the required length are investigated separately whether it is satisfied in both orthogonal directions (YY), only in one direction (NY) or not satisfied at all (NN).

The results in Figure 2.9 indicate that the percentage of masonry buildings in which the wall length requirement is not satisfied at least in one orthogonal direction is 16 % in the general databases. 13 % of the masonry buildings in Dinar database and 25 % of the Zeytinburnu database contribute to this result. When non-conforming buildings are considered, it is seen that 11 % of the buildings do not satisfy the wall length requirements in both orthogonal directions, which increases the potential seismic risk for the people living in these buildings.

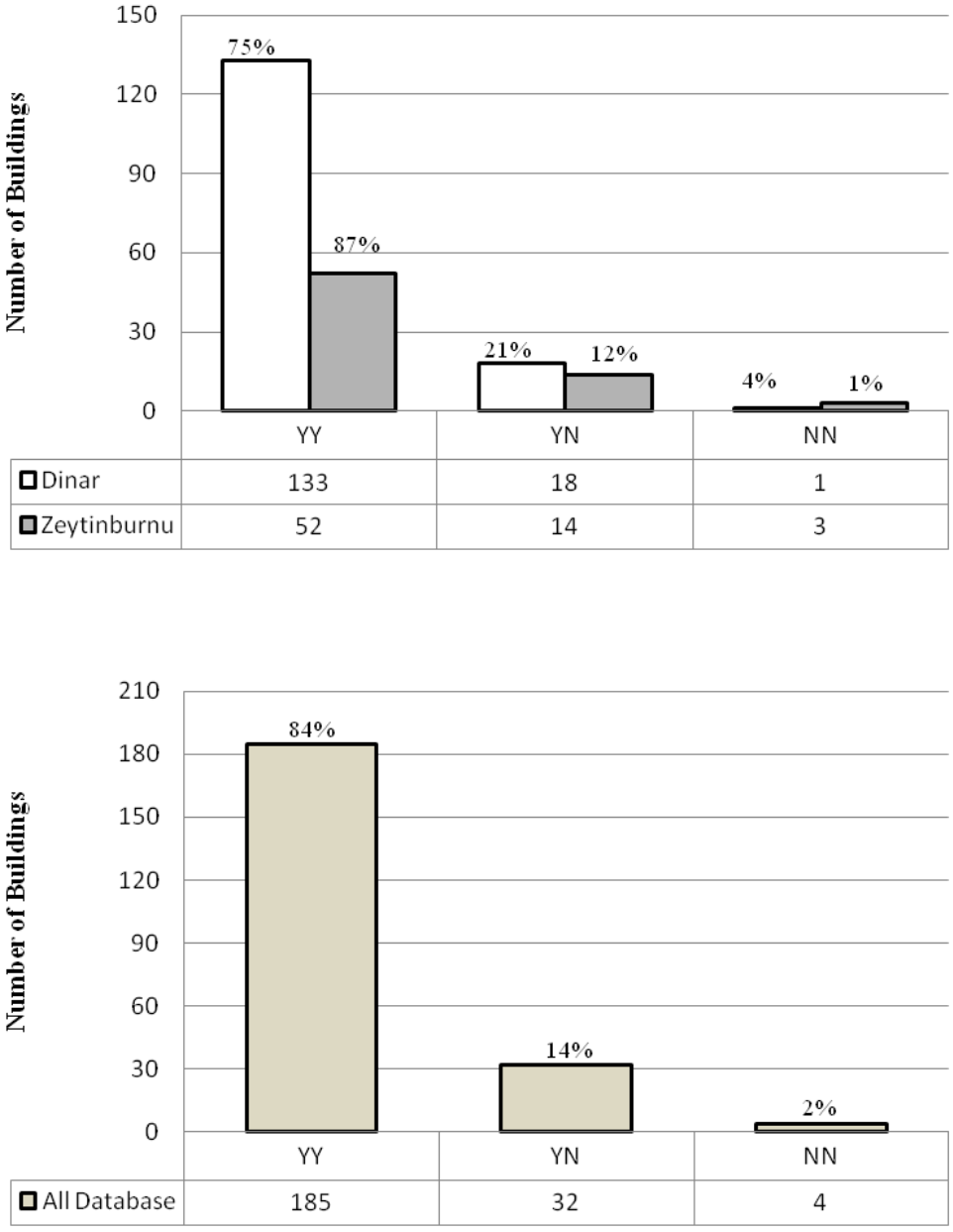

Figure 2. 9. Distribution of buildings in Dinar and Zeytinburnu databases according to required wall length according to the formulation in the code.

In terms of dimensions and locations of the openings in masonry walls, four criteria are considered. They are all taken from the existing earthquake code and can be defined as follows:

- The criterion C2 : The plan length of the wall segment between the corner of a building and the nearest window or door opening should not be less than 1.5 m in the first and second seismic zones ($L_{w1} \geq 1.5$ m in Figure 2.3).

- The criterion C3 : The openings in load-bearing walls considered in this study, plan lengths of load-bearing walls between window or door openings should not be less than 1.0 m in the first and second seismic zones ($L_{w2} \geq 1.0$ m in Figure 2.3).

- The criterion C4 : The plan length of each window or door opening should not exceed 3.0 m ($L_{b1} \leq 3.0$ m and $L_b \leq 3.0$ m in Figure 2.3).

- The criterion C5 : The total plan lengths of window or door openings along the unsupported length of any wall should not be more than 40% of the unsupported wall length ($(L_{b1} + L_{b2}) \leq 0.40\ L_n$ in Figure 2.3).

Since all these criteria are somewhat related to L_d/A ratio, it is accepted as the criterion C1 which is discussed above but not listed in the criteria list.

Figure 10 indicates that, in terms of distribution of database buildings according to the four aforementioned code criteria, the most critical criterion seems to be the criterion C5 when compared to the others. Since only 7% of the buildings in Zeytinburnu database conform to the criterion C2, 95% of the Dinar database fails to conform this criterion. Almost half of the buildings in both Dinar and Zeytinburnu data sets comply with the criterion C3. It is notified that nearly all the buildings satisfy the criterion C4.

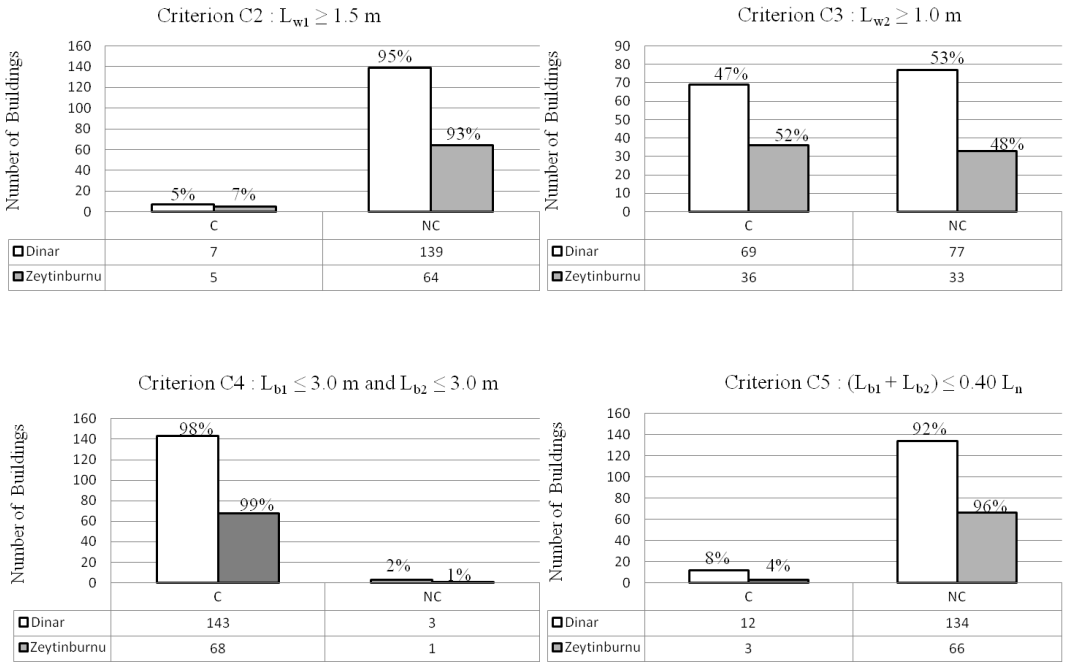

Figure 2. 10. Distribution of buildings according to openings in walls

The distribution of masonry buildings according to load-bearing wall material in the considered databases is shown in Figure 2.11. In this figure, the abbreviations SC, HC, CC, SM and A stand for masonry buildings with wall material types of solid clay brick, hollow clay brick, cellular concrete block, stone masonry and adobe, respectively. The abbreviation HY denote masonry structures with hybrid walls, i.e. walls constructed with more than one material type in a single housing.

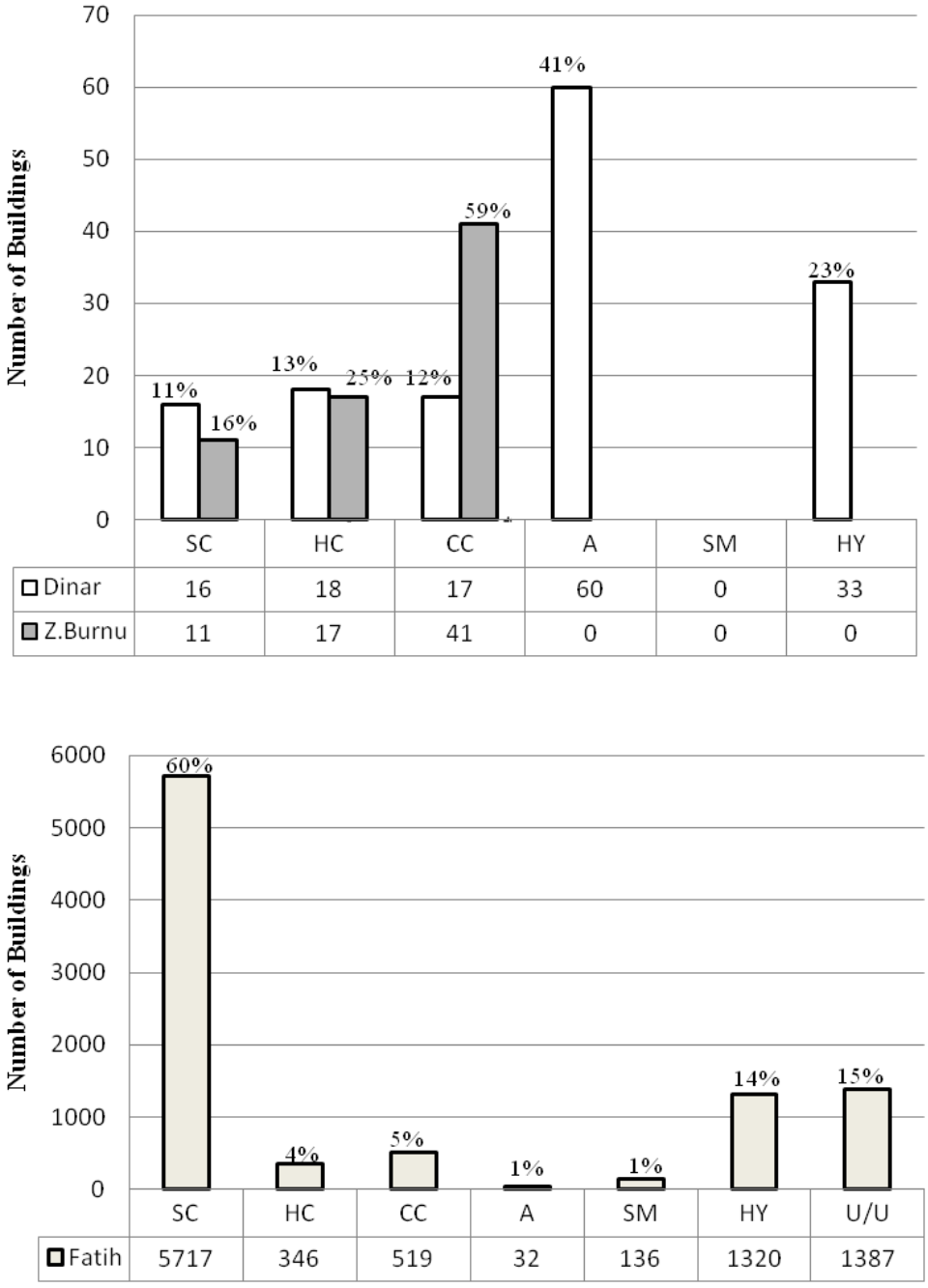

Figure 2. 11. Distribution of database buildings according to load bearing wall material

Figure 2.11 indicates that, almost 40 % of the buildings in Dinar seem to be constructed by adobe walls whereas the cellular concrete is the governing wall material type in Zeytinburnu by representing nearly 60 % of the buildings. It is interesting to observe that there is no building in Dinar is constructed by only stone masonry. Moreover, masonry buildings with hybrid load bearing walls do not exist in Zeytinburnu database. On the other hand, in Fatih database, it is seen that while solid clay is the principal wall material type, there also masonry buildings with walls constructed by stone masonry or cellular concrete or adobe. While the second governing wall material type is hybrid walls in Fatih, there are still unidentified wall material type which is shown with the abbreviations U/U.

It can be stated that economical issues, availability and easiness in transportation have significant effect on the selection of the wall material in local construction practice. As an example, adobe construction, which is very common in the rural regions of Turkey, has some advantages like economical feasibility, acoustic and heat insulation however it has poor performance under earthquake forces. However the material strength of adobe is very low which leads to poor performance of masonry buildings during earthquakes. Especially masonry structures having more than one story constructed with adobe were completely collapsed or suffered irreparable damage during past earthquakes. In addition, adobe masonry buildings with heavy earthen roof are very risky for the people that live in these dwellings since the roof buries the inside of the building during earthquake.

Like adobe, cellular concrete, which is commonly used in the construction of masonry buildings in urban regions, possess low strength and should not be used in the construction of load-bearing walls in earthquake-prone regions. Unfortunately, according to Figure 2.11, it is seen that major part of the masonry buildings in Dinar and Zeytinburnu database and the significant portion of the Fatih database is under high seismic risk due to employment of inappropriate wall material types. In contrast to Dinar and Zeytinburnu databases, which have small percentage of buildings with this type of wall material, the major part of the Fatih database is comprised of

buildings with solid clay brick walls. Due to past experiences, the best seismic performance belongs to buildings with solid clay brick walls since these units have high inelastic displacement capacity and damping properties when compared to the others. Although there seems to exist no stone masonry buildings in the databases, actually this is not the case. In Dinar database, there are structures constructed with stone masonry walls plus other materials (especially for inner walls), which are all included under the heading “hybrid masonry structures”.

CHAPTER 3

FRAGILITY OF TURKISH MASONRY BUILDINGS BY CONSIDERING IN-PLANE FAILURE MODES

3.1. GENERAL

Fragility curves provide estimates for the probability of reaching or exceeding predefined limit states at given levels of seismic hazard intensity. In this chapter, fragility curves of Turkish masonry buildings are generated by considering in-plane failure modes only and by using detailed analytical tools. A force-based approach is selected for the generation of fragility curves. The reason behind this choice is that unreinforced masonry buildings are generally classified as non ductile and relatively undeformable structural systems, in which the brittle load bearing walls have limited deformation capacities beyond the elastic range under earthquake loading. Hence for a masonry structure that reaches to its elastic capacity, the range of inelastic behavior is rather limited before experiencing heavy damage or partial/total collapse. For this reason, it is more appropriate to define limit states in terms of force capacity rather than deformation capacity.

Generation of fragility curves for Turkish masonry structures by considering in-plane failure modes is presented as a flowchart in Figure 3.1. First, generic building models are developed in accordance with the major structural parameters explained in Chapter 2, which represent inherent characteristics of Turkish masonry buildings. The material properties are then defined by considering Turkish construction practice. At this point, the procedure is divided into two branches in order to generate

demand and capacity statistics required for the generation of the fragility curves. For the determination of capacity, nonlinear static procedure is applied to the generated models. Then the limit states are attained based on the capacity evaluation. The uncertainty in capacity is taken into consideration. For the determination of demand, a set of ground motion records are selected in order to enable record-to-record variability. Seismic hazard parameter is selected as peak ground acceleration (PGA) due to not only its simplicity but also being appropriate in order to assess the fragility of rigid masonry structures. Then time-history analyses are employed in order to obtain seismic response of generic building models by applying the selected set of ground motion records. The final step is to compare the demand and capacity statistics (in terms of shear force) to determine the probabilities of exceedance of the prescribed limit states given the intensity of seismic hazard in terms of PGA. The selected fragility function is the standard normal cumulative distribution.

In Chapter 2, it was concluded that there exist four major structural parameters that characterize the seismic vulnerability of unreinforced masonry structures in Turkey: number of stories, material properties of walls (type, quality, and strength), plan geometry and considerations about wall length and openings in walls. These parameters are considered also for the classification of fragility curves derived for Turkish masonry buildings. They are further divided into sub-classes in order to represent all the classes of masonry buildings that are present in the existing building stock. Overall, 120 different classes are defined, which means 120 fragility curve sets are generated. The following sections give the details of the fragility curve generation procedure that is illustrated in Figure 3.1. The last part of this chapter is devoted to the verification of the generated fragility curves by comparing the estimated damage obtained from the fragility curves with the actual damage after Dinar (1995) earthquake as assessed from the Damage Evaluation Forms.

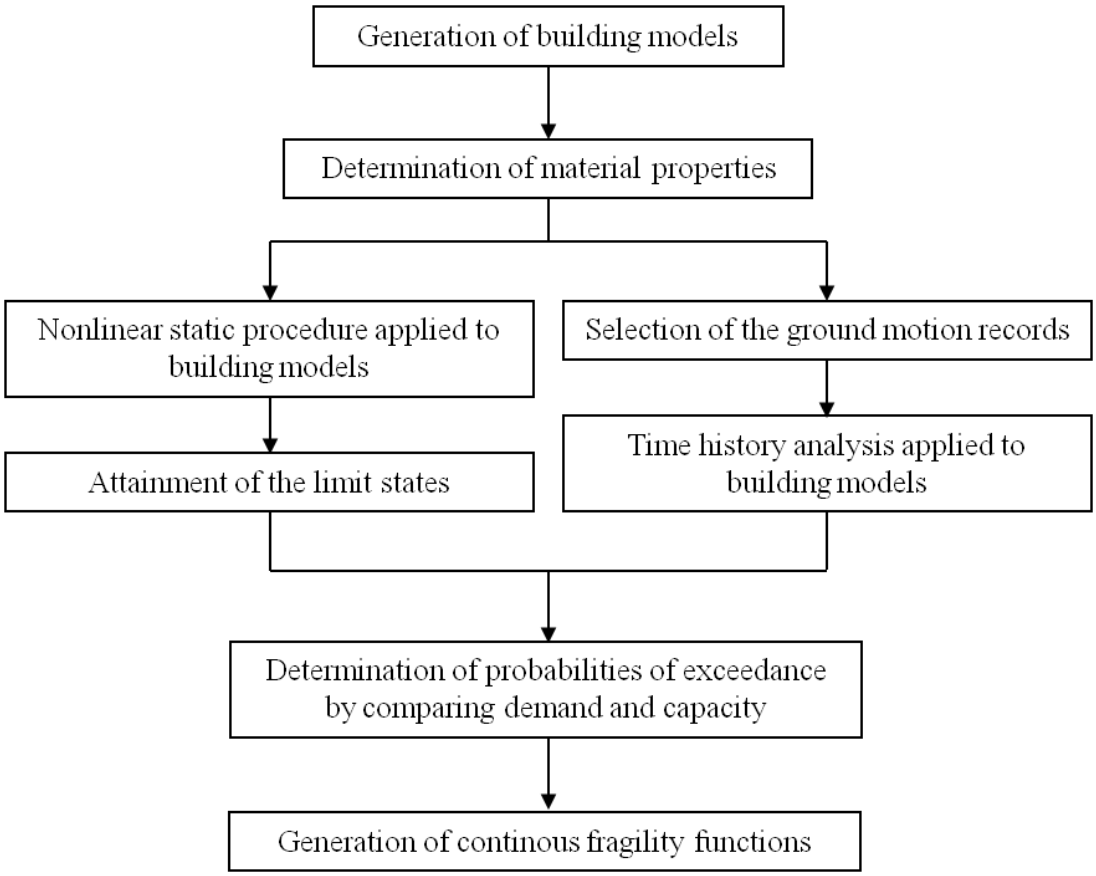

Figure 3. 1. General outline of the method used for the generation of fragility curves of Turkish masonry buildings

3.2. DETERMINATION OF FRAGILITY CLASSES FOR TURKISH MASONRY BUILDINGS

Turkish masonry buildings are classified according to four major structural parameters based on the observed characteristics from existing urban and rural building databases. These are number of stories, load-bearing wall material, plan geometry and considerations about wall length and openings in walls.

According to number of stories, masonry buildings are classified as N1, N2, N3, N4 and N5. The number in each alphanumeric abbreviation represents the number of

stories of the considered building sub-class. For instance, N2 denotes the subclass that includes masonry buildings with two stories.

Load bearing wall material is the second parameter used for the classification of the masonry buildings. It is a parameter formed by considering three different criteria: type of masonry unit, material strength and inspected quality of the material. These three criteria are combined together to develop the subclasses D1, D2, D3 and D4. The details of these subclasses are given in Section 3.4.

The third classification parameter is the regularity in plan. Since regularity and symmetry in plan are important factors affecting the seismic behavior of masonry buildings, they are classified as either regular (R1 sub-class) or irregular (R2 sub-class) regarding their plan geometry. While rectangular buildings or buildings with re-entrant corners but that do not violate the plan irregularity dictated by TEC-07 are considered in R1 subclass, all the other buildings are considered in R2 subclass. These sub-classes are used to define the geometry of the generic building models. The details are given in Section 3.3.

The last parameter contains the requirements regarding the required wall length and layout of openings in walls, referring to clauses in TEC-07. It combines five different code criteria described in Chapter 2 in order to generate the corresponding three sub-classes; W1, W2 and W3. The details are given in Section 3.3.

As a conclusion, five N sub-classes (N1, N2, N3, N4, N5), four D sub-classes (D1, D2, D3, D4), two R sub-classes (R1, R2) and three W sub-classes (W1, W2, W3) forms total of 120 classes of masonry buildings for which fragility curve sets for the in-plane behavior are generated in this study. The procedure used for generating the fragility curves is explained in the proceeding sections in detail.

3.3. DEVELOPMENT OF ANALYTICAL MODELS

Six different generic story plans are developed for Turkish masonry buildings by considering the combinations of R and W subclasses; R1-W1, R1-W2, R1-W3, R2-W1, R2-W2, R2-W3 since these are the geometrical structural parameters among the selected ones.

As mentioned above, R1 sub-class represents masonry buildings with rectangular plan layouts or buildings with re-entrant corners but that do not possess A3-type of plan irregularity stated by TEC-07. All other buildings (buildings that possess A3-type of plan irregularity or buildings which have non-parallel axes of structural walls, L-shaped or U-shaped buildings, etc.) are considered in R2 sub-class.

W sub-classes represent the classification of buildings with respect to required length of walls and size and distribution of openings in walls. In order to achieve this, five criteria (C1-C5) defined in Chapter 2 are considered. Accordingly the subclasses are established as follows:

W1 subclass represents masonry buildings which obey the code principles and possess adequate lateral wall resistance. In this subclass, masonry buildings are complied with not only L_d/A criteria, which is denoted as C1, by considering as 0.30 and but also the code criteria C2-C5.

W2 subclass represents masonry buildings which obey some of the code principles such as C1, which is complied with the code by taking into consideration L_d/A criteria as 0.25, and C4 and C5 but also possess structural deficiencies by not complying with C2 and just satisfying C3.

W3 subclass represents masonry buildings which do not obey most of the code principles and possess inadequate lateral wall resistance. C1 is not complied with the code by taking into account L_d/A criteria as 0.20. While this building subclass does not comply with the code criteria C2 and C3, the criterion C4 is “just” satisfied and the criterion C5 is satisfied.

The above conditions are reflected in the generated story plans as seen in Appendix A. The plan irregularity is introduced by shifting center of rigidity (CR) away from center of mass (CM). This is obtained by changing the even distribution of wall segments in plan for irregular (R2) layouts. The reason for doing this is that from the analytical point of view, R1 and R2 sub-classes can also be distinguished from each other by considering the eccentricity between CM and CR of the plan layout of the building. If CM and CR are apart from each other, this means that due to the distribution of masonry walls in plan, some extra shear forces are induced. These forces are balanced by the torsional moment which is equal to the product of the total shear force on the walls and the eccentricity between CM and CR. Such buildings can be treated as irregular due to uneven distribution and placement of load-bearing walls in plan. On the other hand, buildings, in which CM and CR are very close to each other, can be treated as regular buildings. In the development of the story plans of the analytical models, this approach has been considered. Accordingly, the parameters e_x and e_y in Table 3.1 represent the eccentricities between CM and CR as a ratio of total plan length in two orthogonal directions. For regular plan layouts (R1-W1, R1-W2, R1-W3), CM and CR are assumed to coincide and therefore there is no eccentricity for these cases. For irregular layouts (R2-W1, R2-W2, R2-W3), there exists some eccentricity, which increases with the increasing level of non-uniformity in the arrangement of walls in story plan (W1 to W3).

All generic story plans possess the same plan area 74.5 m^2 (9.8m×7.6m). The last five columns in Table 3.1 present the compliance of the generic story plans with the code criteria C1-C5. The abbreviations OK, JS and NS mean that the corresponding criterion is either “satisfied (ok)”, or “just satisfied (in the limit)” or “not satisfied”, respectively. The story plans are developed for buildings with single story (N1 sub-class) and duplicated for buildings with more than one story (N2-N5 sub-classes). (see Figure 3.2)

Table 3. 1. Major parameters of the generic storey plans for R-W sub-classes

Story Plan	Area (m^2)	e_x	e_y	L_d/A (C1)	C2	C3	C4	C5
R1-W1	74.5	-	-	0.30	OK	OK	OK	OK
R1-W2	74.5	-	-	0.25	NS	JS	OK	OK
R1-W3	74.5	-	-	0.20	NS	NS	JS	OK
R2-W1	74.5	0.05 L	0.07 L	0.30	OK	OK	OK	OK
R2-W2	74.5	0.09 L	0.12 L	0.25	NS	JS	OK	OK
R2-W3	74.5	0.13 L	0.25 L	0.20	NS	NS	JS	OK

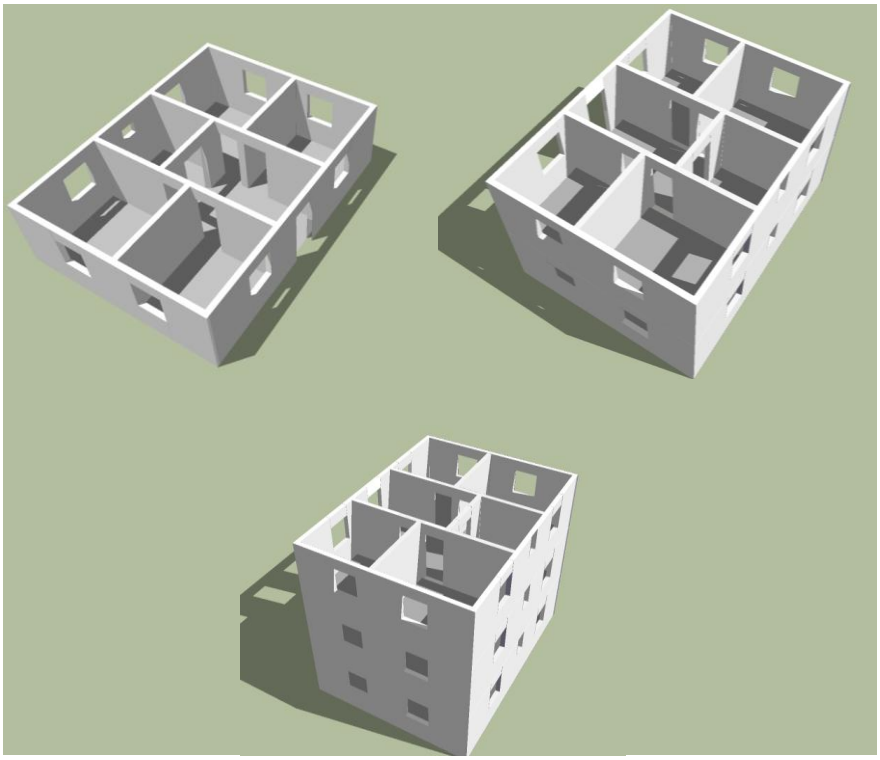

Figure 3. 2. Duplication of R1-W1 story plan in order to construct D2 and D3 sub-classes from D1 sub-class.

3.4. DETERMINATION OF MATERIAL PROPERTIES

The second parameter used for the classification of Turkish masonry structures is the masonry wall material. In this classification, three different criteria are considered: material type, material strength and inspected quality of the material. These three criteria are assessed together to develop the material subclasses D1, D2, D3 and D4 as shown in Table 3.2. The values in cells represent the average compressive strength of that particular material subclass in accordance with previous studies, field observations and the related Turkish Standards (METU-EERC 1996, Sucuoğlu and Erberik 1997, Turkish Standards Institute 1977, 1988, 2001, 2005). Hence the D sub-classes can be defined as follows:

- D1 sub-class represents masonry walls with good quality solid local brick.
- D2 sub-class represents masonry walls with good quality hollow factory brick or mode-rate quality solid local brick.
- D3 sub-class represents masonry walls with good quality concrete masonry unit, stone or adobe; moderate quality hollow factory brick; or poor quality solid clay brick.
- D4 sub-class represents masonry walls with moderate and poor quality concrete masonry unit, stone or adobe; or poor quality hollow factory brick.

Table 3. 2. Building sub-classes due to material type, strength and inspected quality

Masonry Wall Material	Mean Compressive Strength Values (MPa)		
	Good Quality	Moderate Quality	Poor Quality
Solid Local Brick	D1	D2	D3
Hollow Factory Brick	D2	D3	D4
Concrete Masonry Unit, Stone or Adobe	D3	D4	D4

One of the main sources of uncertainty in fragility curve generation procedure comes from material variability. In Turkey, the properties of masonry materials vary significantly since they are not produced in a standard manner. For this reason, compressive strength of masonry (f_m) has been chosen as a random variable in order to account for the uncertainty in the determination of the capacity statistics. Statistical variation of f_m for each subclass (D1-D4) is described by two distinct descriptors: mean (μ) and coefficient of variation (COV), the ratio of standard deviation (σ) to mean. The corresponding values are given in Table 3.3. Furthermore, sketch of probability density functions, PDF, for f_m of each D-subclass are presented in Figure 3.3.

Table 3. 3. Mean strength and coefficient of variation of material sub-classes

Material Sub-class	μ (MPa)	COV
D1	8	0.250
D2	6	0.275
D3	4	0.350
D4	2	0.400

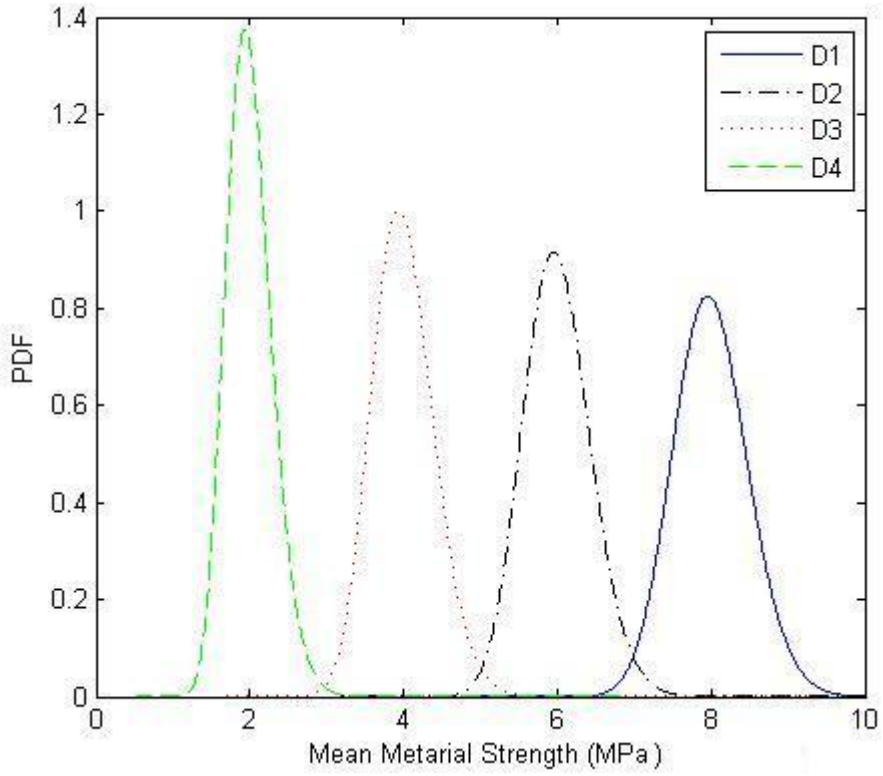

Figure 3. 3. Sketch of probability density functions for f_m of material sub-classes.

3.5. THE ANALYSIS PLATFORM USED: MAS

MAS is an Fortran based computer platform developed according to some analytical models proposed for the three dimensional, linear and nonlinear earthquake analysis of unreinforced and reinforced brick masonry buildings (Mengi et al. 1992). Analytical models were proposed based on experimental results on shake-table tests, which were performed on clay brick masonry wall specimens to in-plane earthquake excitations at the laboratories of the Earthquake Engineering Research Center, University of California at Berkeley (Mengi and McNiven 1989, McNiven and Mengi 1989).

The models generated in MAS program involve some assumptions. The first one is the rigid diaphragm modeling proposed by A.Ghali and A.M.Nevile (1978). The floors of masonry building are assumed to be reinforced concrete slabs which are infinitely rigid in their own planes. There are also some geometrical assumptions about the model such that the mass of the stories are lumped at floor levels and the location of the centroid of the wall elements remains the same for all stories. In addition, there exist some assumptions related to the mechanical properties of the masonry elements that are used in the formulation of nonlinear response of masonry buildings under earthquake excitation. One of these assumptions is that bending rigidity of wall elements in their planes is very large when compared to their shear rigidity which means that in-plane behavior of wall elements is governed by shear deformations. Furthermore, out-of-plane rigidity of the wall elements is neglected for unreinforced masonry buildings. The axial deformations of the wall elements are also neglected in the program but torsional rigidity is considered.

The assumptions in MAS program stated above uttered that the in-plane shear modulus (G) of a masonry wall element and its viscous counterpart (G') are the major parameters that simulate the nonlinear response of unreinforced masonry walls subjected to dynamic loading. The relationship between the deformation state of a masonry wall and the in-plane shear modulus G and its viscous counterpart G' was investigated experimentally by Mengi and McNiven (1989). Due to the results of shake-table tests, in which burned clay brick units were used for masonry wall specimens, a skeleton curve was proposed to simulate the variation of in-plane shear modulus G and its viscous counterpart G' with the shear strain for a masonry wall element as seen in Figure 3.4.

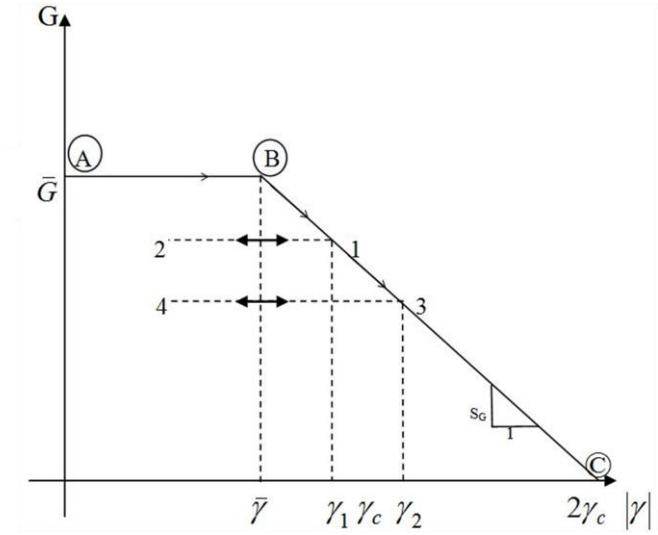

(a)

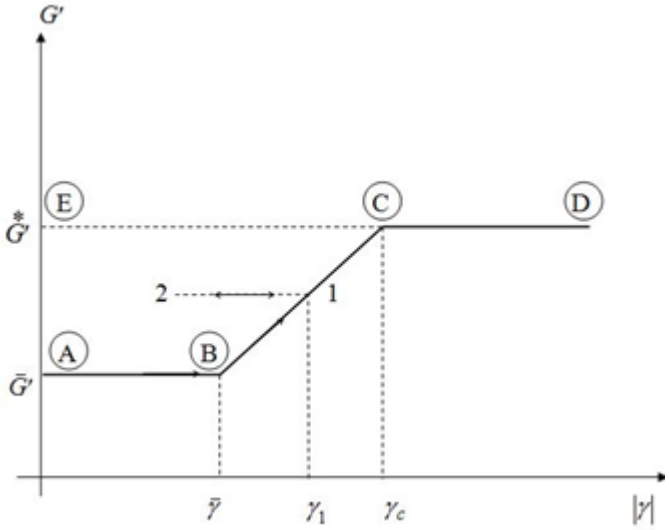

(b)

Figure 3. 4. The variations of the a) shear modulus (G) and b) its viscous counterpart (G') with the shear strain (Mengi et al., 1992)

In Figure 3.4, $\bar{G}$ is elastic shear modulus, $\bar{\gamma}$ is elastic shear strain limit, γ_c is the shear strain at ultimate shear stress, $\bar{G}'$ is the viscous damping coefficient in the linear range and $\overset{*}{G}'$ is the viscous damping coefficient after shear strain exceeds γ_c.

It should be noted that, proposed bilinear form of G and the trilinear form of G' in Figure 3.4 is valid for masonry wall panels constructed from burned-clay bricks with an average workmanship and mortar quality. With the contribution of Benedetti and Benzoni (1984) and Ottazzi et al. (1989), a general form of G, involving also adobe brick and stone brick masonry materials, is proposed by Mengi et al. (1992):

$$G = \begin{cases} \bar{G} & \text{for } |\gamma| \le \bar{\gamma} \\ \bar{G}\,\dfrac{|\gamma|}{\bar{\gamma}}\left\{1+(c-1)\dfrac{(|\gamma|-\bar{\gamma})}{(\gamma_c-\bar{\gamma})^2}[2(\gamma_c-\bar{\gamma})-(|\gamma|-\bar{\gamma})]\right\} & \text{for } |\gamma| > \bar{\gamma} \end{cases} \tag{3.1}$$

The parameter c in Equation 3.1 is an independent parameter which is the ratio of ultimate shear stress, τ_c, to elastic shear stress limit, $\bar{\tau}$. The modified form of G in Equation 3.1 is shown in Figure 3.5. In the modified formulation, there exist two enhancements. The first one is the nonlinear part of G after $|\gamma|=\bar{\gamma}$ for a wall panel that is made of any masonry material in general. The second one is the ultimate shear strain at which $G = 0$ given by the following equation.

$$\gamma^* = \bar{\gamma} + (\gamma_c - \bar{\gamma})\left(1+\sqrt{\frac{c-1}{c}}\right) \tag{3.2}$$

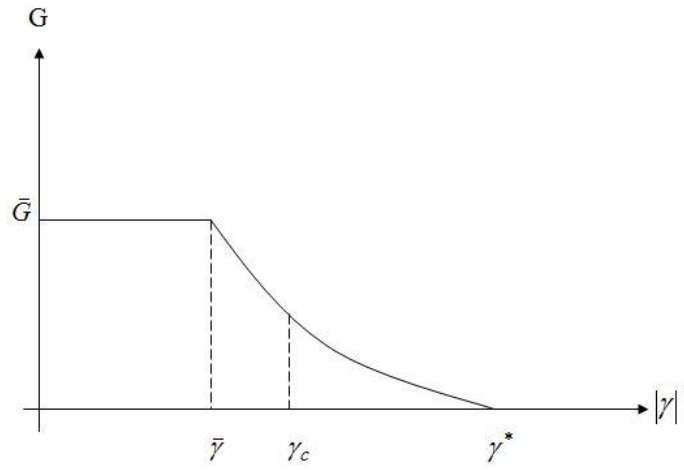

Figure 3. 5. Skeleton curve of G for a wall panel made of general masonry material

As stated before, f_m has been considered as a random variable to account for the material variability for masonry. Starting from this point on, the determination of the parameters in Figure 3.4 , ($\bar{G}$, $\bar{G}'$, $\overset{*}{G}'$, γ_c, $\bar{\gamma}$) is discussed in the following paragraphs.

According to the FEMA 356 (2000), the relationship between the compressive strength of masonry, f_m , and elastic shear modulus, $\bar{G}$, is defined by the following relationships, where E is the elasticity modulus of masonry.

$$E = 550 f_m \tag{3.3}$$

$$\bar{G} = 0.4E \tag{3.4}$$

Viscous damping coefficient in the elastic range, $\bar{G}'$, can also be described as a function of elastic shear modulus by using the formulation stated by Mengi et al. (1992):

$$\bar{G}' = \bar{G}\left(\frac{\xi_n T_n}{\pi}\right) \tag{3.5}$$

In Equation 3.5, parameters ξ_n and T_n are the damping ratio and the natural period of the masonry building for the corresponding n^{th} mode. Damping coefficient is considered as constant (10% of the critical damping) in the linear elastic range (Mengi et al. 1992, Sucuoglu and Erberik 1997). Natural period of the masonry building is also estimated by using an empirical formulation:

$$T = 0.06n \tag{3.6}$$

where n is the number of stories.

In addition to $\bar{G}$ and $\bar{G}'$, other parameters of masonry wall elements are required to be obtained in order to construct the skeleton curves that simulate the variation of in-plane shear modulus, G, and its viscous counterpart, G', with the shear strain. One of these material parameters is $\overset{*}{G}'$, which is the viscous damping coefficient after shear strain exceeds the ultimate shear strain, γ_c. $\overset{*}{G}'$ is considered as $2\bar{G}'$ throughout the analyses.

The ultimate shear strain, γ_c, is obtained from the Equation 3.7 by considering the bilinear relationship between shear stress and shear strain when $|\gamma| > \bar{\gamma}$:

$$\gamma_c^2 - (2c\bar{\gamma})\gamma_c + c\bar{\gamma}^2 = 0 \tag{3.7}$$

According to Mengi et al. (1992) and Sucuoglu and Erberik (1997), it is appropriate to assume parameter c as 1.4. The other parameter in the Equation 3.7 is $\bar{\gamma}$, which is the elastic shear strain limit and it is calculated as :

$$\bar{\gamma} = \frac{\tau_c}{c\bar{G}} \tag{3.8}$$

The parameter τ_c, which stands for the ultimate shear stress is obtained by the expression proposed by Turnsek and Cacovic (1970)

$$\tau_c = \frac{f_t^{'}}{1.5}\sqrt{1+\frac{\sigma_y}{f_t^{'}}} \qquad (3.9)$$

where $f_t^{'}$ is the tensile strength which can be assumed as $0{,}16f_m$ and σ_y is the vertical stress on the wall element.

3.6. DETERMINATION OF CAPACITY

The capacity statistics of analytical masonry building models are obtained through pushover analysis by using the software MAS. The uncertainty in capacity is taken into consideration by employing the material variability as discussed above. Generation of the random variables is one of the most important issues for the evaluation of structural reliability. Although many methods have been proposed in the literature, Latin Hypercube Sampling (LHS) Method, which was developed by McKay et al (1979), is selected for this study since it provides reasonable accuracy without considering large sample size like the classical Monte Carlo Method (Rubinstein 1981) requires. Hence it may be considered as a constrained sampling technique (Ayyub and Lai 1989). The details of the method can be found elsewhere (Wyss and Jorgensen 1998).

By using the random variable f_m, the material properties which are used as input parameters to MAS program can be determined as mentioned above. Hence 20 values are generated for f_m by LHS method using the mean and standard deviation characteristics of each sub-class separately. Then material input parameters are calculated for each sample to be used for the pushover analysis of MAS. This means 20 pushover curves are generated for each sub-class of buildings by considering the material variability (Figure 3.6).

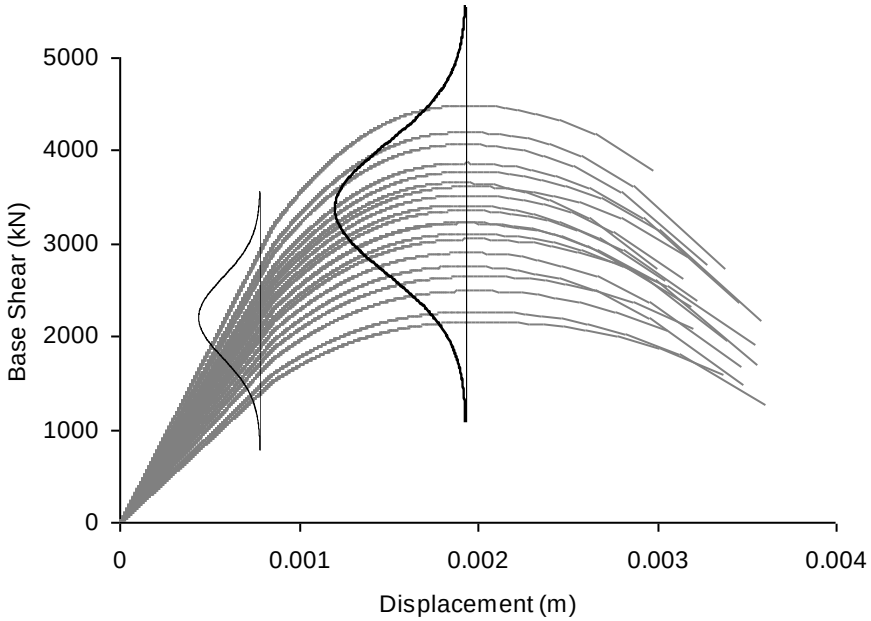

Figure 3. 6. Twenty capacity curves for a specific building class obtained by sampling material properties

Two limit states, which are named as LS-I (serviceability) and LS-II (ultimate) are monitored. This in turn means that three damage states are considered as "None/Light", "Moderate" and "Severe/Collapse". LS-I corresponds to the shear force level for which linear elastic behavior comes to an end by the exposure of visible cracks in masonry components. LS-II represents the maximum shear force capacity after which there exists a severe degradation (Figure 3.7). Since there exist 20 pushover curves for each building class, this means that there are 20 values for each limit state, for which a statistical distribution can be fitted. This is schematically shown in Figure 3.6 for LS-I and LS-II. Hence for each limit state, a mean value of shear force ($V_{LS,i}$) can be obtained with a known standard deviation. This statistical information is then used in the construction stage of the fragility curves.

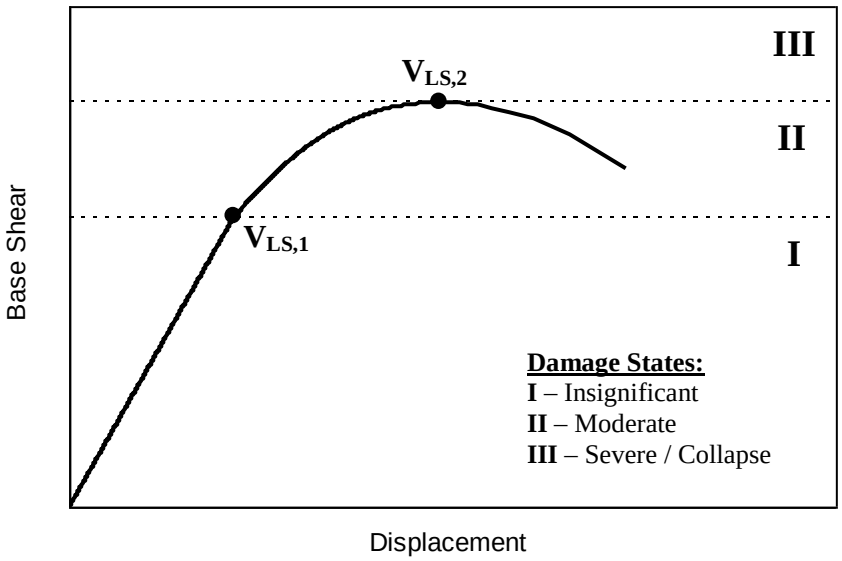

Figure 3. 7. Damage and limit state definitions for masonry buildings.

3.7. DETERMINATION OF DEMAND

In order to obtain the demand statistics, first ground motion records to be used in the fragility curve generation process are selected and then these records are used to conduct time-history analysis for the determination of shear force demand of generic masonry buildings in each class.

3.7.1. Selection of Ground Motion Records

The selection of ground motion records is one of the important stages of the procedure. In this study, peak ground acceleration (PGA) is considered as the hazard parameter to be used in order to generate the fragility functions of rigid masonry structures. 50 ground motion records with PGA values ranging between 0.01 and 0.8g, from low to high intensities. PGA values of the records are uniformly distributed in this defined range without having any gap in between with the purpose of obtaining the probabilities of exceedance for each limit state in a consistent manner. All selected records are taken from stiff sites with a formation of dense soil

or rock in accordance with the fact that ground motions with stiff site characteristics amplify the response of rigid masonry structures with low fundamental periods.

Selected ground motion records are listed in Table 3.4 with an increasing trend with respect to PGA values. The abbreviations in the first line of Table 3.4 can be explained as follows:

- ECODE: Identification code of each earthquake record listed in the database
- ENAME: Name by which the earthquake is commonly known.
- ECTRY: Name of the country where the earthquake occurred.
- Date: Occurrence date of the earthquake.
- Comp: Used component of the selected earthquake record.
- Ms: Surface-wave magnitude.
- PGA: The simplest but essential hazard parameter for force based fragility curve generation corresponds to the maximum response of stiff Single-Degree-of-Freedom (SDOF) systems such as masonry buildings due to the direct relationship between acceleration and force.
- PGV: The sign of maximum energy revealed from the acceleration cycle during the earthquake. It is considered as a more reliable indicator of strong motion intensity than other kinematic parameters. However it is a more suitable parameter to be used for ductile structural systems like reinforced concrete frame buildings, which can experience significant inelastic behavior under dynamic loading conditions.
- Δt_{eff} : Effective duration of earthquake record is a time interval which contributes to the significant part of the vibratory response of SDOF systems.

A practical way of calculating this duration employs Equation 3.10, proposed by Arias (1970):

$$I_a = \frac{\pi}{2g}\int_0^{\infty} a(t)^2 dt \qquad (3.10)$$

where I_a is the Arias Intensity in units of length per time, $a(t)$ is the acceleration-time history in units of g, and g is the acceleration of gravity. Arias Intensity is a ground motion parameter that captures the potential destructiveness of an earthquake as the area under the spectrum of total energy of absorbed by undamped SDOF systems at the end of ground excitation. It is defined by Trifunac and Brady (1975) that Δt_{eff} is the duration between the instants when Arias Intensity reaches the 5% and 95% of its final value.

3.7.2. Conducting Time-History Analysis to Obtain Demand Statistics

The base shear demand of masonry buildings under consideration is determined by conducting time-history analyses through MAS program. The demand statistics are obtained in terms of PGA within a range from 0.01g to 0.8g by employing the selected set of ground motion records in order to consider record-to-record variability. Elastic shear modulus $\bar{G}$ and its viscous damping counterpart $\bar{G}'$ are considered as random variables in the analyses.

Figure 3.8 represents a set of time history analysis results (in terms of the relationship between base shear demand and PGA) for a specific building class. The next step is to fit a curve to this scattered data. Observing the trend, it seems to be suitable to employ power fit. Furthermore it is possible to obtain high R^2 statistics with this simple type of function. Hence power fit with two constants (a and b) to be determined (Equation 3.11) is assumed to represent the relationship between shear force demand and PGA for each building subclass.

$$V_D = a(PGA)^b \tag{3.11}$$

The dispersion associated with the linear fit equation that is used to estimate the uncertainty in demand as

$$\beta_D = \sqrt{\ln(1+s^2)} \tag{3.12}$$

where s^2 is defined as the square of the standard error. By following the same steps, mean shear force demand (i.e. power fit equation) and the associated uncertainty (β_D) for each building class can be obtained.

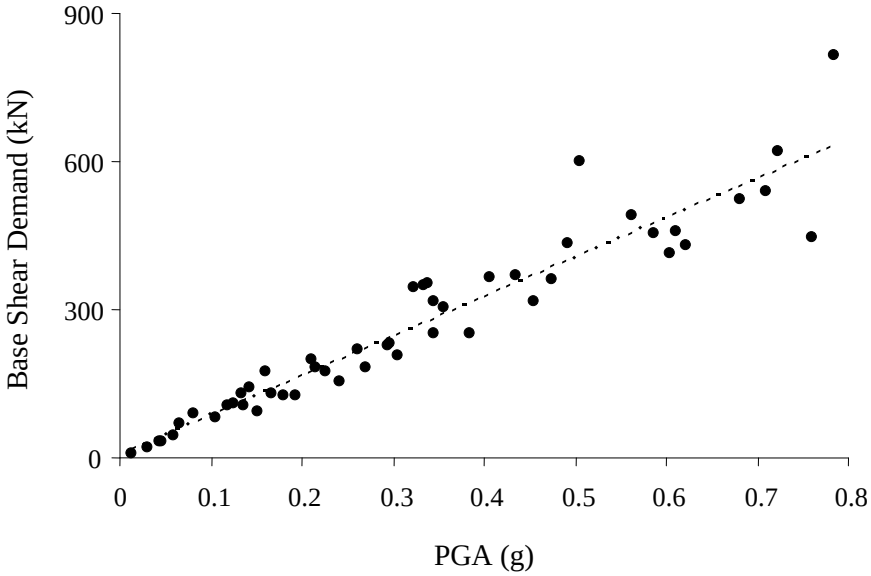

Figure 3. 8. The relationship between base shear demand and PGA together with the power fit for a specific building class.

Table 3. 4. Characteristics of the selected ground motion records

No	ECODE	Earthquake	Country	Date	Location	Comp	Ms	PGA (g)	PGV (cm/s)	EI (cm/s)	Δt_{eff}
1	MNJ90Y02	Manjil	Iran	20.06.1990	Building & Housing Research Center, Tehran	EW	7.3	0.01	1.24	2.92	13.61
2	VRN90X01	Vrancea	Romania	30.05.1990	Vrancioaia	NS	6.8	0.03	2.18	5.09	12.20
3	MAR99Y16	Marmara	Turkey	17.08.1999	Istanbul	T	7.8	0.04	6.84	15.90	37.35
4	MAR99Y14	Marmara	Turkey	17.08.1999	Bursa	T	7.8	0.05	7.90	24.53	34.21
5	MAR99X16	Marmara	Turkey	17.08.1999	Istanbul	L	7.8	0.06	8.46	15.27	38.12
6	IZM92X01	İzmir	Turkey	06.11.1992	Kusadasi Meteorology Station	L	6	0.07	4.34	9.03	10.59
7	IZM92Y01	İzmir	Turkey	06.11.1992	Kusadasi Meteorology Station	T	6	0.08	4.84	10.72	9.51
8	MAR99Y11	Marmara	Turkey	17.08.1999	Heybeliada Senotarium	EW	7.8	0.11	14.92	34.50	35.54
9	MAR99Y06	Marmara	Turkey	17.08.1999	Goynuk State Hospital	EW	7.8	0.12	11.04	24.81	11.41
10	HOR83X01	Horasan	Turkey	30.10.1983	Horasan Meteorology Station	NS	6.7	0.13	36.92	119.46	19.73

Table 3.4. Characteristics of the selected ground motion records (continued)

No	ECODE	Earthquake	Country	Date	Location	Comp	Ms	PGA (g)	PGV (cm/s)	EI (cm/s)	Δt_{eff}
11	MAR99Y12	Marmara	Turkey	17.08.1999	Arcelik	EW	7.8	0.13	38.19	48.57	29.90
12	MAR99X06	Marmara	Turkey	17.08.1999	Goynuk State Hospital	NS	7.8	0.14	9.68	22.54	11.59
13	MAR99Y03	Marmara	Turkey	17.08.1999	Gebze	EW	7.8	0.14	34.72	51.16	8.47
14	BUC77Y02	Bucharest	Romania	04.03.1977	Vrancioaia	EW	7.1	0.15	25.64	65.70	12.31
15	HOR83Y01	Horasan	Turkey	30.10.1983	Horasan Meteorology Station	EW	6.7	0.16	26.02	95.54	18.36
16	MAR99X02	Marmara	Turkey	17.08.1999	İzmit	NS	7.8	0.17	32.04	59.82	15.17
17	CLI80Y01	Campano-Lucano	Italy	23.11.1980	Bagnoli-Irpino	EW	6.9	0.18	30.45	67.22	31.81
18	BUC77X02	Bucharest	Romania	04.03.1977	Vrancioaia	NS	7.1	0.19	70.55	141.77	8.11
19	MAR99X12	Marmara	Turkey	17.08.1999	Arcelik	NS	7.8	0.21	14.19	25.72	32.38
20	CLI80X03	Campano-Lucano	Italy	23.11.1980	Sturno	NS	6.9	0.22	33.06	99.31	40.02

Table 3.4. Characteristics of the selected ground motion records (continued)

No	ECODE	Earthquake	Country	Date	Location	Comp	Ms	PGA (g)	PGV (cm/s)	EI (cm/s)	Δt_{eff}
21	MAR99Y02	Marmara	Turkey	17.08.1999	İzmit	EW	7.8	0.23	54.28	84.25	14.03
22	MTN79Y02	Montenegro	Form. Yugoslavia	15.04.1979	Ulcinj, Hotel Olimpic	EW	7	0.24	47.08	99.62	25.99
23	DNZ76Y01	Denizli	Turkey	19.08.1976	Directorate of Public Works and Settlement	EW	5.1	0.26	15.46	23.22	5.91
24	MAR99X03	Marmara	Turkey	17.08.1999	Gebze	NS	7.8	0.27	45.59	80.09	7.53
25	MTN79X02	Montenegro	Form. Yugoslavia	15.04.1979	Ulcinj, Hotel Olimpic	NS	7	0.29	38.64	99.43	25.05
26	KLM86Y01	Kalamata	Greece	13.09.1986	Kalamata-Prefecture	N355	5.8	0.30	32.27	53.54	7.08
27	MTN79Y01	Montenegro	Form. Yugoslavia	15.04.1979	Petrovac, Hotel Oliva	EW	7	0.31	25.31	47.24	13.36
28	CLI80Y03	Campano-Lucano	Italy	23.11.1980	Sturno	EW	6.9	0.32	55.36	131.27	38.53
29	FRU76Y02	Friuli Aftershock	Italy	15.09.1976	Forgaria Cornio	EW	6.1	0.33	23.80	35.34	2.76
30	TBS78Y01	Tabas	Iran	16.09.1978	Dayhook	N80W	7.3	0.34	17.68	54.69	32.40

Table 3.4. Characteristics of the selected ground motion records (continued)

No	ECODE	Earthquake	Country	Date	Location	Comp	Ms	PGA (g)	PGV (cm/s)	EI (cm/s)	Δt_{eff}
31	DNZ76X01	Denizli	Turkey	19.08.1976	Directorate of Public Works and Settlement	NS	5.1	0.35	24.18	28.51	5.02
32	FRU76X02	Friuli Aftershock	Italy	15.09.1976	Forgaria Cornio	NS	6.1	0.35	23.09	25.64	3.87
33	FRL76X01	Friuli	Italy	06.05.1976	Tolmezzo, Diga Ambiesta	NS	6.5	0.36	20.62	35.74	4.36
34	TBS78X01	Tabas	Iran	16.09.1978	Dayhook	N10E	7.3	0.39	24.58	67.80	33.44
35	MAR99Y05	Marmara	Turkey	17.08.1999	Sakarya	EW	7.8	0.41	79.80	94.78	15.52
36	LPT89X04	Loma Prieta	USA	18.10.1989	Gilroy Array #1	0	7.1	0.44	31.91	36.51	6.62
37	MTN79X01	Montenegro	Form. Yugoslavia	15.04.1979	Petrovac, Hotel Oliva	NS	7	0.45	38.82	87.07	12.00
38	FRU76X01	Friuli Aftershock	Italy	15.09.1976	Breginj Fabrika IGLI	NS	6.1	0.47	27.73	27.68	3.60
39	NPS86X03	North Palm Springs	USA	08.07.1986	Whitewater Trout Farm	180	6	0.49	34.72	46.90	5.44
40	FRU76Y01	Friuli Aftershock	Italy	15.09.1976	Breginj Fabrika IGLI	EW	6.1	0.51	21.15	23.35	2.33

Table 3.4. Characteristics of the selected ground motion records (continued)

No	ECODE	Earthquake	Country	Date	Location	Comp	Ms	PGA (g)	PGV (cm/s)	EI (cm/s)	Δt_{eff}
41	LPT89X16	Loma Prieta	USA	18.10.1989	LGPC	0	7.10	0.56	94.76	259.32	10.18
42	VTR80Y01	Victoria	Mexico	06.09.1980	Cerro Prieto	135	6.40	0.59	19.86	44.72	7.56
43	LPT89Y16	Loma Prieta	USA	18.10.1989	LGPC	90	7.10	0.61	50.97	110.09	7.82
44	NPS86Y03	North Palm Springs	USA	08.07.1986	Whitewater Trout Farm	270	6	0.61	31.48	39.30	3.41
45	VTR80X01	Victoria	Mexico	06.09.1980	Cerro Prieto	45	6.40	0.62	31.60	73.60	8.57
46	SSH87X02	Superstition Hills	USA	24.11.1987	Superstition Mountain	45	6.60	0.68	32.54	63.57	12.28
47	MGH84X04	Morgan Hill	USA	24.04.1984	Coyote Lake Dam	195	6.1	0.71	51.64	73.73	4.08
48	LND92X05	Landers	USA	28.06.1992	Lucerne	275	7.50	0.72	97.60	177.94	13.12
49	UMI97Y01	Umbro Marchigiano	Italy	26.09.1997	Nocera Umbra	EW	5.9	0.76	29.86	41.89	4.50
50	LND92Y05	Landers	USA	28.06.1992	Lucerne	0	7.50	0.78	31.87	67.43	13.77

3.8. DEVELOPMENT OF FRAGILITY CURVES

The information obtained from two branches (capacity and demand) shown in Figure 3.1 is now gathered in order to obtain the fragility curves of masonry buildings. For this purpose, the formulation proposed by Wen et al (2004) is employed.

$$P[LS > ls_i \mid PGA = pga] = 1 - \Phi\left[\frac{\ln(V_{LS,i}) - \ln(V_D)}{\sqrt{\beta_C^2 + \beta_D^2 + \beta_M^2}}\right] \quad (3.13)$$

In the proposed equation, $P[LS > ls_i \mid PGA = pga]$ corresponds to the probability of exceeding the i^{th} limit state for a given PGA level and, in the rest of the study, its abbreviation is shown as $P(LS_i / PGA)$. Symbol Φ stands for the standard normal cumulative distribution function. Parameter $V_{LS,i}$ represents the median base shear capacity of the i^{th} limit state obtained from pushover analysis as explained in Section 3.6 whereas parameter V_D is the median base shear demand that is obtained from the power fit associated with base shear demand vs. PGA relationship. The terms in the denominator stand for the uncertainties involved in the generation of fragility curves. Among these, β_C stands for the uncertainty in capacity, obtained from the standard deviation of the statistical distribution for each limit state. Parameter β_D is the uncertainty related with demand and it is obtained from Equation 3.12. The last uncertainty term, β_M, in the denominator associated with analytical modeling is assumed to be 0.3 throughout the study as it is proposed in Wen et al (2004).

The parameters in Equation 3.13 have been determined for all building classes. After that it is simple to plot fragility curves of masonry buildings by substituting the values into Equation 3.13 but it is not easy to plot all fragility curves since there exist 120 building classes times 2 fragility curves for each class, which makes 240 fragility curves for the whole masonry building stock. Instead some typical curves are examined to assess the physical validity of the generated curves.

In order to distinguish the building classes from each other and identify a certain building class, the following notation is introduced for the classification of Turkish masonry buildings: the letter M is used as a prefix and the succeeding four numbers represent in order the number of stories (N subclass from 1 to 5), material properties (D subclass from 1 to 4), plan regularity (R subclass from 1 to 2) and the considerations about the wall length and openings in walls (W subclass from 1 to 3), respectively. For instance, M3412 stands for the building class for 3-story, regular masonry buildings with moderate or poor quality cellular concrete block and that partially comply with the code requirements for the wall length and placement of openings in walls with some violations.

Figure 3.9 shows the comparison of fragility curves with respect to number of stories, material properties, plan regularity and considerations regarding wall length and openings in walls. All the curves have been generated for the ultimate (second) limit state. The masonry building classes are selected in such a way that one parameter is varied at a time while the other parameters are kept as constants.

Under same circumstance, Figure 3.9.a illustrates the effect of number of stories of masonry buildings in terms of the probability of suffering heavy damage or collapse. This probability for 1-story buildings (2% for PGA level of 0.5g) appear to be negligible when compared to the probabilities for 4 or 5 story buildings as 78% and 89% respectively for PGA level of 0.5g.

The results of material properties showed similar trends for masonry buildings with structural walls having lesser quality and low strength (i.e. D4 subclass) as shown in Figure 3.9.b. As moving from material subclass D3 to D4, the probability of occurrence of heavy damage or collapse increases from 27% to 78% (PGA level of 0.5g) by keeping all the remaining parameters as constant.

Plan irregularity is one of the important parameter that has a considerable effect on the probability of suffering heavy damage or collapse of masonry buildings as shown in Figure 3.9.c. In comparison to regular masonry buildings with a probability of

27% for PGA level of 0.5g, irregular masonry buildings has higher risk of collapse (71% for PGA level of 0.5g) with similar properties.

The effect of minimum wall length and openings in walls on probability of exceeding the limit state of masonry buildings are illustrated in Figure 3.9.d. Although the probability of masonry building classes W1 and W2 are close to each other as 15% and %25 respectively (for PGA level of 0.5g), the corresponding probability of class W3 is 71% (for PGA level of 0.5g), which is considerably higher than the other classes.

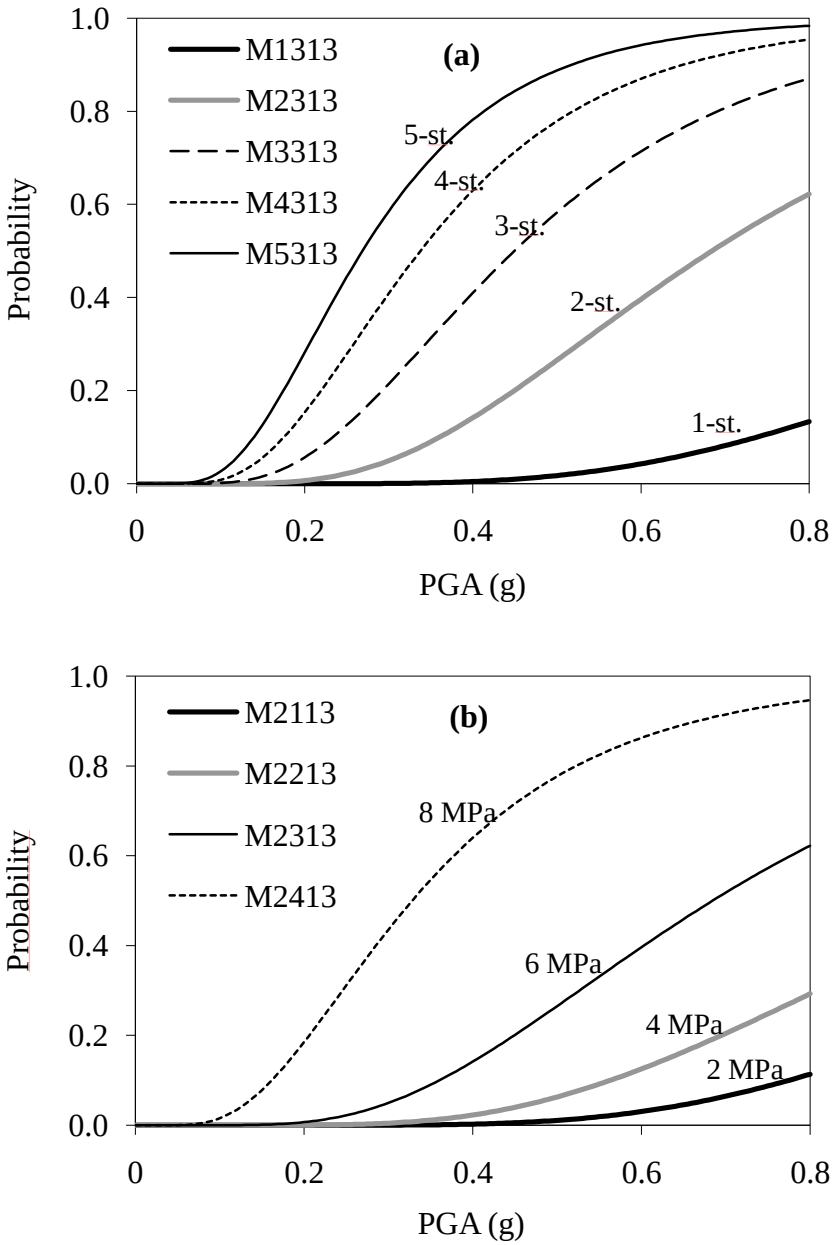

Figure 3. 9. Comparison of the fragility curves in terms of a) number of stories, b) material properties, c) plan regularity and d) considerations regarding wall length and openings in walls.

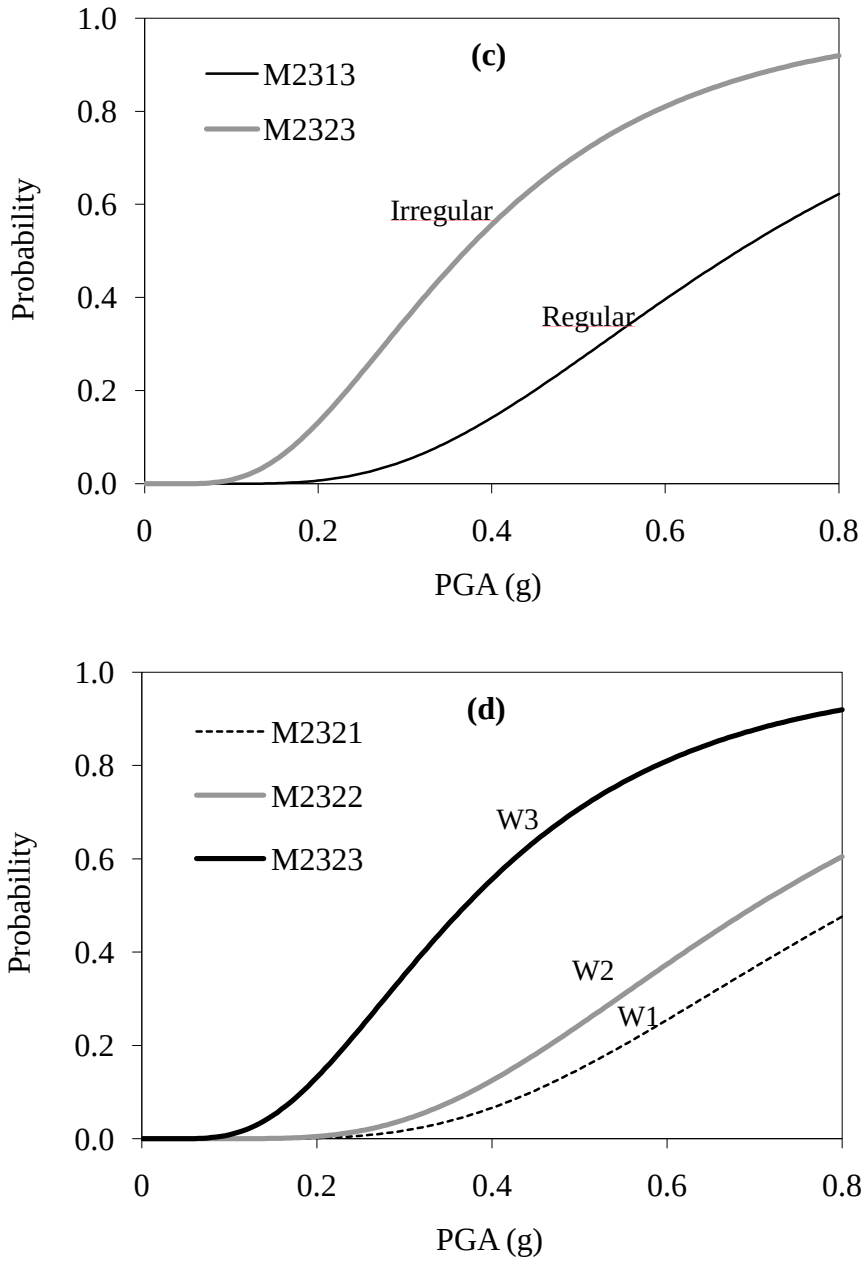

Figure 3.9 Comparison of the fragility curves in terms of a) number of stories, b) material properties, c) plan regularity and d) considerations regarding wall length and openings in walls (continued).

In the context of aforementioned figures (3.9.a-b-c-d), the probability of suffering heavy damage or collapse increases with the increase in number of stories (from N1 to N5), plan irregularity (from R1 to R2) and code violations regarding the wall length and openings (from W1 to W3). Conversely, supposed probability increases with the decrease in material strength value (from D1 to D4) for the selected classes of masonry buildings, which are all consistent with the expectations.

3.9. VERIFICATION OF FRAGILITY CURVES

In this section of this chapter, the verification of the fragility curves is illustrated with a comparative approach where the observed damage sustained by a group of masonry buildings after the 1995 Dinar earthquake is compared with the estimated damage by employing the fragility curves that have been constructed for masonry buildings. This verification is so valuable since it provides the information on the accuracy of the generated fragility curves and gives an idea for the estimation of damage distribution on comparable grounds with the actual field data

After the earthquake in Dinar, several teams of engineers performed a post-earthquake damage assessment of 140 masonry buildings. The quantification of structural damage was performed for rural type masonry structures by using the standard Damage Evaluation Form (General Directorate of Disaster Affairs 1990). In this form, damage points were given for the walls of the most damaged story of the masonry structure as well as for the stairs and roof. Damage is classified into 5 groups as undamaged, minor, moderate and severe or collapse. The significance of the damage states is given in Table 3.5.

In the first phase of the comparative approach, the selected masonry buildings in Dinar are classified according to the building classes proposed in the generation of fragility curves. Hence a fragility curve set is assigned to each building according to

subclass properties such as number of stories, material type, geometry in plan and the wall ratio.

Secondly, on-site ground motion intensity value is acquired for each building in terms of PGA, which is gathered from a previous study about synthetic seismograms generated by using a realistic source model for the 1995 Dinar earthquake (Anderson et al. 2001, Sucuoglu et al. 2003). The city was separated into four distinct zones according to topographical and geotechnical features. A total of 29 synthetic seismogram sites were selected in these zones. Local site conditions, the number of buildings and the statistical properties of PGA are listed in Table 3.6 according to related zones defined for the city. The majority of the selected masonry buildings (73%) are located in Zone 2, while the remaining buildings are in Zone 1 and 3.

Then, on-site PGA values were assigned to the selected masonry buildings by considering the variability of PGA in that zone. After that the damage state probabilities for each building are calculated as a function of the assigned PGA value as presented in Figure 3.10. The probabilities of having insignificant damage, moderate damage and severe damage (or collapse) for an on-site PGA value of 0.5g are obtained as 22%, 51% and 27%, respectively, for a demonstrative set of fragility curves that belongs to a class of masonry buildings.

Table 3. 5. Damage scores used in Damage Evaluation Form

Damage State	Score
Undamaged	0
Minor	1 - 3
Moderate	4 - 6
Severe	7 - 9
Collapse	> 9

Table 3. 6. Properties of seismic zones in Dinar

Related Zone	Site Conditions	No. of Buildings	PGA	
			Mean	COV
1	Rock	27	0.318	0.22
2	Stiff Soil	102	0.517	0.29
3	Soft Soil	11	0.636	0.22
4	Soft Soil	0	0.636	0.22

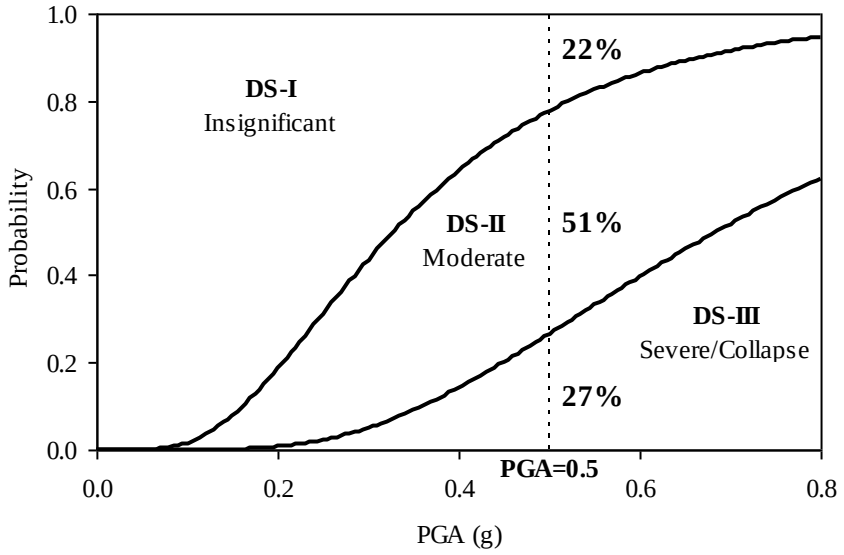

Figure 3. 10. Damage state probabilities obtained from a demonstrative set of fragility curves for a PGA level of 0.5g.

A single-valued vulnerability score (VS) has to be developed by multiplying the damage state probabilities with the corresponding damage state constants for the assigned PGA value in order to compare the estimated damage with the observed damage for the masonry buildings under consideration. The damage state multipliers for DS-I, DS-II and DS-III (see Figure 3.10) are assumed as 0.0, 0.5 and 1.0,

respectively. The vulnerability score should be between 0 and 1 where the higher VS indicate that the building is more vulnerable to seismic action under the given intensity of shaking. As an example, the VS score of the building can be calculated according to given fragility curve set in Figure 3.10 for PGA level of 0.5g;

$$VS = 0.0 \times 0.22 + 0.5 \times 0.51 + 1.0 \times 0.27 = 0.525$$

The scatter diagram in Figure 3.11 represents the vulnerability scores of all the selected masonry buildings, which are obtained and compared with the observed damage. The results illustrates reasonable agreement between the level of inspected visual damage as assessed from the Damage Evaluation Form and the vulnerability score using the fragility curve sets of masonry building classes.

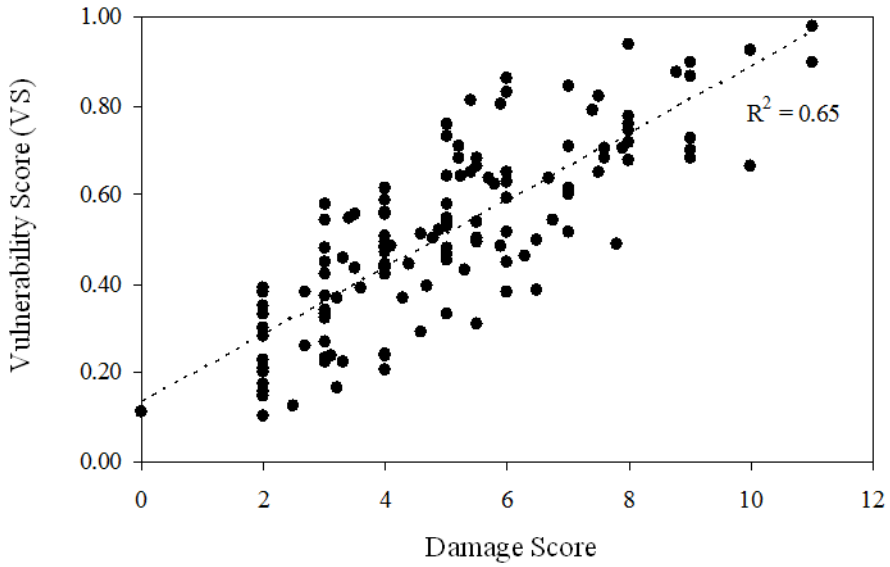

Figure 3. 11. The scatter diagram of estimated damage versus reported damage score.

Subsequent to visual damage inspection, it was time to come to a decision about the masonry buildings that were affected by the Dinar Earthquake; to repair or to

demolish. While making this decision, the economic feasibility of executing such a huge structural rehabilitation was taken into consideration as well (Wasti et al 1998). The distribution of repaired and demolished masonry building percentages with VS intervals as presented in Figure 3.12. As the VS scores moves from low to high values, percentage of repaired buildings decreases whereas the percentage of demolished buildings increases. This outcome indicates that vulnerability scores can be employed as an alternative approach on the repair or demolition decisions of damaged masonry buildings.

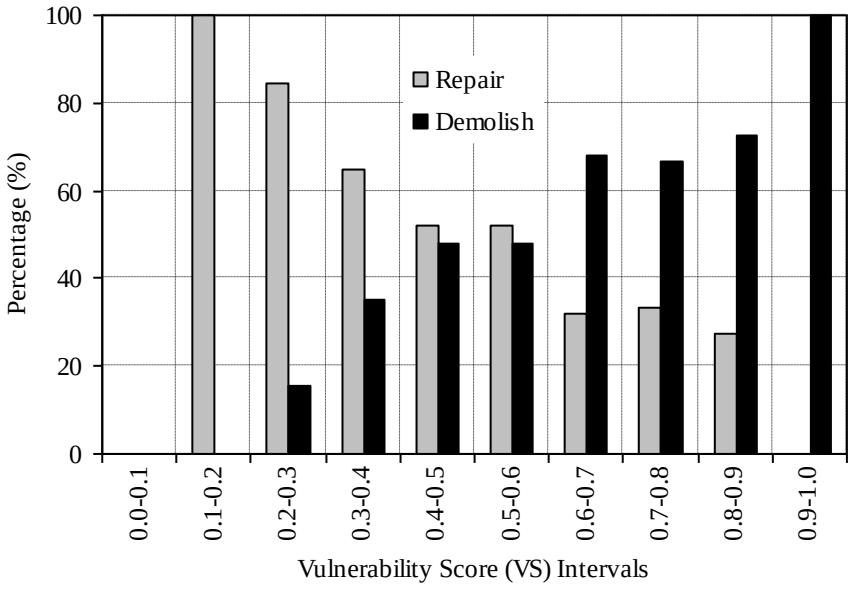

Figure 3. 12. Proportions of repaired and demolished masonry buildings in each VS interval.

CHAPTER 4

FRAGILITY OF TURKISH MASONRY BUILDINGS BY CONSIDERING OUT-OF-PLANE FAILURE MODES

4.1. GENERAL

In the previous chapter, vulnerability of Turkish masonry buildings was considered by using in-plane failure modes. However, according to the past observations after major earthquakes, one of the most dominant modes of failure for unreinforced masonry buildings in Turkey has been encountered as the out-of-plane failure of walls. The structural deficiencies that lead to this type of failure can be stated as poor wall-to-floor and wall-to-wall connections due to insufficient anchorage, absence of horizontal rigid diaphragms, poor material quality and high slenderness ratio (i.e. ratio of wall height to its thickness). Hence it is misleading to evaluate the seismic vulnerability of masonry structures without considering the out-of-plane behavior. In addition to this, out-of-plane wall failures impose a significant risk to the people living in these buildings, since they may be trapped in by this type of failure, which may lead to partial or complete collapse of the building. The fatalities in collapsed masonry buildings in Turkey are mostly due to this specific type of failure.

As stated by Paulay and Priestley (1992), out-of-plane response of unreinforced masonry walls is one of the most complex and ill-conditioned problems in seismic analysis of building structures. The reason is that the behavior is governed both by strength and stability. Hence many different approaches have been considered to solve this problem in the past. The first attempts started with the tests conducted by

ABK Joint Venture (1981). In this extensive series of tests, dynamic loading was applied to 22 wall specimens with different vertical stress levels and slenderness ratios. As a result, ABK proposed maximum allowable slenderness ratios in terms of the vertical stress level and peak input velocities at the top and bottom of the wall. These results have been used extensively in proceeding years, especially in FEMA and ASCE guidelines (FEMA 1997, ASCE 2000, ASCE 2007). Later on it was stated that the proposed ratios were rather conservative (Simsir 2004, Sharif et al., 2007).

Two different analytical modeling approaches are available to examine out-of-plane behavior of URM walls: strength (or stiffness)-based models and rigid-body rocking models. Strength-based models can be employed in linear static, nonlinear static, linear dynamic and nonlinear dynamic types of analysis. For dynamic analysis, either single-degree-of-freedom (SDOF) (Doherty et al 2002) or multi-degree of freedom (MDOF) (Simsir 2004) idealization can be assumed.

Rigid-body rocking models have been employed based on the fact that after the wall cracks significantly, its motion is based on the rigid body motion of blocks separated by cracks rather than the elastic or material properties of the wall. The study of rigid-body rocking motion of blocks goes back to Housner (1963). Thanks to this pioneer study, Makris and Konstantinidis (2003) worked on the dynamic response of rocking bodies by considering rigid body motion. Although they claim that this approach yields more reliable results than strength-based approach, it is evident that rigid-body based analysis methods are much more difficult to apply since it is not possible to define a unique model frequency or use viscous damping in the case of rigid-body models (Sharif et al. 2007).

As seen in previous paragraphs, research on out-of-plane response of unreinforced masonry walls includes many methods from the simplest to the most complex ones. In this study, a force-based method is selected due to some reasons. First, the method should be simple and practical since it is going to be applied to a population of buildings rather than an individual building in a short period of time. Furthermore,

the selected method should be consistent with the one used for in-plane fragility of masonry buildings, in which a force-based approach was selected, so that they could be used together to yield the overall vulnerability of unreinforced masonry buildings. Eventually the method possesses many assumptions and simplifications. But all of them are justifiable in terms of earthquake engineering and structural mechanics.

The following sections give the details of the procedure that has been proposed to assess the out-of-plane fragility of unreinforced masonry buildings in Turkey as illustrated in Figure 4.1. The last section of this chapter is devoted to the verification of the out-of-plane fragility curves. For this purpose, structural damage observed after the 2010 Elazığ earthquake is considered since rural masonry dwellings generally suffered out-of-plane damage during this particular earthquake.

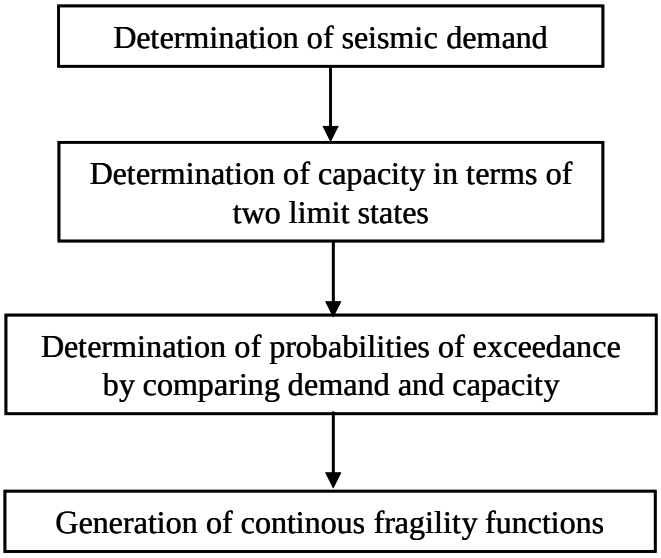

Figure 4. 1. Outline of the method used for the generation of fragility curves of Turkish masonry buildings for out-of-plane action

4.2. DETEMINATION OF SEISMIC DEMAND

The details of the interaction between in-plane and out-of-plane responses of masonry walls during seismic action were presented by Paulay and Priestley (1992). Considering the seismic energy path in Figure 4.2, the ground acceleration seems to be amplified by in-plane loaded walls and the floor diaphragms. In most cases, this interaction is too complex, inducing out-of –phase responses between walls and uneven amplification factors between floors. However it can always be stated that the amplification is most significant in the uppermost story of the building, with largest values of floor accelerations. In addition to this, the vertical stress, which helps in resisting the out-of-plane deformation of a masonry wall, is lowest in these stories. Therefore, the face-loaded (out-of-plane) walls of the uppermost stories are the most vulnerable parts of masonry buildings regarding the out-of-plane action. This has been verified in previous major earthquakes (see Figure 4.3).

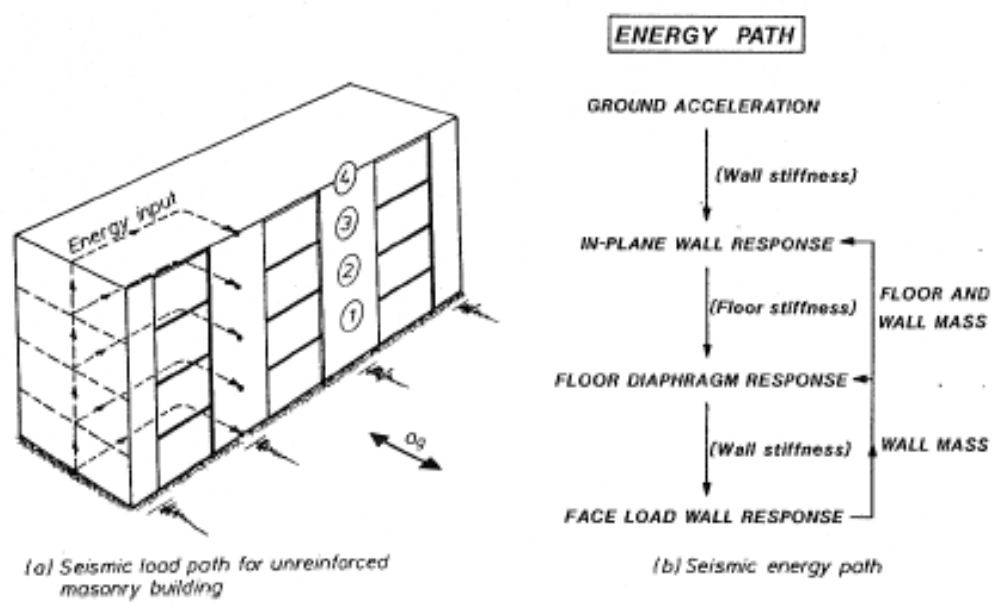

Figure 4. 2. Seismic response of an unreinforced masonry building
(Paulay & Priestley 1992)

Figure 4. 3. Typical examples for out-of-plane failure of unreinforced masonry walls in the uppermost stories of damaged buildings during a) Loma Prieta earthquake (1989), b) Northridge California earthquake (1994).

Nevertheless, it can be assumed that if floor slabs have considerable in-plane rigidity, the amplifications of the out-of-plane loaded wall accelerations by floor response can be neglected and the floor accelerations become equal to the accelerations of the in-plane loaded walls at the floor height (Lang 2002). Hence it is possible to estimate the story accelerations from the spectral acceleration of an equivalent SDOF is presented in a conservative manner as recommended by Paulay and Priestley (1992). This is illustrated in Figure 4.4 for a five story unreinforced masonry building.

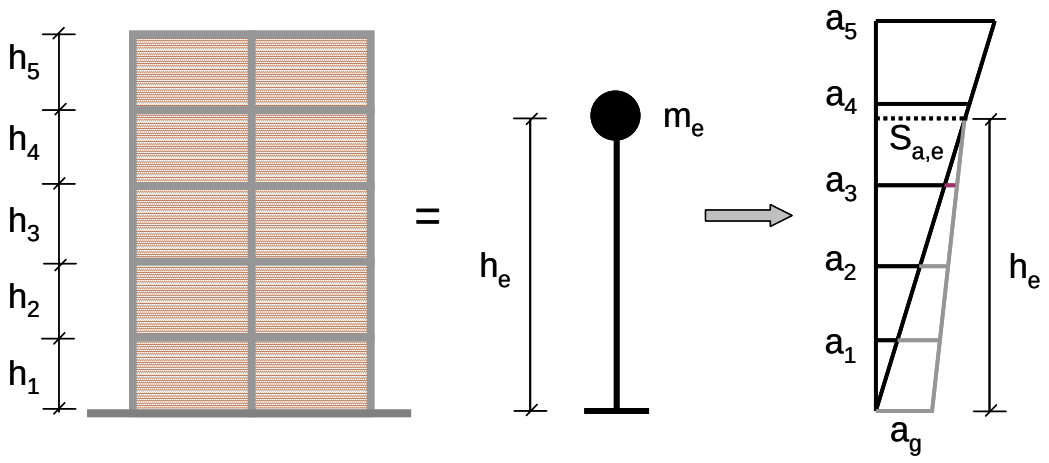

Figure 4. 4. Superposition of the peak ground acceleration and story accelerations by using equivalent SDOF idealization

In the figure, m_e and h_e stand for the equivalent mass and height of the idealized SDOF system, respectively and they are represented by the following equations

$$m_e = \sum_{i=1}^{n} m_i \phi_i \tag{4.1}$$

$$h_e = \frac{\sum_{i=1}^{n} h_i m_i \phi_i}{\sum_{i=1}^{n} m_i \phi_i} \tag{4.2}$$

where m_i is the concentrated mass and ϕ_i is the first mode displacement at the i^{th} floor level normalized such that the first mode displacement at the top storey $\phi_n=1$,h_i is the height of the i^{th} floor level and n is the number of stories. Parameter $S_{a,e}$ in Figure 4.4 acts on the equivalent height h_e and it represents the elastic spectral acceleration at the fundamental period of the building subjected to a specific ground motion record, which is obtained by carrying out spectrum analysis with idealized SDOF systems. Just like in the case of in-plane motion, fundamental period of unreinforced masonry buildings is estimated by using the empirical formulation

$$T = 0.06n \tag{4.3}$$

where n is the number of stories. However, calculating $S_{a,e}$ as a function of a single period value may be misleading since elastic response spectrum is very erratic in short period range. Instead, an averaging process is considered in this study, where $S_{a,e}$ is obtained in a range of periods with lower and upper bounds of T and 2T, respectively. Previous studies (Erberik 2008) indicated that the upper bound could be taken as 2T since this approximately represents the period of a masonry structure in which load bearing walls have started to experience damage by cracking due to seismic action. Hence $S_{a,e}$ values are calculated for 50 ground motion records listed in Table 3.4 and used as the seismic demand input parameter. Example of how $S_{a,e}$ is calculated from elastic response spectra is illustrated in Figure 4.5.

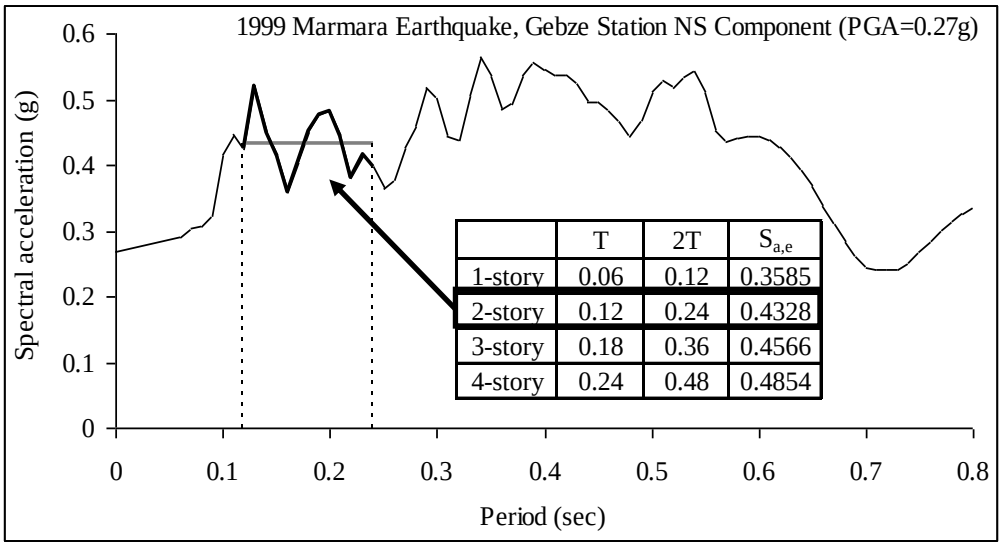

	T	2T	$S_{a,e}$
1-story	0.06	0.12	0.3585
2-story	0.12	0.24	0.4328
3-story	0.18	0.36	0.4566
4-story	0.24	0.48	0.4854

Figure 4. 5. Calculation of average $S_{a,e}$ values for unreinforced masonry buildings from one to four stories high subjected to NS component of Gebze record (PGA=0.27g) from the 1999 Marmara earthquake, Turkey.

As it is seen from Figure 4.4, at heights above h_e of the equivalent SDOF system, the storey acceleration at the i^{th} storey (a_i) is governed by the first mode shape distribution, which is assumed to be linear, from the spectral acceleration, $S_{a,e}$

$$a_i = \frac{S_{a,e}}{h_e} \sum_{j=1}^{i} h_j \tag{4.4}$$

At heights below h_e, influence of the peak ground acceleration, a_g, is taken into account by a linear interpolation between a_g and $S_{a,e}$

$$a_i = a_g + \frac{\sum_{j=1}^{i} h_j (S_{a,e} - a_g)}{h_e} \tag{4.5}$$

where h_j stands for the storey height between each floor level. Thanks to Equations 4.4 and 4.5, accelerations at each storey level can be calculated. Considering a wall panel between any two floor levels, for instance i^{th} and $(i-1)^{th}$ floors, it is assumed that acceleration on the wall (a_{wall}) is constant over the floor height as calculated from Equation 4.6 although the response acceleration indeed varies with height and maintains its maximum value at mid-height and minimum value at floor levels (see Figure 4.6.a). This is not a very conservative assumption as stated by Menon and Magenes (2008).

$$a_{wall} = \frac{a_i + a_{i-1}}{2} \tag{4.6}$$

Using this assumption, out-of-plane loading of a masonry wall (q) due to inertia can be expressed as

$$q = m\, a_{wall} \tag{4.7}$$

where m is the mass per unit length. Different boundary conditions can exist between walls and floors (horizontal boundaries) and also between walls connecting in a perpendicular manner at corners (vertical boundaries). If the wall is not properly connected to adjacent perpendicular walls or if the wall is long enough then it is possible to model the wall as a strip or beam element in one dimension while calculating the maximum demand created by the seismic action. Since this part of the study aims at assessing the seismic vulnerability of masonry building due to out-of-

plane action, it is proper to assume the worst case scenario for face-loaded walls: poor wall-to-wall connections and long walls with out-of-plane stability problems. Turkish earthquake code (2007) limits the unsupported length of unreinforced masonry walls (L_{max} in Figure 4.6.b) in order to avoid out-of-plane instability. Maximum length is permitted as 5.5 m in seismic zone 1 and 7.5 m in all other seismic zones. However, in practice, such long walls can be frequently encountered in Turkish masonry buildings. For these walls, it is not a false assumption to consider the wall as a one-way spanning beam at the mid-section of the wall as shown in Figure 4.6.b. Furthermore, neglecting the two-way action is conservative and since the proposed method has been intended to be applied to a population of buildings, this level of conservatism is tolerable and on the safe side. Hence based on above discussions, the critical wall, for which the out-of-plane action is to be examined, is treated as an equivalent beam of unit length which is supported by the upper and lower floors.

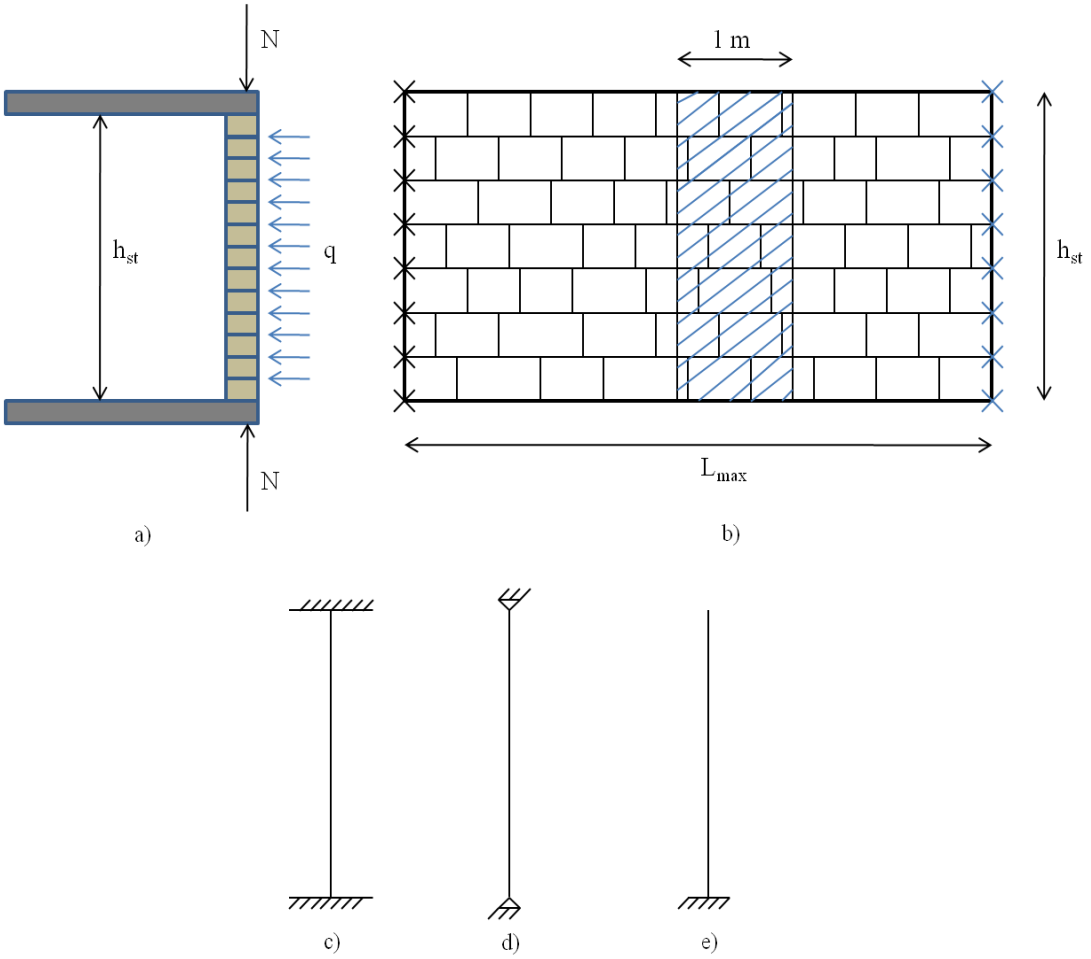

Figure 4. 6. a) Out-of-plane loaded wall, b) one way spanning strip assumption, c) fixed boundary condition, d) hinge boundary condition (simple beam), e) cantilever boundary condition

Depending on the characteristics of wall-to-floor connection, maximum moment demand in wall element, M_d, can be expressed as such that;

1. For a built in beam (Figure 4.6.c), simulating a concrete floor system with continuous horizontal ring beams, and where the normal forces are usually high, preventing the top and the bottom of the wall element to rotate; or for a

timber floor system with ties connecting the wall element to the floors, the maximum moment demand can be calculated as,

$$M_d = \frac{qh_{st}^2}{12} \tag{4.8}$$

2. For a simply supported beam (Figure 4.6.d), representing a floor system with joints at the top and bottom of the wall element, the maximum moment demand is,

$$M_d = \frac{qh_{st}^2}{8} \tag{4.9}$$

3. In the case of a cantilever (Figure 4.6.e), standing for a gable wall or a balustrade; or load-bearing walls of single story rural masonry dwellings which have nearly no connection to the roofs, the maximum moment demand can be expressed as

$$M_d = \frac{qh_{st}^2}{2} \tag{4.10}$$

In the above equations, h_{st} represents the wall height in that particular story. It is important to note that all demand calculations are carried out for the most critical face-loaded masonry wall, which is located in the upper most story for multi-story buildings, assuming that the wall is not connected to other structural members in a proper way and it is long enough to invoke out-of-plane instability under seismic action. All assumptions are made, trying to stay on the conservative side, since the methodology is proposed for a population of buildings rather than a single building.

4.3. DETEMINATION OF SEISMIC CAPACITY

According to the developed procedure for this study, determination of seismic demand can only be meaningful with the determination of seismic capacity of masonry walls. As it is done in in-plane analysis, limit states for the masonry

buildings considering out-of-plane failure should be determined. However limit states are defined for this case in terms of moment per unit length.

The first limit state, LS-I, can be quantified by examining the out-of-plane moment versus curvature relationship of the masonry wall under consideration as proposed by Paulay and Priestley (1992). The onset of cracking (see Figure 4.7.a) is determined by the linear stress distribution which is equal to zero at the extreme fiber. Therefore, cracking moment capacity at the onset of cracking, $M_{C,cr,}$ can be calculated as follows.

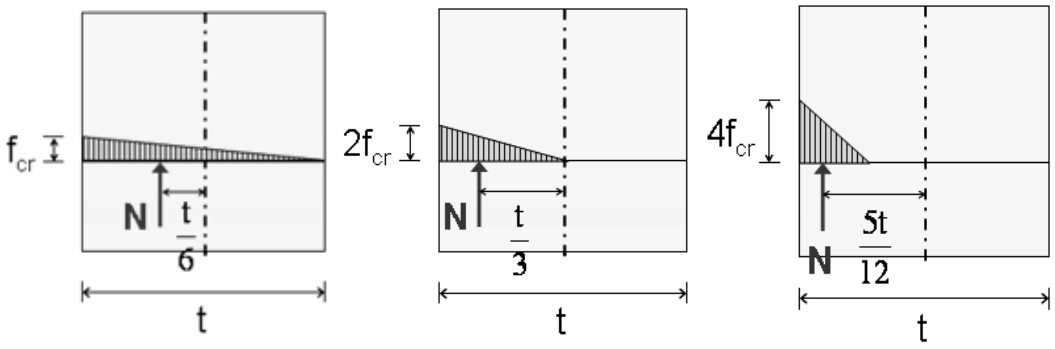

a) b) c)

Figure 4. 7. Stress distributions in the center of the masonry wall at different stages of out-of-plane action: a) onset of cracking, b) half-cracked, c) 3/4 cracked

$$M_{C,cr} = \frac{Nt}{6} \tag{4.11}$$

where N is the resulting gravity load due to loads on floors and self weight of the wall and t is the thickness of the wall considered. Accordingly, the corresponding curvature at the onset of cracking can be calculated by assuming a linear distribution of strains along the thickness of the wall

$$\varphi_{C,cr} = \frac{f_{cr}}{EI_m} \tag{4.12}$$

where $\varphi_{C,cr}$ is the curvature capacity at the onset of cracking, f_{cr} is the cracking strength, E is the elasticity modulus of masonry and I_m is the moment of inertia. In a similar fashion (ϕ_C, M_C) points can be obtained at different stages of out-of-plane action, i.e. 1/4 cracked, half cracked, 3/4 cracked, and so on. In these calculations, tensile strength of masonry has been neglected. By joining the obtained points, one can construct the moment curvature relationship for out-of-plane motion as shown in Figure 4.8.b. This is a typical curve generated for the face-loaded wall A (see Figure 4.8.a) at the uppermost story of an existing four story unreinforced brick masonry building in Istanbul, for which the story plan is also given in the same figure. The hollow dots on the curve represent different stages of cracking along the thickness of the wall. First cracking occurs at a very early stage as seen in the figure. Hence it is highly conservative to consider first cracking as the serviceability limit state. With a closer look to the moment curvature relationship, it is observed that the change in tangent slope starts at a point between 20% and 30% cracking along the thickness of the wall (Figure 4.9). This means that it would be more appropriate to consider later stages of cracking as the serviceability limit state. Hence the serviceability limit state (i.e. LS-I) is considered as the stage when 1/4 (25%) of the wall thickness has been cracked. In this case, the moment capacity at LS-I ($M_{LS,1}$) becomes

$$M_{LS,1} = \frac{Nt}{4} \tag{4.13}$$

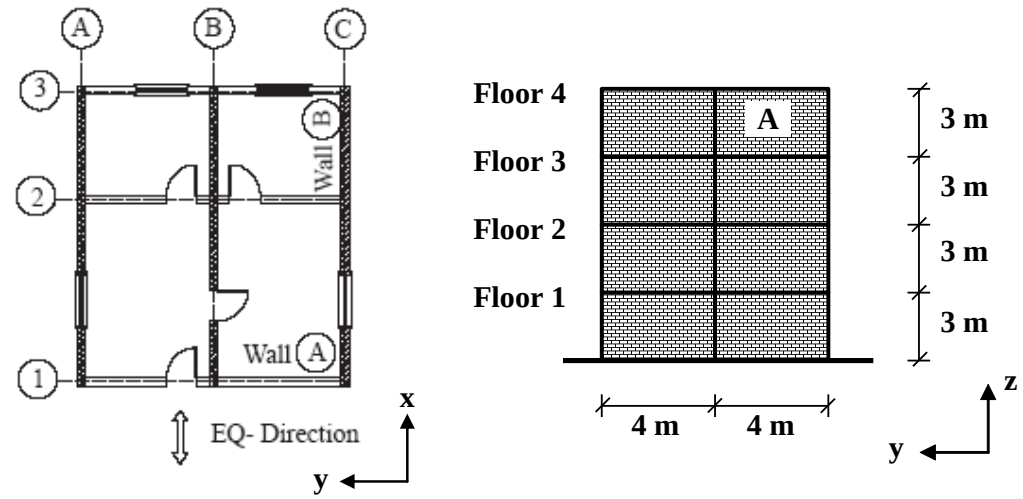

(a)

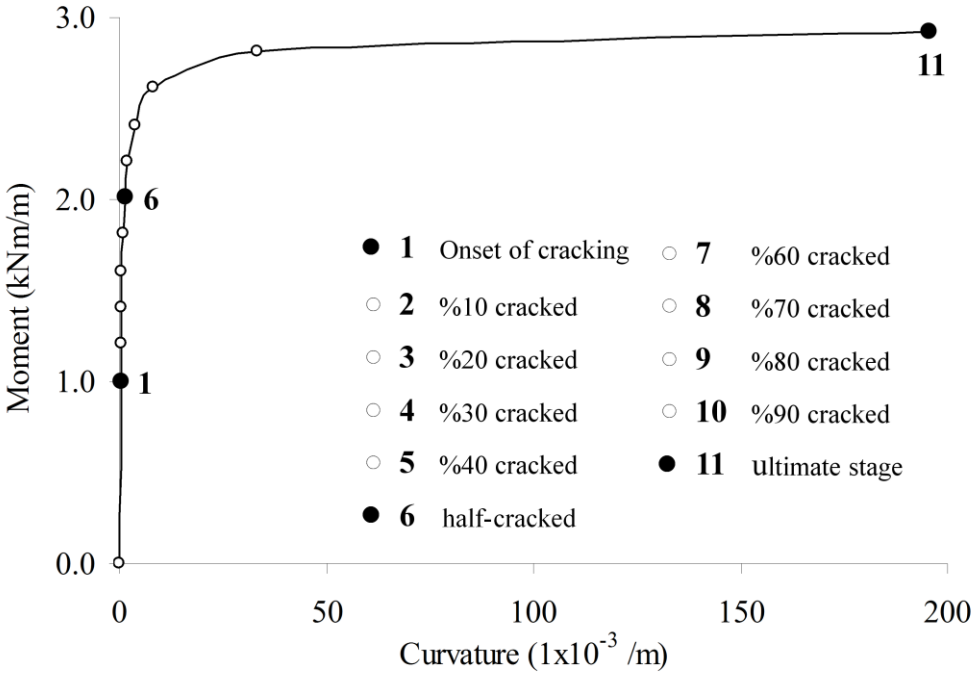

(b)

Figure 4. 8. a) An existing four story unreinforced masonry building in Istanbul, b) Out-of-plane moment curvature relationship for the uppermost story wall A of the building

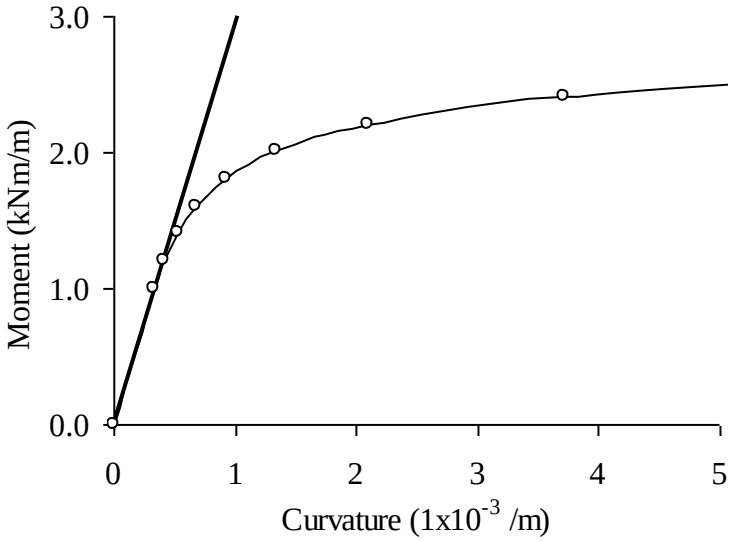

Figure 4. 9. A closer look at the moment curvature relationship of Figure 4.8.b

The ultimate limit state, which is denoted as LS-II, is attained by the ultimate moment of the masonry wall at the onset of out-of-plane failure (see stage-11 in Figure 4.8.b). After cracking occurs, the crack will propagate through the thickness of the wall together with increase in compressive stress and decrease in depth of compression zone decrease until the compressive strength of masonry orthogonal to the mortar bed (f_m) is reached ultimately. The stress distribution at ultimate can be approximated by a rectangular stress block as shown in Figure 4.10. Hence the ultimate moment capacity ($M_{LS,2}$) is calculated as

$$M_{LS,2} = N\left(\frac{t-a}{2}\right) < 3\,M_{cr} \tag{4.14}$$

where “a” is the width of the stress block, which can easily be calculated from the force equilibrium in Figure 4.10 as follows.

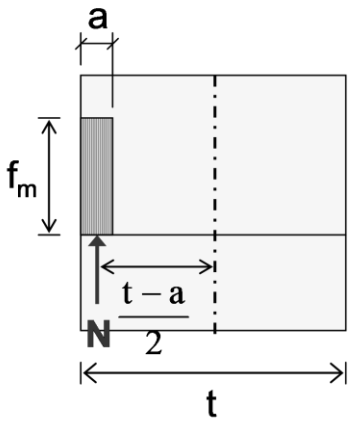

Figure 4. 10. Stress distribution at the central crack at the ultimate stage

$$a=\frac{N}{f_m\, l} \tag{4.15}$$

In Equation 4.15, parameter "l" stands for the load per 1 meter length of the stress block, which is taken as 1 meter. With the combination of Equations 4.14 and 4.15, it can be written as

$$M_{LS,2}=\frac{Nt}{2}\left(1-\frac{N}{f_m t}\right) \tag{4.16}$$

However, it has been stated by some researchers that out-of-plane behavior of unreinforced masonry walls is governed by displacement rather than strength (Doherty et al 2002, Griffith et al 2003, Menon and Magenes 2008). In fact, using a strength-based approach is rather conservative since it has been shown that dynamically loaded walls can experience acceleration demand in excess of the threshold value obtained through static analysis. Hence it was decided to multiply $M_{LS,2}$ by a factor in order to obtain more realistic results for the ultimate stage. For the quantification of this multiplication factor, the research study conducted by Lagomarsino and Magenes (2009) has been employed. The researchers examined a

number of masonry walls under static and dynamic loading conditions. At the end they concluded that the static acceleration at the onset of failure is on the average about 75% of the corresponding dynamic acceleration obtained through the dynamic analysis of the wall by rigid body kinetics. Considering this information, multiplication factor in this study is selected as 4/3 and then Equation 4.16 becomes

$$M_{LS,2} = \frac{2Nt}{3}\left(1 - \frac{N}{f_m t}\right) \tag{4.17}$$

To conclude, the limit states (denoted as LS-I and LS-II) for out-of-plane action have been obtained in terms of out-of-plane moment and are given in Equations 4.13 and 4.17.

4.4. GENERATION OF FRAGILITY CURVES FOR OUT-OF-PLANE BEHAVIOUR

After obtaining the demand and the capacity (in terms of limit states LS-I and LS-II) for out-of-plane action, the fragility curves can be generated by considering the same formulation that has been used for in-plane fragility generation (Equation 3.13) with slight modifications. For out-of-plane action, the response parameter is considered as out-of-plane moment instead of shear force, which has been used for in-plane action.

$$P(LS_i / PGA) = 1 - \Phi\left[\frac{\ln(M_{LS,i}) - \ln(M_D)}{\sqrt{\beta_C^2 + \beta_D^2 + \beta_M^2}}\right] \tag{4.18}$$

In the proposed equation, $P(LS_i / PGA)$ corresponds to the probability of exceeding the i^{th} limit state for a given PGA level. Symbol Φ stands for the standard normal cumulative distribution function. Parameter $M_{LS,i}$ represents the median moment capacity at the i^{th} limit state (obtained at the onset of cracking or at the ultimate stage when the out-of-plane failure of the masonry wall panel is about to occur) whereas

parameter M_D is the median moment demand. The terms in the denominator stand for the uncertainties involved in the generation of fragility curves. Among these, β_C stands for the uncertainty in capacity, obtained from the standard deviation of the statistical distribution for each limit state. Parameter β_D is the uncertainty related with demand and it is obtained from Equation 3.12. The last uncertainty term, β_M, associated with analytical modeling, is assumed to be 0.3 throughout the study as it is proposed in Wen et al (2004).

In order to attain the statistical variation of demand and capacity for masonry walls, some of the parameters are considered as random variables. These parameters are height of the masonry wall (h), gravity load acting on the masonry wall (N), compressive strength of masonry wall material (f_m) and unit weight of masonry wall material (γ_m). The statistical variation of wall height is obtained by considering the related information in the existing building databases. Accordingly, mean values and coefficient of variation (COV) are presented in Table 4.1 in terms of masonry unit type. The variability of unit weight of each material, which is also listed in Table 4.1, has been obtained by expert judgment.

Table 4. 1. Statistical descriptors of wall height and thickness as random variables

Masonry Unit Type	Wall Height (m)		Unit Weight (kN/m^3)	
	μ	COV	μ	COV
Solid Brick	2.70	0.20	16.0	0.25
Hollow Brick	2.65	0.20	14.0	0.25
Cellular Concrete Block	2.65	0.20	14.0	0.25
Stone	2.60	0.20	20.0	0.30
Adobe	2.50	0.20	12.0	0.30

The vertical load acting on the wall panel per meter, N, is calculated by considering the requirements of TEC-07. Statistical variation of N is described by the mean value (μ), which is taken as 40 kN/m for the uppermost story of a typical masonry building (since this is the critical story for out-of-plane behavior) and COV for this case is considered as 0.4. For other stories of the same building, these values eventually vary since the overburden on the top of walls changes from story to story. The variability in material strength (f_m) was already considered in Section 3.4 for different masonry unit types. The same values are employed also for out-of-plane action.

The following example illustrates how the fragility curves for out-of-plane behavior are generated. Consider a typical three story masonry building made of hollow clay brick units, which is vulnerable to out-of-plane action (poor wall-to-wall or wall-to-floor connections, high slenderness ration of walls, poor material quality, etc.). Fragility curve sets are to be generated for two cases: presence of rigid RC slab (nearly fixed boundary conditions) or presence of wooden flexible floors (nearly hinged boundary conditions). Figure 4.11.a-b shows demand statistics for these two cases in terms of the out-of-plane moment acting on the most critical face-loaded wall in the first, second and third stories, respectively. Symbols represent the scatter in demand in terms of maximum moment experienced during each ground motion record listed in Table 3.4. Lines denote the best fit to the scatter data for each story. According to the figures, moment demand increases with increasing story number, i.e. it is maximum at the uppermost story of the building as expected. It is also observed that moment demand is more pronounced for hinged type of connection when compared to fixed type for all stories. The limit state values for these two cases are given in Table 4.2 in terms of out-of-plane moment capacity. The figures indicate that the out-of-plane moment capacity is independent of the type of wall-to-floor connection. This can be clearly seen by looking at Equations 4.13 and 4.16, which are functions of axial load, thickness and material strength only. In addition to this, the moment capacity seems to decrease as the story number increases, an opposite trend when compared to seismic demand on the face loaded masonry walls.

Table 4. 2. Out-of-plane moment capacity in terms of story number and wall-to-floor connection type

	Out-of-Plane Moment Capacity for Fixed Wall-to-Floor Connection		Out-of-Plane Moment Capacity for Hinged Wall-to-Floor Connection	
	LS-I (kNm/m)	LS-II (kNm/m)	LS-I (kNm/m)	LS-II (kNm/m)
First Story	8.728	17.890	8.728	17.890
Second Story	5.819	13.123	5.819	13.123
Third Story	2.909	7.160	2.909	7.160

By considering demand and capacity parameters together in Equation 4.18, fragility curves are generated for LS-I and LS-II and for different stories. Figure 4.11 and 4.12 present the fragility curves for fixed and hinged connections separately. From the figures it is clear that the seismic vulnerability in the out-of-plane direction is critical for the upper-most stories of masonry buildings as observed in damage surveys after major earthquakes. As it seen from Figure 4.12 b, for a hazard level of 0.6g, the probability of out-of-plane failure in the first story walls of a three story masonry building with RC floor slabs is nearly zero (only 1%) whereas this probability increases to 66% in the uppermost story walls. Out-of-plane vulnerability seems to increase further in the presence of wooden floors, Figure 4.13 b, for which the out-of-plane failure probability has been calculated as 87%.

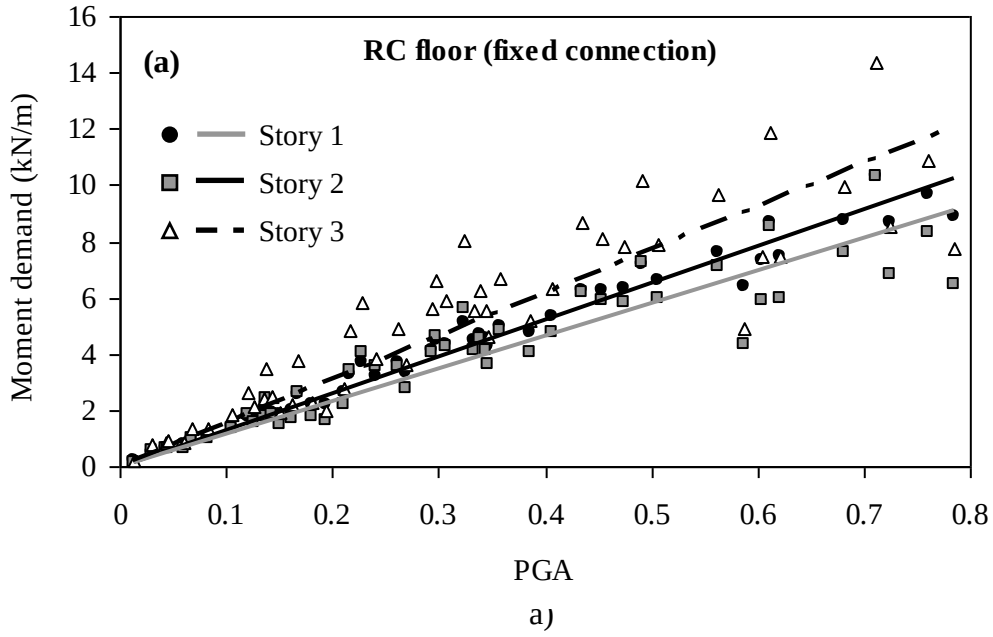

a)

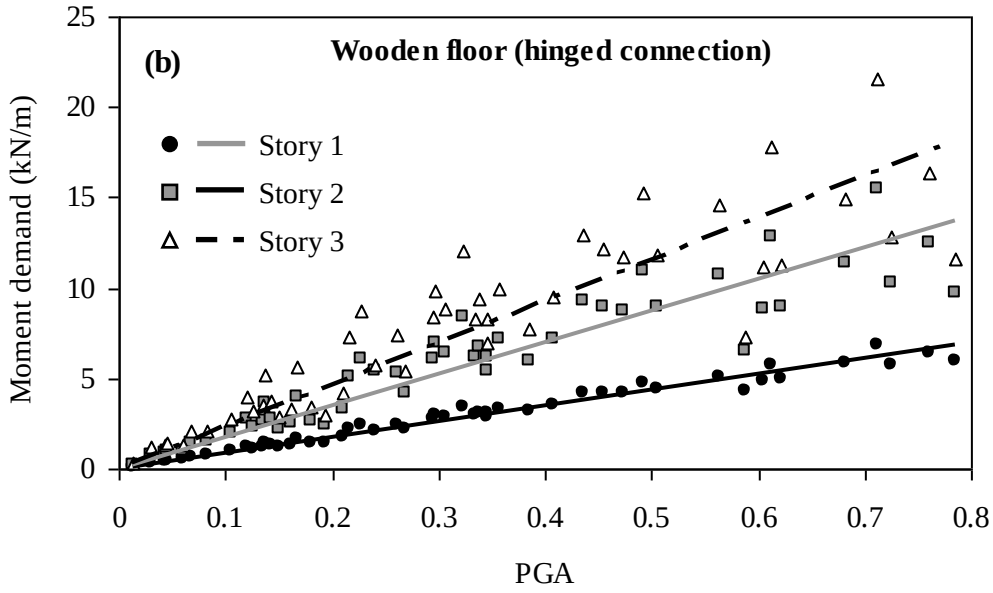

b)

Figure 4. 11. Relationship between out-of-plane moment and PGA in different stories of a typical masonry building, which has a) fixed, b) hinged, wall-to-floor connections

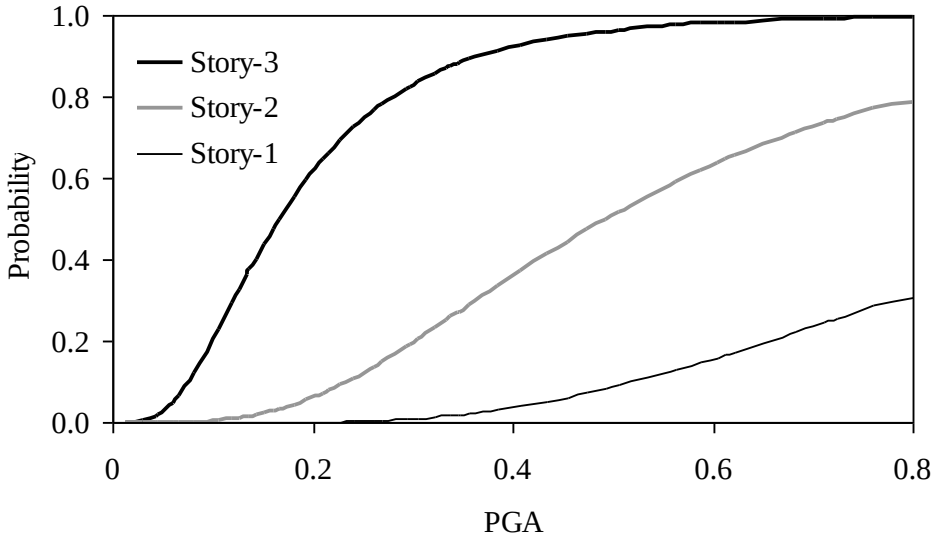

a)

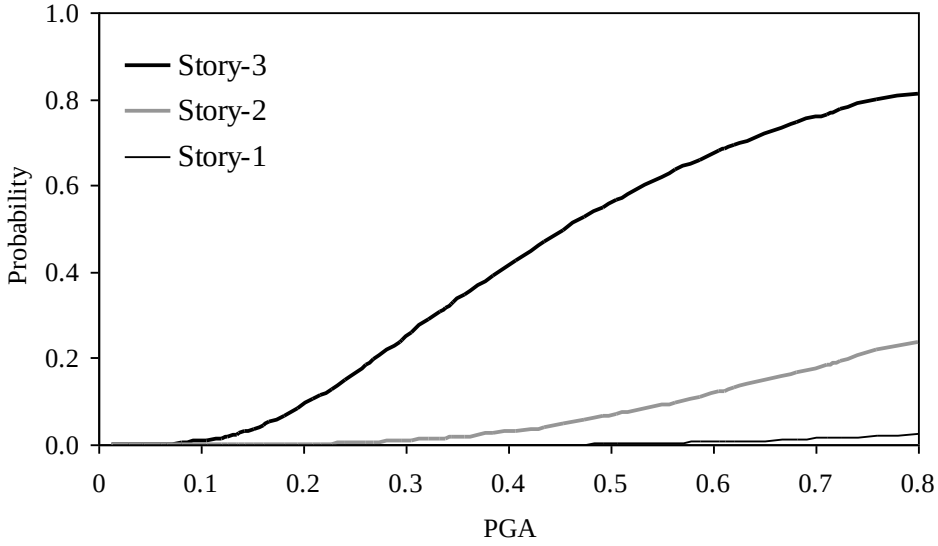

b)

Figure 4. 12. Fragility curves for a typical three story unreinforced masonry building with RC floor slab (fixed wall-to-floor connection) according to the story number where the critical face-loaded wall is located and for a) LS-I, b) LS-II

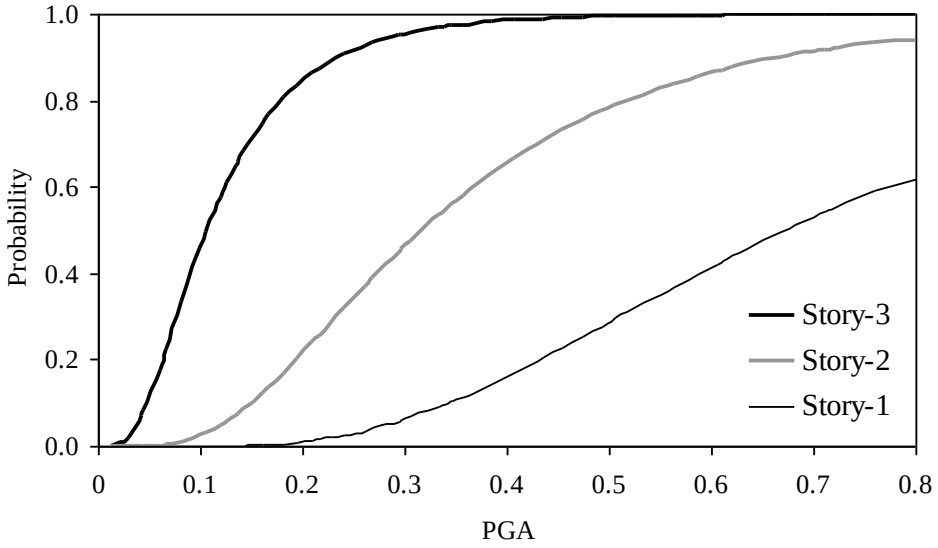

a)

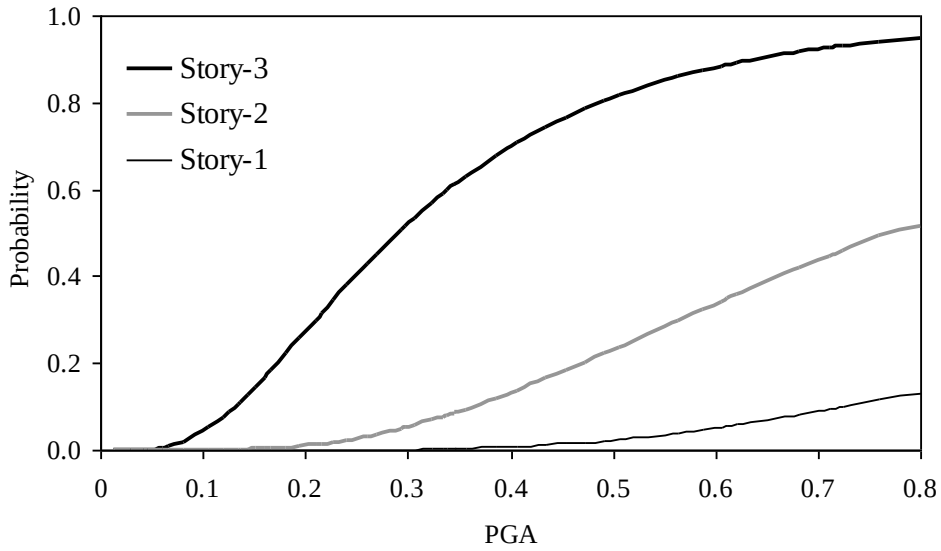

b)

Figure 4. 13. Fragility curves for a typical three story unreinforced masonry building with wooden floor slab (hinged wall-to-floor connection) according to the story number where the critical face-loaded wall is located and for a) LS-I, b) LS-II

It has been observed that wall-to-floor connections in some of the unreinforced masonry buildings in Turkey is so poor that the walls act like cantilevers during out-of-plane action. This is generally true for rural non-engineered masonry dwellings. In such cases the most critical wall can be assumed to behave like a cantilever component in out-of-plane action during earthquake. This is illustrated in Figure 4.14, which shows the comparison of probabilities of out-of-plane failure for the most critical walls of two cases above and a single story masonry building for which there exist no wall-to-floor connection practically so that the walls are assumed to act like cantilevers. The fragility curves reveal that the cantilever-like walls in single story building are more vulnerable than uppermost story walls in three story buildings with either RC or wooden floor slabs in terms of out-of-plane action. Out-of-plane failure in single story masonry building seems to definitely occur at a hazard level of 0.45g whereas the probability of failure at the same intensity is 50% for three story masonry building with RC floor slabs and 77% for three story masonry building with wooden floor slabs.

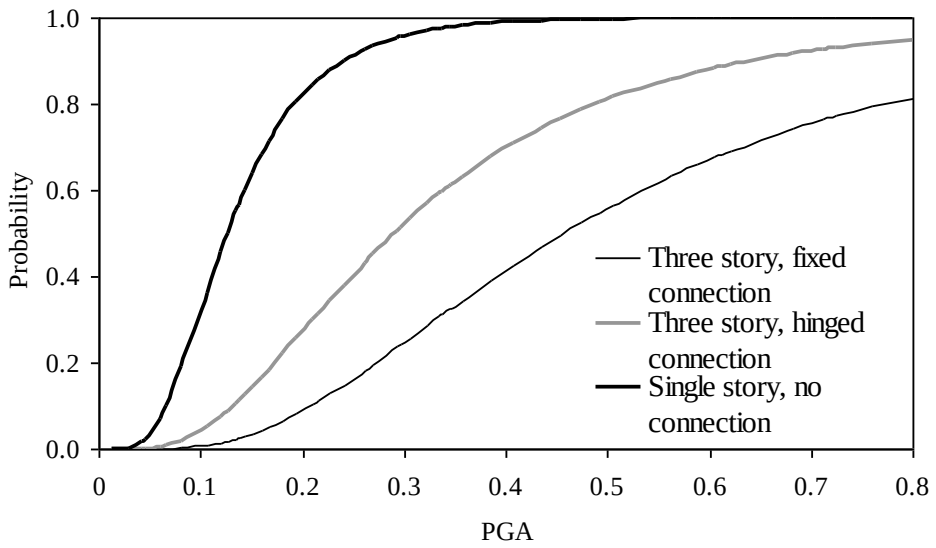

Figure 4. 14. Fragility curves for the ultimate limit state of the critical walls of three case study masonry buildings: single story, no wall-to-floor connection; three story, hinged wall-to-floor connection and three story, fixed wall-to-floor connection.

Overall, all these trends seem to physically match with general structural considerations in terms of out-of-plane behavior. The validity of the fragility curves is discussed in the next section by comparing the generated curves with the actual field data.

4.5. VERIFICATION OF FRAGILITY CURVES FOR OUT-OF-PLANE BEHAVIOUR

Due to lack of data, it is not an easy task to validate out-of-plane vulnerability of masonry structures by considering observed damage statistics. Even though there exits some data, it is not easy to decide whether structural damage has been caused by out-of-plane or in-plane deficiencies of building structures since the data has not been collected intentionally by taking these specific cases into account. Hence only a crude comparison can be made in order to show that the estimated and the observed numbers have the same order of magnitude.

In this study, the 2010 Elazığ (Turkey) earthquake and the rural masonry buildings that were affected in the earthquake region were selected for validation. There are some reasons of selecting this event as the case study. First, two different teams from Middle East Technical University Earthquake Engineering Research Center (METU-EERC) went to the affected region just after the earthquake and had the chance to observe the actual damage (Bakır et al. 2010, Askan et al. 2010). Second, the teams observed that due to typical deficiencies of rural masonry construction in the region, out-of-plane damage prevailed in-plane damage in most of the cases (Figure 4.15).

A moderate earthquake (M_L=5.8) occurred in eastern part of Anatolia on March 8, 2010, with a focal depth of 5 km. It was named as “Elazığ Earthquake” since the epicenter of the earthquake was located in this province. The earthquake mostly affected the rural areas and killed 42 people while 137 was injured (Yılmaz and Uran 2010). The earthquake caused major structural damage in few villages (Okçular,

Göçmezler, Kayalık, Yukarı Kanatlı, Yukarı Demirci and Tabanözü). All the fatalities were reported in these villages due to the collapse of rural non-engineered masonry buildings. According to Governorship of Elazığ (2010), among 8723 dwellings that were affected from the earthquake, 3005 (34%) of them were heavily damaged or collapsed, 1643 (19%) of them were moderately damaged and 4075 (47%) were slightly damaged or experienced no damage at all.

The building stock in the affected region is composed of one or two story masonry buildings that have been constructed by using adobe or rubble stone units. The floor-to-wall and wall-to-wall connections are generally so poor that the load-bearing walls can not act together (Figure 4.16). In other words, it is not possible to maintain box-like behavior during seismic action. Some dwellings in the region have heavy earthen toppings. Probably the deaths were caused by out-of-plane failure of the load bearing walls first and then by collapse of these heavy roofs into the building so that no one could escape out. This has been verified by officials and local residents who reported that most of the deaths were caused by either chocking under soil or due to falling stones (Askan et al 2010, Yılmaz and Uran 2010). Due to economical reasons and construction practice in the region, mud mortar is being used as a bonding agent in load bearing walls. Hence both in-plane and out-of-plane resistance of such walls is very low, leading to a highly vulnerable structure under seismic action. That is why such a moderate earthquake caused extensive damage and a considerable number of physical and economical losses.

Figure 4. 15. Examples of masonry dwellings damaged during the 2010 Elazığ earthquake with out-of-plane failure of exterior walls (photos taken by the METU-EERC team)

Figure 4. 16. Poor wall-to-wall and floor-to-wall connections leading to out-of-plane type of damage during the 2010 Elazığ earthquake (photo taken by the METU-EERC team)

The most adversely affected village during the earthquake was Okçular. In this village, 19 people died and out of 175 dwellings, 148 (~85%) either collapsed or experienced heavy damage (Figure 4.17). At the time of the main shock, 30 unoccupied dwellings collapsed completely, which most probably avoided more deaths and injuries (Askan et al 2010).

Figure 4. 17. An overview of Okçular village (photo taken by METU-EERC team)

Verification study is focused on Okçular, since this is the most adversely affected village during the earthquake and the METU-EERC teams spent a considerable amount of time in this earthquake affected region, examining 70 damaged buildings. The distribution of the inspected buildings according to type is as follows: 14 one-story adobe masonry (20%), 8 two-story adobe masonry (11%), 25 one-story stone masonry (36%), 11 two-story stone masonry (16%), 3 one-story brick masonry (4%), 4 two-story brick masonry (6%) and 5 reinforced concrete frame building (7%). Since 40% (70 out of 175 buildings) of the existing building stock in Okçular village has been examined on site, it seems reasonable to estimate the building inventory before earthquake by extrapolating the number of observed buildings to the number of existing buildings. After extrapolation, a total of 175 existing buildings in Okçular village are listed as follows: 35 one-story adobe masonry buildings, 20 two-story adobe masonry buildings, 63 one-story stone masonry buildings, 27 two-story stone

masonry buildings, 7 one-story brick masonry buildings, 10 two-story brick masonry buildings and 13 reinforced concrete frame buildings.

The observations in the village revealed that the common type of construction (56% of the total building stock) is single story dwellings made of adobe or rubble stone as the load-bearing wall material. The quality of material is very poor and generally mud mortar has been used in construction. In most cases, heavy earthen roofs have been utilized. The wall-to-roof connections are so poor that most of the walls have acted as if they were cantilever walls during the ground shaking and experienced collapse in the out-of-plane direction (Figures 4.15 and 4.16). Taking all these observations into consideration, the fragility curves for out-of-plane behavior are generated for one-story adobe and stone masonry buildings as seen in Figure 4.18. The corresponding fragility curves for in-plane behavior are also placed in the figures for the sake of comparison. In the figures OP stands for out-of-plane whereas IP stands for in-plane. In addition, LS1 represents the first (serviceability) limit state whereas LS2 represents the second (ultimate) limit state. Looking at the figures it can be stated that out-of-plane behavior governs for these two building types, which is a consistent trend when compared to field observations.

Observations in the field indicated that in most of the two-story adobe and stone masonry dwellings, the roof system has been upgraded and instead of earthen topping, light metal sheets which are supported by wooden girder and columns have been used (Figure 4.19). When compared to the poor wall-to-roof connection of one-story buildings in the region, this is an enhanced system where the walls can be assumed to be supported by joints at the top and bottom ends. But this roof system has still problems and it is vulnerable to out-of plane action under seismic loading.

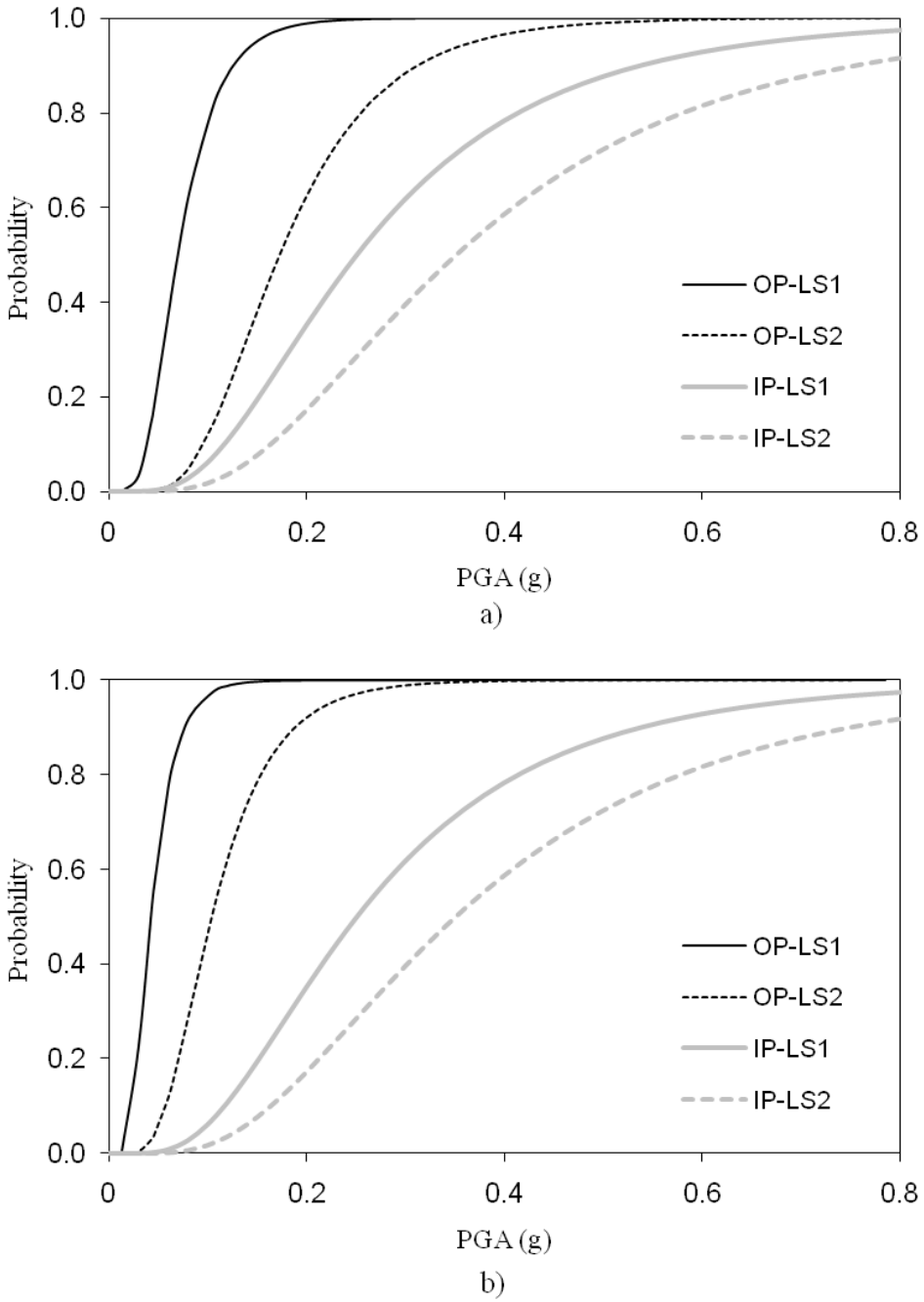

Figure 4. 18. Out-of-plane and in-plane fragility curves for a) one-story adobe masonry buildings, b) one-story stone masonry buildings

a)

b)

Figure 4. 19. a) Two story stone masonry building with roof made of metal sheets, b) roof system with wooden logs as girders and columns (photos taken by METU-EERC team).

Figure 4.20 presents the out-of-plane (for the second story) and in-plane fragility curves for two-story adobe and stone masonry buildings. In adobe masonry buildings, for the serviceability limit state, out-of-plane behavior seems to govern significantly, but for the ultimate limit state, the curves for out-of-plane and in-plane fragility seem to be nearly coincident. This shows that the probability of experiencing an out-of plane wall failure in the second floor due to amplified floor acceleration, reduced axial load on the wall and deficiencies in the wall-to-floor connection is nearly the same with the probability of experiencing an in-plane shear failure at the ground story walls due to very low strength of adobe units with respect to the density of the material. In stone masonry buildings, out-of-plane behavior seems to govern for both limit states since the in-plane strength of stone is more than that of adobe. Another reason is that mud mortar is washed out from the joints of walls made of irregular rubble stone due to weather conditions in time, leading to unstable walls with dry joints which are highly vulnerable to seismic action.

In one- or two-story brick masonry buildings, generally hollow factory brick units have been used. The floors are rigid reinforced concrete slabs often with horizontal lintel beams at the top of the walls. This enables the most effective wall-to-floor connection among the masonry buildings in the affected region. Due to good connection details and rigid diaphragms, these buildings are more vulnerable to in-plane shear rather than out-of-plane deformations as observed in the affected region (Figure 4.21). The same trend is also seen in the fragility curves for one- and two-story brick masonry buildings (Figure 4.22). For both limit states, in-plane behavior seems to govern, especially for the ultimate limit state.

Overall, the fragility curves yield consistent trends when compared with site observations for the building types in the affected region.

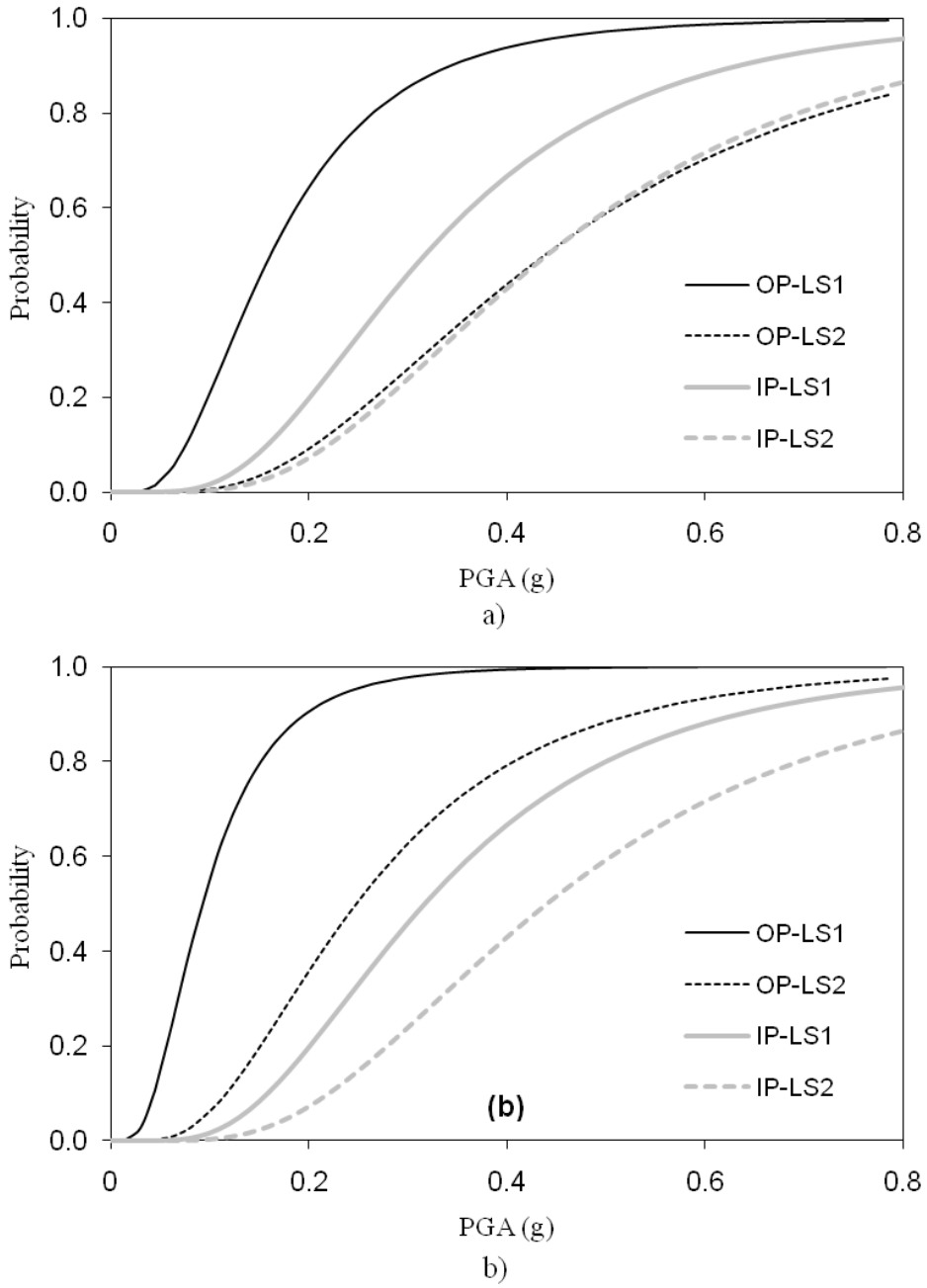

Figure 4. 20. Out-of-plane (for the second story) and in-plane fragility curves for a) two-story adobe masonry buildings, b) two-story stone masonry buildings

Figure 4. 21. Damaged brick masonry buildings in Okçular village with typical in-plane shear cracks (photos taken by METU-EERC team).

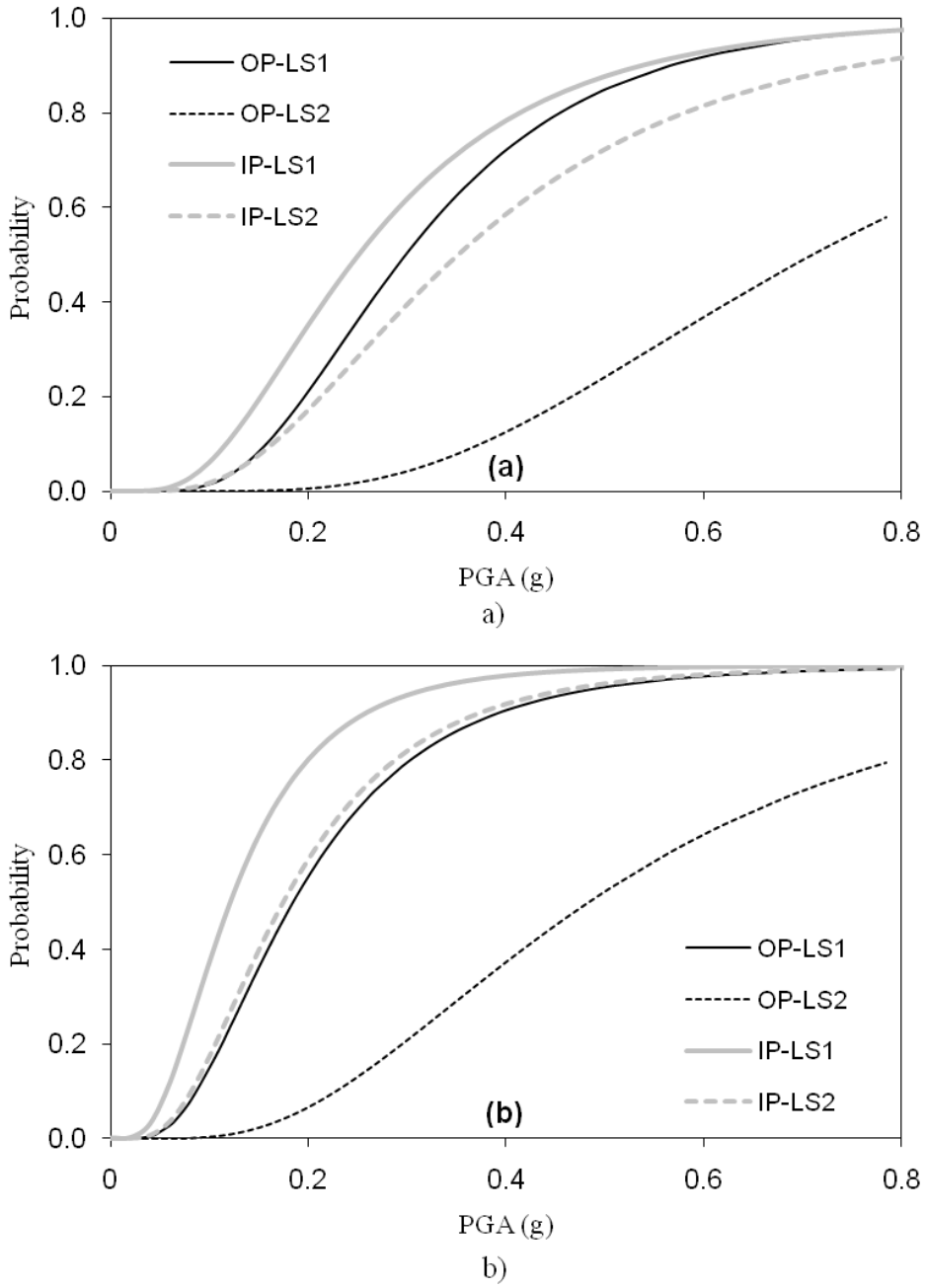

Figure 4. 22. Out-of-plane and in-plane fragility curves for a) one-story brick masonry buildings, b) two-story brick masonry buildings

After obtaining the building inventory and the fragility information, the next step is to determine the seismic hazard intensity in the region. In other words on-site values of PGA should be determined in order to calculate damage state probabilities of all structural types in Okçular village. This can be achieved by utilizing empirical attenuation relationships.

In a recent study, several ground motion prediction equations (GMPEs) are utilized in order to simulate the variation of ground motion characteristics with distance for the 2010 Elazığ earthquake (Akkar et al, 2010). Selected GMPEs for the study belong to Kalkan and Gülkan (2004) [KG04], Boore and Atkinson (2008) [BA08], and Akkar and Cagnan (2010) [AC10], Grazier and Kalkan (2007) [GK07], Campbell and Bozorgnia (2008) [CB08], and Chiou and Youngs (2008) [CY08]. The predictions are plotted in Figure 4.23 together with the recorded values at nearby stations during the earthquake. The bar chart in Figure 4.23 shows the standard error of predictions for each GMPE. Predictions of BA08 and CY08 seem to the best ones that represent the attenuation of ground motion parameters for the 2010 Elazığ earthquake. Hence the distance of case study region, i.e. the Okçular village, from the seismic source is calculated in accordance with distance definitions used in GMPEs. The average of the predicted values for BA08 and CY08 is assumed as the on-site PGA value for the Okçular village, which is 0.39g. It is interesting to observe that most of the GMPEs overestimate the actual PGA recorded at stations. This is due to two reasons. First, since the 2010 Elazığ earthquake was a shallow one with a depth of 5 km, it affected a limited area and the earthquake waves attenuated very rapidly. Therefore, ground motion data shows faster attenuation at far distances (Zor et al., 2007). Second, the GMPEs have been developed by considering Turkish ground motion databases that include records mostly from western and northern Anatolia earthquakes. So the tectonic characteristics of the eastern Anatolian region are not fully reflected by the available GMPEs due to lack of data.

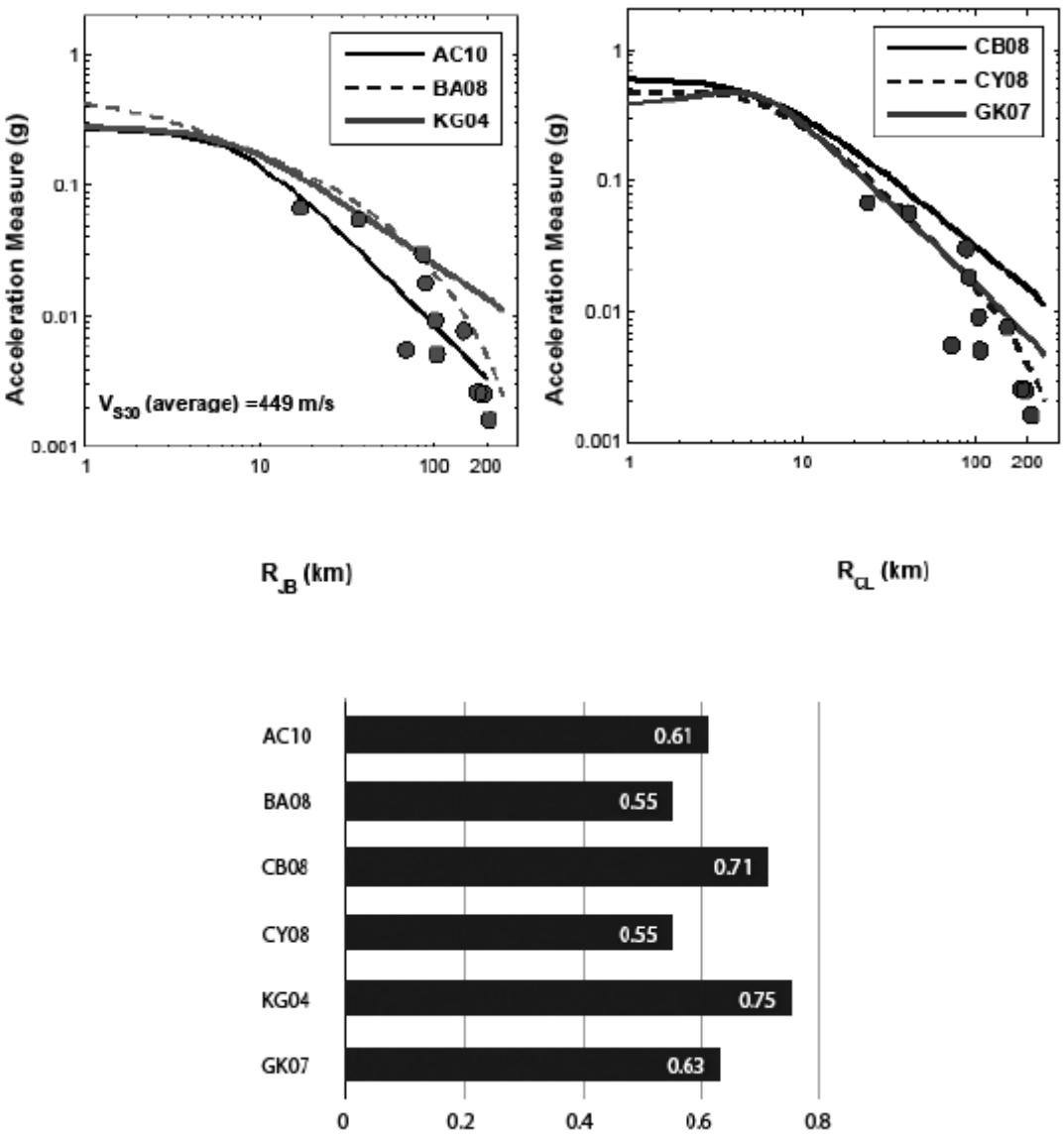

Figure 4. 23. Comparison of PGA values recorded from the main shock with different GMPEs together with standard error of predictions computed for each GMPE (taken from Akkar et al 2010)

The final step in verification is to use predicted on-site PGA value (0.39g) in order to compute damage state probabilities by using the fragility curves shown in Figures 4.18, 4.20 and 4.22 for different types of masonry buildings. The values are

presented in Table 4.3 together with the governing type of behavior for the masonry building types under consideration. All of the RC frame buildings are assumed to have experienced none-to-light damage during the earthquake, which is consistent with field observations in Okçular village.

Table 4. 3. Estimated damage state probabilities for the building types in Okçular village

Building Typology	No. of Buildings	Governing Behaviour	Damage State Probability		
			None or Light	Moderate	Heavy or Collapse
One-Story Adobe Masonry	35	Out-of-Plane	0.00	0.03	0.97
Two-Story Adobe Masonry	20	Out-of-Plane + In-Plane	0.06	0.49	0.45
One-Story Stone Masonry	63	Out-of-Plane	0.00	0.00	1.00
Two-Story Stone Masonry	27	Out-of-Plane	0.01	0.19	0.80
One-Story Brick Masonry	7	In-Plane	0.22	0.20	0.58
Two-Story Brick Masonry	10	In-Plane	0.02	0.06	0.92
RC frame	13	N/A	1.00	0.00	0.00

In order to compare the estimated overall damage with the observed one, combined fragility information is obtained by using the formulation proposed by Shinozuka et al (2000). Combined fragility is obtained from

$$F_c = \sum_{i=1}^{M} P_i F_i \tag{4.19}$$

where

$$P_i = \frac{N_i}{N_t} \tag{4.20}$$

and

$$N_t = \sum_{i=1}^{M} N_i \tag{4.21}$$

In Equations 4.19, 4.20 and 4.21, F_c stands for the combined fragility, F_i represents the fragility curve for the i^{th} structural type and P_i shows the probability with which i^{th} structural type is chosen at random from the combined population of buildings. N_t is the total number of buildings with N_i being the number of buildings for the i^{th} structural type.

Using Equations 4.19, 4.20 and 4.21, a single and combined fragility curve can be obtained that represents the complete population of buildings in Okçular village with all structural types. Then for the on-site PGA value of 0.39g, damage state probabilities for the whole building stock are obtained. Then these numbers are compared with the actual ones observed from field observations. As seen in Figure 4.24, the estimated and observed values are pretty close to each other. This means the proposed fragility functions can estimate the actual damage distribution in Okçular village with a reasonable degree of accuracy.

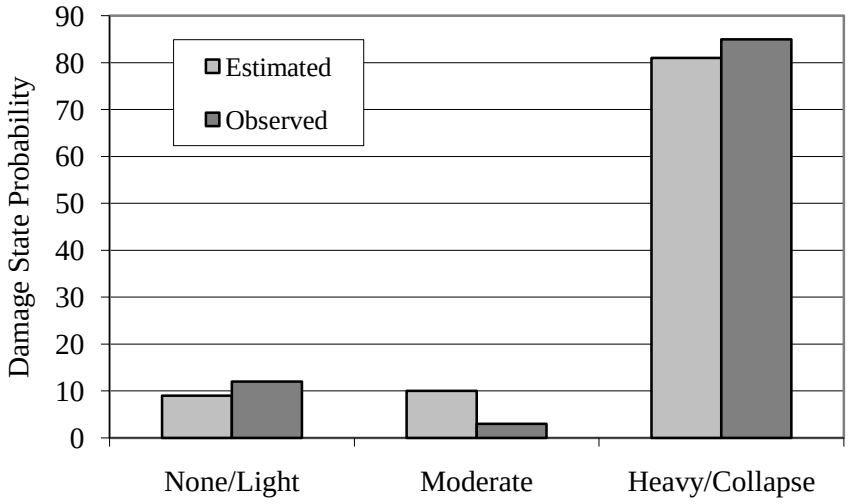

Figure 4. 24. Comparison of damage state probabilities obtained from generated fragility curves with the ones obtained from field observations for Okçular village during the 2010 Elazığ earthquake.

CHAPTER 5

SEISMIC SAFETY EVALUATION OF EXISTING UNREINFORCED MASONRY BUILDINGS IN FATIH: A CASE STUDY

5.1. GENERAL

The efficiency of the mitigation efforts and post-disaster decision making process depends on the accuracy of the estimation of the expected damage and the associated loss in earthquake prone regions. Hence evaluation of seismic safety of existing masonry buildings is the most important part of this study. As stated by Erberik (2008), taking into consideration the estimated damage as a measure of seismic vulnerability is a reasonable way for the determination of the assessment of seismic performance of different masonry building types. Up to this chapter, the seismic performance of masonry buildings in Turkey is reflected in the form of fragility curves by considering not only in-plane failure modes but also, unlike other studies, out-of-plane failure modes. Finally, the last chapter of this study is devoted to efforts for the embedment of the generated fragility information into seismic safety evaluation studies in Fatih sub-province, a highly populated earthquake–prone district in Istanbul. In the first part of this chapter, seismic safety evaluation will be performed without considering out-of-plane behavior since the relevant data is missing and has not been collected during sidewalk survey in Fatih sub-province. In the second part of the chapter, by conservatively assuming that all the buildings are vulnerable to out-of-plane action (i.e. poor wall-to-wall and wall-to-floor

connections, presence of long and slender walls, etc.), the seismic safety of the same building stock is re-evaluated and the results are compared.

5.2. SEISMIC SAFETY EVALUATION OF UNREINFORCED MASONRY BUILDINGS IN FATIH BY CONSIDERING ONLY IN-PLANE ACTION

Shortly after the devastating Kocaeli and Düzce earthquakes in 1999, Japan International Cooperation Agency (JICA) conducted a detailed earthquake loss estimation study together with the Istanbul Metropolitan Municipality (IMM) and released a report in 2002 (JICA & IMM 2002). This study was based on a scenario earthquake on the western section of the North Anatolian Fault with a magnitude M=7.5. They attempted to simulate the historical earthquake that occurred in 1766 in Istanbul. The most striking outcome of JICA study was the fact that the estimated earthquake losses in Istanbul after a devastating scenario earthquake are unacceptably high. This serious issue motivated IMM to kick off an "Earthquake Master Plan for Istanbul (EMPI)" in 2003 in order to find sustainable solutions for the complex problem of risk mitigation and planning. In EMPI, multi-level strategies have been developed in order to prevent or mitigate seismic risk, prepare emergency rescue and restoration plans for the earthquake prone areas identified in accordance with the risk priorities determined by the JICA study (Erberik 2010).

Fatih sub-province in Istanbul, which is the subject of the case study of thesis, is inspected within the scope of the EMPI. In order to evaluate the seismic safety of existing buildings and to develop strengthening strategies for those which seem to be risky comparatively, masonry buildings in Fatih are examined separately with a two staged procedure which was calibrated in the Zeytinburnu sub-province of Istanbul since it is selected as the pilot study region. While the vulnerability of the masonry buildings are investigated in the first stage, the buildings accepted as seismically

vulnerable are analyzed by using a more detailed procedure in the second stage which is beyond the scope of this study.

The evaluation procedure starts with sidewalk survey of the masonry buildings in Fatih which means that, without entering inside the building, the masonry structures are examined by considering some major structural parameters. The Damage Evaluation Form that is used to gather the information of the buildings by the observers is given in Appendix B. As it is seen from the form; the sidewalk survey starts with taking into consideration the plan geometry of the building. Although some specific geometrical patterns have been proposed such as rectangular, trapezoidal (with non-parallel axes) or L-shaped, it is also possible to draw the plan geometry if it is not defined in the form. Then there exists a section related to the identification of the investigated masonry building. This part generally contains the address information of the building. In order to describe the buildings' geographical position correctly, its geographical coordinates are required to define according to Global Positioning System. The next section in the form is about general description of the building. The section starts with the questions regarding the number of stories and whether there is basement in the building. Next, load bearing wall material type is identified according to the defined materials in the form by the observer. After the length of the plan of the buildings and the openings in the walls are estimated by rule of thumb, the distribution of the openings in vertical alignment is also investigated by only just looking at the building. The buildings are classified as "regular", "semi-regular" and "irregular" in terms of vertical alignment of their openings. Simple illustrations of regular and irregular classes and example photos of buildings from Fatih database are given in Figure 5.1. This parameter is important since it affects the stress path of the building while transferring the seismic forces in the building safely to the foundation and back to the ground.

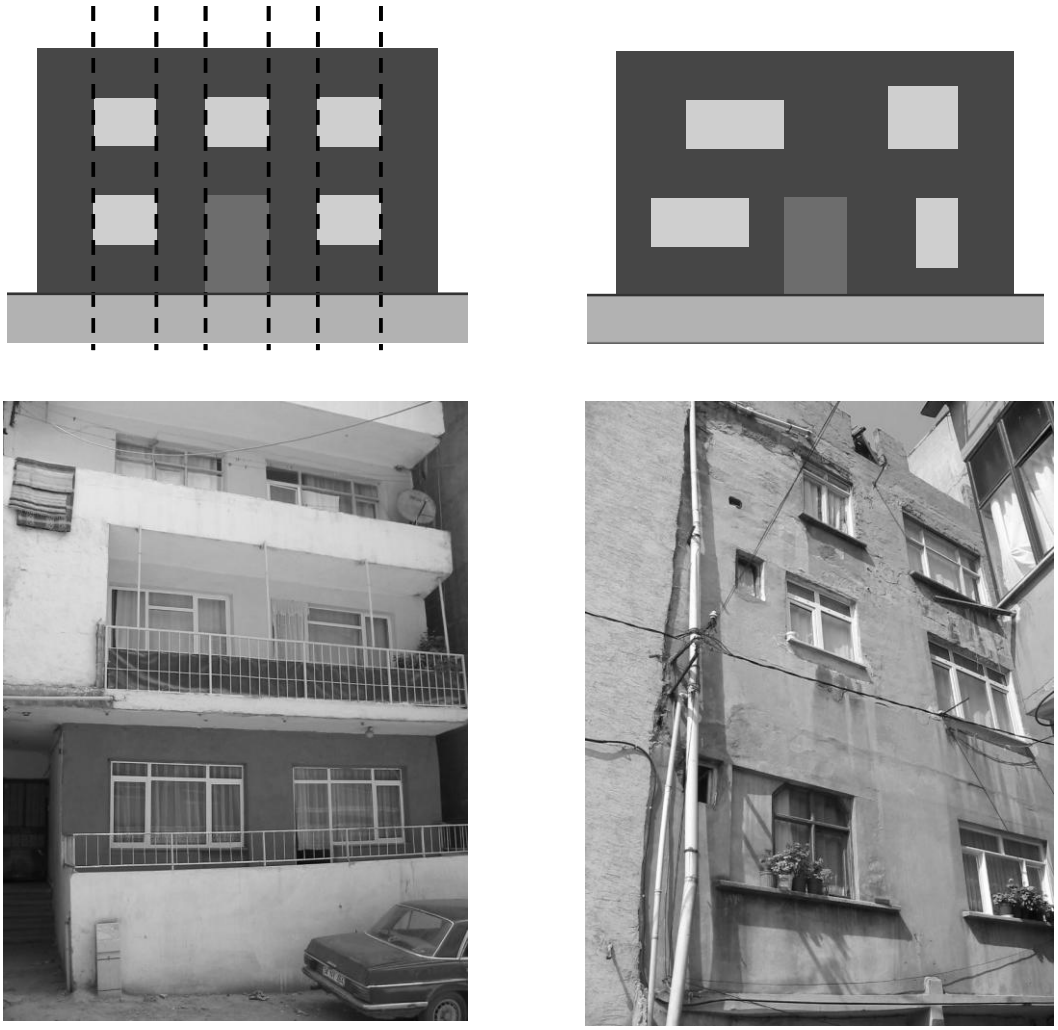

Figure 5. 1. Classification of masonry buildings according to vertical alignment of openings: a) regular, b) irregular

Another structural parameter to be determined is the floor type of the building, i.e. reinforced concrete or timber, if it is possible to obtain this valuable information without entering the building. Next parameter is the statue of the structure, i.e. separate or adjacent (in the middle or at the corner). These cases are illustrated in Figure 5.2. The worst case is being adjacent and at the corner of the building aggregate since such buildings has been observed to experience severe damage in past earthquakes due to hammering and inertial effects of the adjacent building

block. Two related parameters for adjacent buildings that are also present in the form are whether the building height and floor levels are different or not in adjacent buildings. If the building heights and/or floor levels are different for adjacent buildings, then hammering effect becomes detrimental due to specific dynamic characteristics of these interacting buildings. Some local damages at the impact regions can be encountered which may endanger the safety of the building (see Figure 5.3). Photos of example buildings from Fatih database with different statue are shown in Figure 5.4. Furthermore, Figure 5.5 presents a case where hammering effect can be serious since the floor levels and heights of adjacent buildings are different.

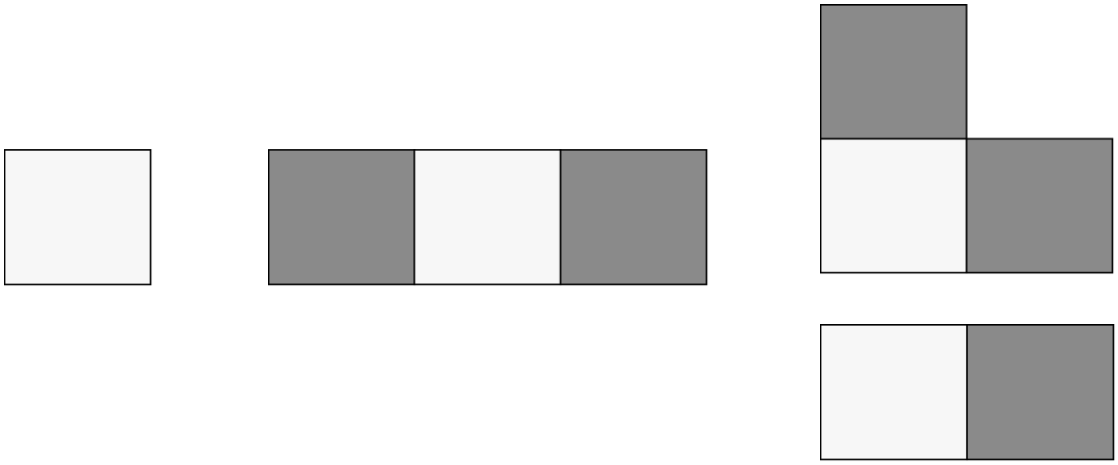

(a) (b) (c)

Figure 5. 2. Classification of buildings according to statue; a) separate, b) adjacent and in the middle, c) adjacent and at the corner

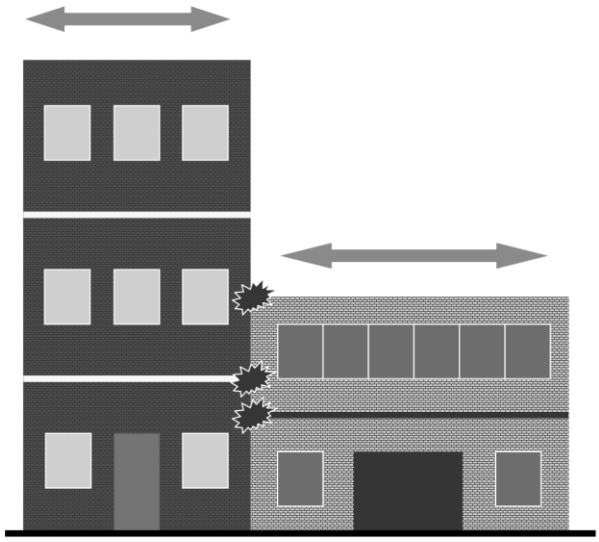

Figure 5. 3. Hammering effect for buildings with different heights and floor levels

(a)

(b) (c)

Figure 5. 4. Example buildings from Fatih database with a) separate, b) adjacent (in the middle), c) adjacent (at the corner) statue

Figure 5. 5. An example masonry building aggregate from Fatih database for which the floor levels of adjacent buildings have different elevations

The remaining parameters in this section of the form are roof type, slope of the ground that the building is located and apparent quality of the building. The last parameter is highly subjective and depends on the judgment of the person that investigates the building. Generally material quality, maintenance of the building during service life and age of the building are important parameters for the determination of apparent quality. For the sake of clarity, example photos of buildings which have been classified as “poor”, “moderate” or “good” in terms of apparent quality are presented in Figure 5.6.

In the final section of the form, function of the building is emphasized by considering whether it is residential or commercial. Since the information about masonry buildings in Fatih sub-province in terms of aforementioned structural parameters has been presented in Chapter 2, it will not be discussed here once more.

(a) (b)

(c)

Figure 5. 6. Example buildings from Fatih database with a) good, b) moderate, c) poor apparent quality

After completing the sidewalk survey of 9457 masonry buildings in Fatih sub-province and obtaining the aforementioned data from each building by filling the forms, the next stage is the identification of seismic hazard in the region. Seismic hazard identification is conducted by using a probabilistic approach (Erdik et al, 2006). The study region is divided into 250m x 250m grids, for each of which ground motion parameters to be used in the risk analysis is obtained through hazard analysis. Peak ground acceleration (PGA) of each grid, which is employed as the hazard parameter for masonry structures, are calculated for events with exceedance probabilities of 2%, 10% and 50% in 50 years. These correspond to events with return periods of 2475, 475 and 75 years, respectively. To be in line with the design criteria of the Turkish Earthquake Code (2007), the PGA values for the event with a return period of 475 years is used in the evaluation method which corresponds to 10% exceedance probability in 50 years. The distribution of PGA values obtained from an event with a return period of 475 years in Fatih sub-province is given for each grid in Figure 5.7.

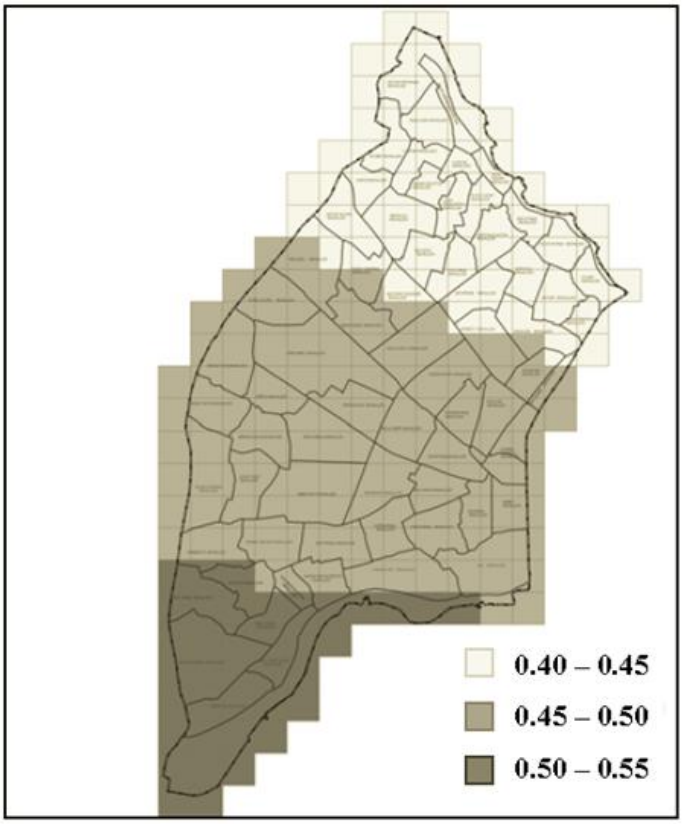

Figure 5. 7. Grid by grid distribution of PGA values in terms of gravitational acceleration (g) for an event with a return period of 475 years in Fatih sub province.

The final stage is to obtain the seismic vulnerability of masonry buildings and to rank them accordingly. In order to achieve this, a building class and a corresponding set of in-plane fragility curves are assigned to each building. Building classification is carried out by using the following structural parameters from sidewalk survey: number of stories (for N sub-classes), plan geometry (for R sub-classes), type of masonry material and apparent quality of the building (for D sub-classes), statue of the building and position of openings in vertical alignment (for W sub-classes). The definitions of these sub-classes were given in Chapter 3. Since a set of fragility curves was generated for each building class, the seismic vulnerability of each building in the database can now be defined in terms of a specific fragility curve set.

Typical buildings from Fatih database, their corresponding building classes and fragility curve sets are shown in Figure 5.8.a-c. For example, Figure 5.8.a presents a single story, regular masonry building with moderate quality hollow clay brick units as the masonry wall material that violates some of the structural requirements regarding adequate wall length and size and arrangement of openings in walls. The corresponding set of fragility curves is M1312, which is given in the same figure. Figure 5.8.b presents a two story, regular masonry building with moderate quality solid clay brick units as the masonry wall material that violates most of the structural requirements regarding adequate wall length and size and arrangement of openings in walls. The corresponding set of fragility curves is therefore M2213, which is given in the same figure. Finally, Figure 5.8.c shows a three story, irregular masonry building with poor quality cellular concrete blocks as the masonry wall material that violates some of the structural requirements regarding adequate wall length and size and arrangement of openings in walls. The fragility curve set assigned for this building is M3422, which is given in the same figure. It can be stated that damage state probabilities for a specific level of seismic intensity differ significantly for different classes of masonry buildings. In all figures, the first (serviceability) and the second (ultimate) limit states seem to be close to each other. This is in accordance with field observations that masonry buildings shift from light to severe damage rapidly with a narrow margin for moderate damage due to their inherent deficiencies regarding in-plane and out-of-plane capacities of load bearing walls.

The input for the fragility functions is the level of seismic hazard for each building in terms of PGA obtained from probabilistic seismic hazard analysis (Figure 5.7), and the output is the damage state probabilities. However a single valued function is required in order to rank these buildings with respect to their seismic vulnerability. This is achieved by using the vulnerability score (VS) that has been introduced in Section 3.8.

$$VS=\sum_{i=1}^{3} w_i P_i \qquad (5.1)$$

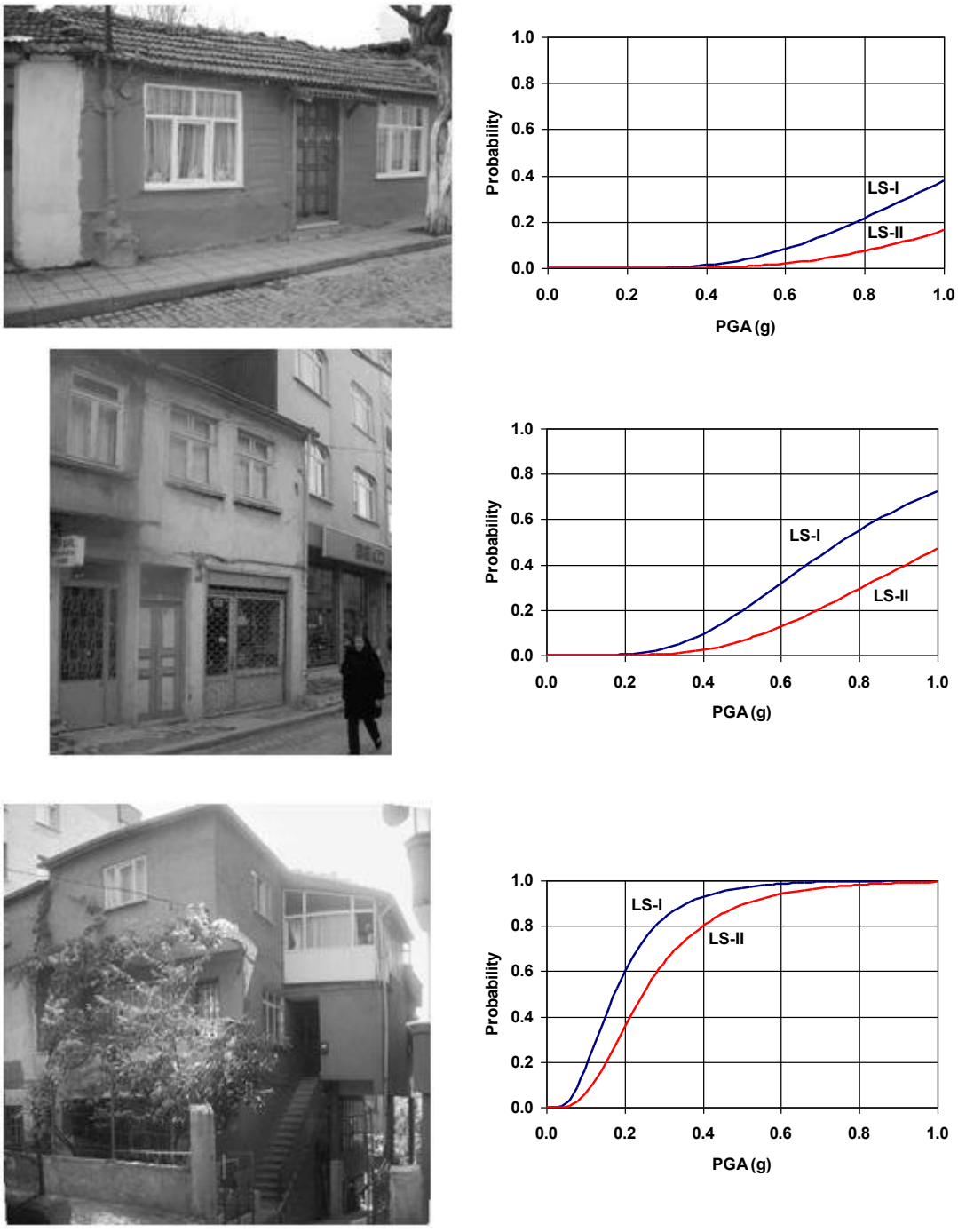

Figure 5. 8 Set of fragility curves for the building class a) M1312, b) M2213, c) M3422.

In Equation 5.1, vulnerability score, VS is computed by the summation of the multiplication of the damage state constants w_i with the damage state probabilities P_i for the assigned PGA values. The damage state constants for DS-I, DS-II and DS-III are assumed as 0.0, 0.5 and 1.0, respectively. Considering example buildings in Figure 5.8.a-c, for the given hazard level of 0.6g, the following VS have been obtained.

VS (for M1312) = 0.0 × 0.92 + 0.5 × 0.06 + 1.0 × 0.02 = 0.051

VS (for M2213) = 0.0 × 0.68 + 0.5 × 0.19 + 1.0 × 0.13 = 0.221

VS (for M3422) = 0.0 × 0.01+ 0.5 × 0.05 + 1.0 × 0.94 = 0.962

The results imply that M2213 is more vulnerable than M1312 but safer than M3422 in terms of seismic actions which is an expected conclusion under the light of our knowledge about our masonry models.

Accordingly, VS for each masonry building in Fatih is calculated. The results are shown in Table 5.1 in terms of the relationship between VS and the number of stories for masonry buildings in Fatih.

Table 5. 1**.** Relationship between VS and the number of stories for masonry buildings in Fatih (Sucuoğlu et al. 2006)

Vulnerabilty Score	**Number of Stories**					**Total**
	1	**2**	**3**	**4**	**5**	
0 ≤ VS < 0.1	907	395	5	0	0	**1307**
0.1 ≤ VS < 0.2	30	146	33	1	0	**210**
0.2 ≤ VS < 0.3	473	364	322	8	1	**1168**
0.3 ≤ VS < 0.4	681	304	295	39	1	**1320**
0.4 ≤ VS < 0.5	152	97	44	239	1	**533**
0.5 ≤ VS < 0.6	0	17	278	283	26	**604**
0.6 ≤ VS < 0.7	0	60	410	49	176	**695**
0.7 ≤ VS < 0.8	173	582	88	273	55	**1171**
0.8 ≤ VS < 0.9	30	231	231	268	169	**929**
0.9 ≤ VS ≤ 1.0	0	136	485	516	380	**1517**
Total	**2446**	**2332**	**2191**	**1676**	**809**	**9454**

It should be noted that the vulnerability score is between 0 and 1. It indicates that the higher VS, the more vulnerable building to seismic action under the given intensity of shaking. As Sucuoğlu et al.(2006) stated that depending on the parametric studies and expert opinions, the buildings which have VS greater than 0.7 is accepted as "High Risk" in terms of seismic safety so about 38% of the buildings in Fatih are decided to be analyzed in a more detailed manner in the second stage of the study. Examples of buildings from Fatih database with relatively high risk (VS >0.7) and relatively low risk (VS <0.7) are given in Figures 5.9 and 5.10.

Figure 5. 9. Examples of unreinforced masonry buildings in Fatih sub-province with relatively high seismic risk (VS>0.7) after vulnerability score assignment

Figure 5. 10. Examples of unreinforced masonry buildings in Fatih sub-province with relatively low seismic risk (VS<0.7) after vulnerability score assignment

5.3. SEISMIC SAFETY EVALUATION OF UNREINFORCED MASONRY BUILDINGS IN FATIH BY CONSIDERING BOTH IN-PLANE AND OUT-OF-PLANE ACTIONS

In the previous section, all the assessment is carried out by considering in-plane modes of behavior for masonry buildings. However out-of-plane vulnerability of unreinforced masonry buildings sometimes precedes in-plane vulnerability due to inherent structural deficiencies like poor wall-to-wall and wall-to-floor connections, poor material quality, presence of long and slender walls, etc. These types of deficiencies are frequently encountered for Turkish masonry buildings and they have caused heavy damage and collapse of the buildings in past earthquakes in Turkey. Therefore out-of-plane vulnerability should not be ignored during seismic safety evaluation of Turkish masonry buildings. However the problem is that the structural parameters required to classify out-of-plane behavior of masonry buildings have not been considered during the development stage of the evaluation form, so this information is missing for masonry building population in Fatih. But for the sake of comparison, it can be assumed that all the buildings are classified as vulnerable to out-of-plane action. This means they are all assumed to have poor connections, long

and slender wall within the building, etc. In fact, this is not true, and it is a very conservative assumption, but the assumption will be used only to see the effect of out-of-plane vulnerability in the overall ranking of buildings in terms of their seismic safety.

In order to take into account the effect of out-of-plane action in the generation of fragility curves, load bearing wall material type and floor type for each masonry building should be assigned in addition to masonry building classification. One of the information gathered from the sidewalk survey is the load bearing wall material type. In the form, it is offered that the load bearing wall material type can be “Adobe”, “Cellular Concrete Block”, “Hollow Brick”, “Solid Brick”, “Stone”, “Mixed Type” and “Unidentified”. Except the last two options, the proposed material types are parallel to our out-of-plane assessment procedure. For the last two options, “Mixed Type” and “Unidentified”, they are accepted as “Hollow Brick” not only to be on the safe side but also to be acquired in abundance and easily in an urban region. This assumption is also consistent since in the classification of masonry buildings in Fatih, the buildings with “Mixed Type” or “Unidentified” load bearing wall materials are assigned as D4 sub-class which can be described as poor quality hollow clay brick. Beside the identification of load bearing wall material type for each masonry buildings, floor type is also established from the information collected by the sidewalk survey. While reinforced concrete floors are accepted as “Good Connection”, timber floors are assumed as “Poor Connection” in terms of floor to wall connections. Moreover, some buildings, which have unidentified floor type, are evaluated as “Poor Connection”.

The VS calculation in Equation 5.1 is now changed into the form that:

$$VS=\sum_{i=1}^{5} w_i P_i \qquad (5.2)$$

The sequence of limit states can change, which affects the calculation of VS. This means the damage state constants can be changed for different cases. But there exist

a systematic way to assign the values for w_i. This is based on the following assumptions and rules:

- Out-of-plane limit state has been attained for a wall or a number of walls. Therefore it may or may not endanger the overall safety of the building. However in-plane limit states are attained for the most critical story (this means the ground story) of the building. If a building experiences significant damage in terms of the in-plane behavior of its load bearing walls, the out-of-plane behavior for that building is assumed to be irrelevant. Briefly if in-plane behavior governs, out-of-plane mode is not considered for that limit state.

- If in-plane behavior governs, damage state constants are increased by 0.50.

- If out-of-plane behavior governs, damage state constants are increased by 0.25.

All possible combinations and sequences of in-plane and out-of-plane modes are listed in Table 5.2, together with their damage state constants w_i. As an illustrative example, corresponding fragility curves of a two story regular masonry building with poor quality solid clay brick units with a reinforced concrete floor (M2323) is shown in Figure 5.11. As it is seen from the figure, it is expected that, in-plane serviceability limit state (IP-LS1) is firstly exceeded for any particular ground motion. Then, out-of-plane limit states, serviceability (OP-LS1) and ultimate (OP-LS2), governs the characteristics of the fragility curve. Finally, in-plane ultimate limit state (IP-LS2) is noticed at the bottom of the figure. Since there are four limit states in two sets of fragility curves, five damage state constants should be applied in the calculation of VS.

Table 5. 2. Damage state constants for the corresponding sequence of limit states

Sequence	w_1	w_2	w_3	w_4	w_5
(OP-LS1),(IP-LS1),(OP-LS2),(IP-LS2)	0.0	0.25	0.50	0.75	1.0
(OP-LS1),(OP-LS2),(IP-LS1),(IP-LS2)	0.0	0.25	0.50	0.75	1.0
(OP-LS1),(IP-LS1),(IP-LS2),(OP-LS2)	0.0	0.25	0.50	1.0	-
(IP-LS1),(OP-LS1),(IP-LS2),(OP-LS2)	0.0	0.50	-	1.0	-
(IP-LS1),(IP-LS2),(OP-LS1),(OP-LS2)	0.0	0.50	1.0	-	-
(IP-LS1),(OP-LS1),(OP-LS2),(IP-LS2)	0.0	0.50	-	0.75	1.0

The damage state constants for DS-I, DS-II, DS-III, DS-IV, DS-V are taken from Table 5.2 as 0.0, 0.5, 0.75, 1.0, respectively. Then VS for the building type M2323 for a hazard level of 0.5g is calculated according to Figure 5.11 with the help of Equation 5.2:

$$VS = 0.0 \times 0.02 + 0.25 \times 0.10 + 0.50 \times 0.17 + 1.0 \times 0.71 = 0.820$$

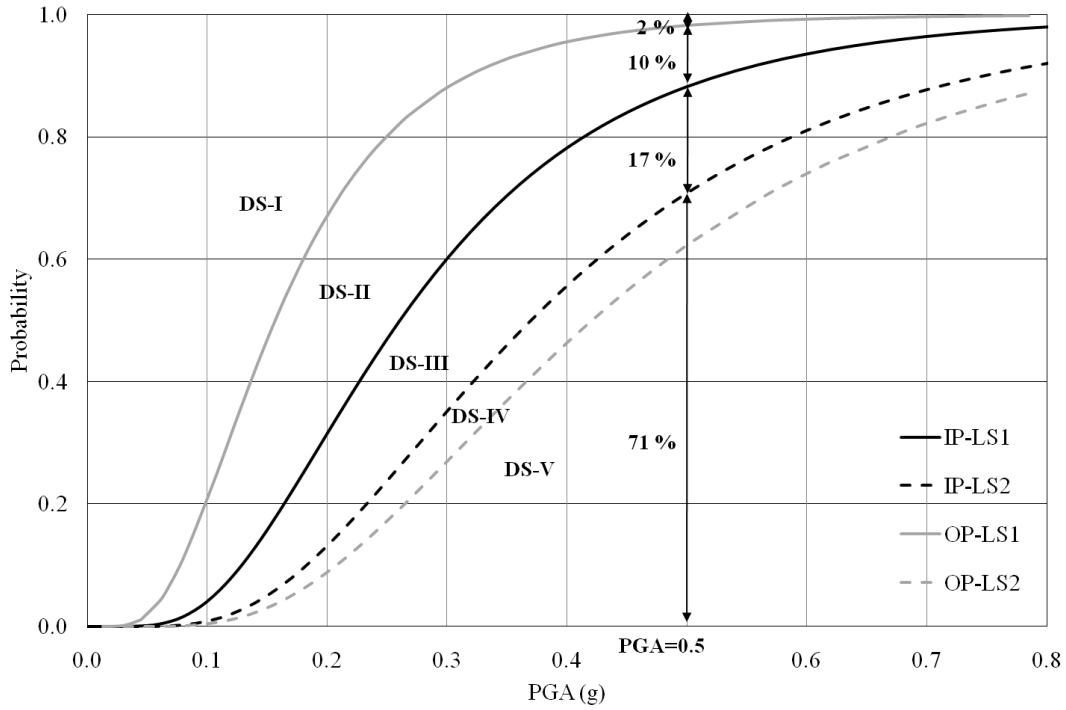

Figure 5. 11. Fragility curves for M2323 by considering in-plane and out-of-plane failure modes.

In this part of this study, VS calculation for each masonry building in Fatih subprovince is carried out with in this context except for the case that the fragility curves of masonry building are dominated by the in-plane action in spite of the contribution of the out-of-plane failure modes. Under this circumstance, the VS value is not changed and the previously calculated score is considered as valid. VS statistics in terms of number of stories by considering in-plane and out-of-plane behavior modes of masonry buildings is presented in Table 5.3

Table 5. 3. Relationship between VS and the number of stories for masonry buildings in Fatih

Vulnerabilty Score	Number of Stories					Total
	1	2	3	4	5	
$0 \leq VS < 0.1$	0	0	0	0	0	**0**
$0.1 \leq VS < 0.2$	0	0	0	0	0	**0**
$0.2 \leq VS < 0.3$	293	0	0	0	0	**293**
$0.3 \leq VS < 0.4$	597	72	0	0	0	**669**
$0.4 \leq VS < 0.5$	752	486	37	0	0	**1275**
$0.5 \leq VS < 0.6$	574	583	498	40	2	**1697**
$0.6 \leq VS < 0.7$	27	175	406	460	76	**1144**
$0.7 \leq VS < 0.8$	124	349	490	150	182	**1295**
$0.8 \leq VS < 0.9$	79	531	173	499	148	**1430**
$0.9 \leq VS \leq 1.0$	0	136	587	527	401	**1651**
Total	**2446**	**2332**	**2191**	**1676**	**809**	**9454**

According to Table 5.3, with the assumption of critical VS as 0.7, 46% of the buildings accepted as having high seismic risk in Fatih sub province of Istanbul. The results show that there is a strong correlation between seismic safety and number of stories. While there exists an abundant number of buildings with three to five stories which has low values of VS in Table 5.1, these buildings now seems to be more vulnerable according to Table 5.2 with the contribution of out-of-plane failure modes. It is also noted that there exist also single story and two story masonry buildings which are labeled to be “Under High Seismic Risk” although they seem to be comply with TEC-07 in terms of number of story. The change of distribution of the seismically vulnerable masonry buildings in terms of number of stories is also shown in Figure 5.12. As it seen from the Figure 5.12, there is a drastic change in the distribution of the masonry buildings which have VS over 0.7. With the contribution of the out-of-plane failure modes, the increase in the number of buildings with increasing number of stories and VS is observed clearly.

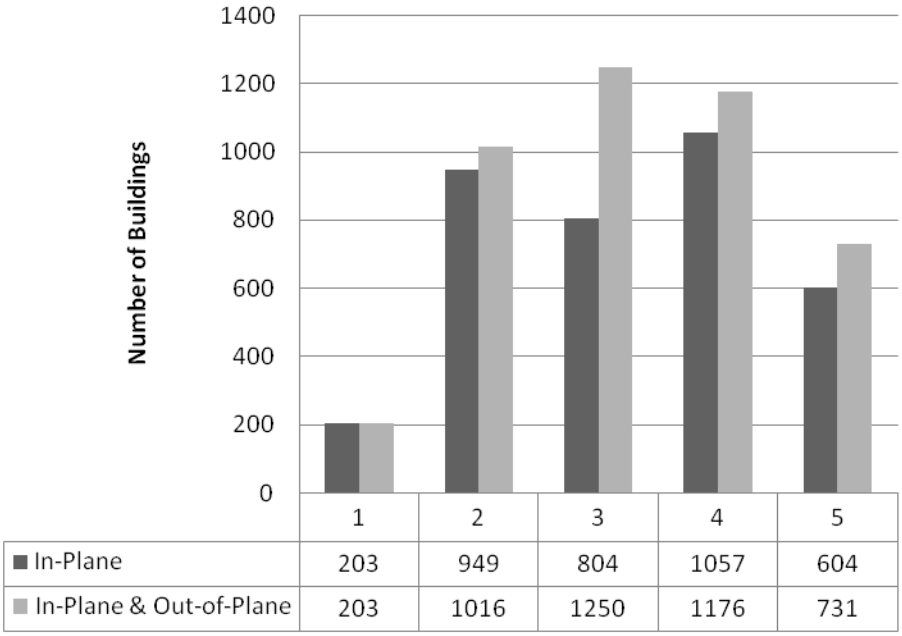

	1	2	3	4	5
In-Plane	203	949	804	1057	604
In-Plane & Out-of-Plane	203	1016	1250	1176	731

Figure 5. 12. The distribution of seismically vulnerable buildings (VS>0.7) in terms of number of stories.

CHAPTER 6

SUMMARY AND CONCLUSIONS

6.1. SUMMARY

This study is focused on the assessment of seismic vulnerability of populations of unreinforced masonry buildings in Turkey for both in-plane and out-of-plane behavior. The analysis tool that is used is fragility curves. Different sets of fragility curves have been generated for in-plane and out-of-plane action by using the same type of formulation.

Three different building databases have been considered in this study in order to examine the inherent characteristics of Turkish masonry buildings. The first one is a rural database that was compiled after the 1995 Dinar earthquake, Afyon Turkey. The other two databases are urban databases, which were compiled for the seismic safety assessment of two sub-provinces in Istanbul; Zeytinburnu and Fatih within the content of Earthquake Masterplan of Istanbul. The statistics obtained from these masonry building databases revealed that the most important structural parameters in the classification of Turkish masonry buildings are the number of stories, load-bearing wall material, plan geometry, and the amount and arrangement of load-bearing walls (required length, openings in walls, etc.). Furthermore, it has been observed that wall-to-wall or wall-to-floor connections, type of floor diaphragm (rigid or flexible), slenderness of load-bearing walls are the other factors that affect the seismic behavior of unreinforced masonry buildings in Turkey.

The fragility curves obtained for in-plane action are generated by using time history (for demand) and pushover (for capacity) analyses for the most critical story of the building, i.e. the ground story. Uncertainty in demand, capacity and modeling are all taken into account and sampling is carried out by Latin Hypercube Method. Two limit states are considered. The hazard parameter is taken as peak ground acceleration. A total of 120 different masonry building classes are considered and a set of fragility curves is generated for each class. Then the generated fragility curves are employed to estimate the damage of masonry buildings in Dinar after the 1995 earthquake. At the final step, the estimated damage is compared with the inspected visual damage as assessed from the Damage Evaluation Form

The fragility curves obtained for out-of-plane action are generated by using equivalent lateral static analysis (for demand) and out-of-plane moment versus curvature analyses (for capacity) for the most critical face-loaded wall of the upper-most story of the masonry building. Uncertainty in demand, capacity and modeling are all taken into account and sampling is carried out by Latin Hypercube Method. Two limit states are considered. The hazard parameter is taken as peak ground acceleration. A total of 9454 different masonry building classes are considered and a set of fragility curves is generated for each class. The sets of fragility curves obtained for in-plane and out-of-plane action complement each other. Finally the generated fragility curves for both in-plane and out-of-plane action are employed to estimate the damage of rural masonry buildings in Elazığ after the 2010 earthquake. Since most of the damaged masonry buildings in the region suffered from out-of-plane vulnerability, this example was a good candidate in order to check the validity of out-of-plane fragility curves by comparing them with the observed damage. The results are quite satisfactory and encourage the use of out-of-plane fragility curves together with in-plane curves.

The final part of the thesis is devoted to the seismic safety assessment of Turkish masonry buildings in Fatih, Istanbul as a case study. First, all the buildings are examined by ignoring the out-of-plane vulnerability. In the second phase of

evaluation, both in-plane and out-of-plane actions are taken into account by introducing the corresponding fragility curve sets, assuming that all the buildings are vulnerable to out-of-plane damage during seismic action. The assessment is carried out through a single-valued parameter, which is named as vulnerability score. By using the score, it becomes possible to rank all the buildings under consideration in terms of their seismic vulnerability.

6.2. CONCLUSIONS

Based on the specific masonry building databases, the gross assumptions and the simplified approaches used in this study, the following conclusions are drawn:

- Masonry buildings in Turkey generally do not obey the code regulations on the maximum number of stories, proper choice of bearing wall material, regularity requirements in plan, the minimum length of walls and the openings in walls. In addition to this, they generally possess poor wall-to-wall or wall-to-floor connections. This is a major reason why such structures suffer significant damage or even collapse during moderate-to-severe earthquakes.

- From the generated sets of fragility curves for in-plane behavior, it is observed that the damage state probabilities are significantly influenced from the number of stories and wall material strength. Regularity in plan, length and arrangement of bearing walls in plan also has significant effect on the damage state probabilities to some extent. This shows that the inherent characteristics of Turkish masonry buildings have been well reflected in the generated set of fragility curves.

- The damage estimated by using the in-plane fragility curve sets is compared with the actually inspected damage as assessed from the Damage Evaluation Form. For the quantification of fragility-based damage, a single-valued index,

"vulnerability score", is proposed. There seems to be a fair agreement between the two damage measures.

- The decisions regarding the repair or demolition of masonry buildings in Dinar due to visual damage inspection are also on comparable grounds with the relative measure obtained from vulnerability score of the same buildings, which has been obtained through in-plane fragility curves.

- From the generated sets of fragility curves for out-of-plane behavior, it is observed that the damage state probabilities are significantly influenced from the type of wall-to floor connection, slenderness ratio of the face loaded wall and the strength of masonry wall. According to the results, non-engineered masonry buildings with very poor wall-to-floor connections, in which the walls imitate cantilever-like behavior, are extremely vulnerable to even low-to-moderate levels of seismic action. For these buildings, out-of-plane behavior surpasses in-plane behavior.

- The fragility based procedure developed in this study can provide an alternative for the seismic safety evaluation of unreinforced masonry buildings in Turkey. Using this procedure, it becomes possible to investigate a large population of masonry buildings located in regions of high seismic risk in a short period of time. The obtained results are valuable in the sense that they can be used as a database during the development of strategies for pre-earthquake planning and risk mitigation for earthquake prone regions of Turkey.

REFERENCES

- ABK Joint Venture, (1981). “Methodology for Mitigation of Seismic Hazards in Existing Unreinforced Masonry Buildings: Wall Testing, Out-Of-Plane”, ABK Topical Report 04.

- Akkar, S. and Cagnan, Z., (2010). “A Local Ground Motion Predictive Model for Turkey and Its Comparison with Other Regional and Global Ground-Motion Models”, Submitted to Bull. Seism. Soc. Am. for publication.

- Akkar, S., Aldemir, A., Askan, A., Bakır, S., Canbay, E., Demirel, O., Erberik, A., Gülerce, Z., Gülkan, P., Kalkan, E., Prakash, S., Sandıkkaya, A., Sevilgen, V., Ugurhan, B. and Yenier, E., (2010). “8 March 2010 Elazığ-Kovancılar (Turkey) Earthquake: Observations on Ground Motions and Building Damage”, Seismological Research Letters (in press).

- American Society of Civil Engineers (ASCE), (2003). “Seismic Evaluation of Existing Buildings”, SEI/ASCE 31-03, Reston Virginia.

- Anderson, J.G., Zeng, Y., Sucuoğlu, H., (2001). “Analysis of Accelerations from the 1 October 1995 Dinar, Turkey, Earthquake”. Bulletin of the Seismological Society of America, 91(6):1433-1445.

- Applied Technology Council, (1985). “Earthquake Damage Evaluation Data for California”, ATC-13, Redwood City, California.

- Applied Technology Council, (1987). “Evaluating the Seismic Resistance of Existing Buildings”, ATC-14, Redwood City, California.

- Arias, A., (1970). "A Measure of Earthquake Intensity," R.J. Hansen, (ed). Seismic Design for Nuclear Power Plants, MIT Press, Cambridge, Massachusetts, pp. 438-483.

- ASCE, (2000). “Prestandard and Commentary for the Seismic Rehabilitation of Buildings”, FEMA 356 Report, prepared by American Society of Civil Engineers for Federal Emergency Management Agency, Washington D.C.

- ASCE, (2007). “Seismic Rehabilitation of Existing Buildings”, ASCE/SEI 41, American Society of Civil Engineers, Reston, VA.

- Askan, A., Gupta, S.P., Ugurhan, B., (2010). “March 8, 2010 Başyurt-Karakoçan (Elazığ) Earthquake, Supplementary Report”, Middle East Technical University Earthquake Engineering Research Center, Ankara.

- Ayyub, B.M., and Lai, K-L. (1989). “Structural Reliability Assessment Using Latin Hypercube Sampling.” Proc., 5th Int. Conf. on Struct. Safety and Reliability, ICOSSAR’89, Vol. 2, ASCE, New York, 1177–1184.

- Bakır, S., Canbay, E., Erberik, A., Gülerce, Z., Aldemir, A., Demirel İ.O., (2010). “March 8, 2010 Başyurt-Karakoçan (Elazığ) Earthquake, Reconnaissance Report”, Middle East Technical University Earthquake Engneering Research Center, Ankara.

- Bayülke, N., (1992) “Yığma Yapılar”, Afet İşleri Genel Müdürlüğü Deprem Araştırma Dairesi, Ankara.

- Belmouden, Y. and Lestuzzi, P., (2007). “On the Seismic Vulnerability Assessment of Unreinforced Masonry Existing Buildings in Switzerland”, Research Report, École Polytechnique Fédérale de Lausanne (EPFL).

- Benedetti, D., Benzoni, G., (1984). “A Numerical Model for Seismic Analysis of Masonry Buildings: Experimental Correlations”, Earthquake Engineering and Structural Dynamics 12: 817-831.

- Benedetti, D., Benzoni, G., Parisi, M.A., (1988). “Seismic Vulnerability and Risk Evaluation for Old Urban Nuclei”, Earthquake Engineering and Structural Dynamics 16: 183-201.

- Boore, D. M. and Atkinson, G. M. (2008). "Ground Motion Prediction Equations for the Average Horizontal Component of PGA, PGV, and 5%-damped PSA at Spectral Periods Between 0.01 s and 10.0 s", Earthquake Spectra, Vol. 24, No. 1, pp. 99-138.

- Brencich, A, Gambarotta, L, Lagomarsino, S (1998). "A Macro Element Approach to the Three-Dimensional Seismic Analysis of Masonry Buildings", 11th European Conference on Earthquake Engineering, Paris.
- Calvi G.M., (1999). "A Displacement-Based Approach for Vulnerability Evaluation of Classes of Buildings", Journal of Earthquake Engineering, 3(3):411-438.

- Campbell, K. W. and Bozorgnia, Y. (2008). "NGA Ground Motion Model for the Geometric Mean Horizontal Component of PGA, PGV, PGD and 5% Damped Linear Elastic Response Spectra for Periods Ranging from 0.01 to 10 s", Earthquake Spectra, Vol. 24, No. 1, pp. 139-172.

- Chiou, B. and Youngs, R.R., (2008). "An NGA for the Average Horizontal Component of Peak Ground Motion and Response Spectra", Earthquake Spectra 24, 173-215

- Coburn, A. and Spence, R., (1992). "Earthquake Protection", John Wiley & Sons, Chichester.

- Council of Europe (1998). "European Macroseismic Scale", edited by G.Grünthal, Centre Europèen de Géodynamique et de Séismologie, Luxembourg.

- D'Ayala D., (2005). "Force and Displacement Based Vulnerability Assessment for Traditional Buildings", Bulletin of Earthquake Engineering 3: 235-265.

- D'Ayala, D., Spence, R., Oliveira, C., Pomonis, A., (1997). "Earthquake Loss Estimation for Europe's Historic Town Centers". Earthquake Spectra, 13(4): 773-793.

- Doherty, K. T., Griffith, M. C., Lam, N., and Wilson, J., (2002). "Displacement-Based Seismic Analysis for Out-of-Plane Bending of Unreinforced Masonry Walls", Earthquake Eng. Struct. Dyn. 31, 833–850.

- Erberik, M.A., Aldemir, A., Ay, B.Ö., (2008). "A Critique on the Turkish Earthquake Code Regulations Regarding Masonry Construction", 8th International Seminar on Structural Masonry, Istanbul,

- Erberik MA.(2008) "Generation of Fragility Curves for Turkish Masonry Buildings Considering In-Plane Failure Modes", Earthquake Eng. and Str. Dyn. 37, 387-405.

- Erdik, M., Durukal, E., Demircioğlu, M., Şeşetyan, K., (2006). "Identification of Seismic Hazard in Fatih sub-province", Earthquake Engineering Department, Kandilli Observatory and Earthquake Research Institute, Boğaziçi University, Istanbul.

- European Committee for Standardization (CEN) (2003), "Eurocode 8: Design of Structures for Earthquake Resistance, Part 1", prEN 1998-1, Brussels, Belgium.

- Federal Emergency Management Agency (FEMA), (2000). "Prestandard and Commentary for the Seismic Rehabilitation of Buildings", FEMA 356.

- Federal Emergency Management Agency (FEMA), (1988). "Rapid Visual Screening of Buildings for Potential Seismic Hazards: A Handbook", FEMA 154, Washington.

- Federal Emergency Management Agency (FEMA), (1988). "Rapid Visual Screening of Buildings for Potential Seismic Hazards: Supporting Documentation", FEMA 155, Washington.

- Federal Emergency Management Agency (FEMA), (1998). "Handbook for the Seismic Evaluation of Buildings: A Prestandard", FEMA 310, Washington.

- Formica, G. (2004). “Multilevel Analysis of Masonry Buildings”, Doctoral Thesis, University of Calabria, Italy.

- Galasco, A., Lagomarsino, S., Penna, A. and Resemini, S., (2004). “Nonlinear Seismic Analysis of Masonry Structures”, 13th World Conference on Earthquake Engineering, Vancouver, B.C., Canada, Paper No. 843

- General Directorate of Disaster Affairs, (1990). “Assessment of Earthquake Damage in Rural Structures”, Ministry of Public Works and Settlement, Ankara.

- Ghali, A. and Neville, A.M., (1978). Structural Analysis, Chapman and Hall,London

- Governorship of Elazığ, (2010). “The Elazığ Earthquake by Numbers”, http://www.elazig.gov.tr/p997-rakamlarla-elazig-depremi.html (last accessed 15/10/2010).

- Graizer, V. and Kalkan, E., (2007). “Ground Motion Attenuation Model for Peak Horizontal Acceleration from Shallow Crustal Earthquakes”, Earthquake Spectra, Vol. 23, pp. 585–613.

- Griffith, M.C., Magenes, G., Melis, G., Picchi, L., (2003). “Evaluation of Out-of-Plane Stability of Unreinforced Masonry Walls Subjected to Seismic Excitation”, Journal of Earthquake Engineering 7(S1): 141-169.

- Housner, G. W., (1963). “The Behavior of Inverted Pendulum Structures During Earthquakes”, Bull. Seismol. Soc. Am. 53, 403–417.

- Japan International Co-operation Agency (JICA), and Istanbul Metropolitan Municipality (IMM), (2002). “The Study on a Disaster Prevention / Mitigation Basic Plan in Istanbul including Seismic Microzonation in the Republic of Turkey, Final Report”, Tokyo-Istanbul.

- Kalkan, E. and Gülkan, P., (2004). “Site-Dependent Spectra Derived from Ground Motion Records in Turkey”, Earthquake Spectra, Vol. 20, No. 4, pp. 1111-1138.

- Kappos A.J., Penelis G.G., Drakopoulos C.G., (2002). "Evaluation of Simplified Models for Lateral Load Analysis of Unreinforced Masonry Buildings", Journal of Structural Engineering, 128(7): 1-8.

- Lagomarsino, S. and Magenes, G., (2009). "Evaluation and Reduction of the Vulnerability of Masonry Buildings", The State of Earthquake Engineering Research in Italy: the ReLUIS-DPC 2005-2008 Project, G. Manfredi, M. Dolce (eds): 1-50.

- Lang, K., (2002). "Seismic Vulnerability of Existing Buildings", Swiss Federal Institute of Technology, Zurich.

- Lourenço, B.B., (1996). "Computational Strategies for Masonry Structures", Doctoral Thesis, Delft University of Technology, The Netherlands.

- Makris, N., and Konstantinidis, D., (2003). "The Rocking Spectrum and The Limitations of Practical Design Methodologies", Earthquake Eng. Struct. Dyn. 32, 265–289.

- McKay, MD., Conover, WJ., Beckman, RJ., (1979). "A Comparison of Three Methods for Selecting Values of Input Variables in the Analysis of Output From a Computer Code", Technometrics, 221:239–245.

- Mengi, Y, McNiven, HD., (1989). "A Mathematical Model for the In-Plane Nonlinear Earthquake Behavior of Unreinforced Masonry Walls, Part 1: Experiments and Proposed Model", Earthquake Engineering and Structural Dynamics 18: 233-247.

- Mengi, Y. and McNiven, HD., (1989). "A Mathematical Model for the In-Plane Nonlinear Earthquake Behavior of Unreinforced Masonry Walls, Part 2: Completion of the Model", Earthquake Engineering and Structural Dynamics 18: 249-261.

- Mengi Y., McNiven, HD. and Tanrıkulu, AD., (1992). "Models for Nonlinear Earthquake Analysis of Brick Masonry Buildings", Report No. UCB/EERC-92/03, Earthquake Engineering Research Center, University of California at Berkeley.

- Menon, A. and Magenes, G., (2008). “Out-of-Plane Seismic Response of Unreinforced Masonry: Definition of Seismic Input”, Research Report ROSE-2008/04, Rose School, EUCENTRE, Pavia, Italy.

- METU-EERC, (1996). “Repair and Rehabilitation Project for Moderately Damaged Masonry Structures after 1995 Dinar Earthquake”, Earthquake Engineering Research Center, Civil Engineering Department, METU, Ankara.

- National Institute of Building Science (NIBS), (1999). Earthquake Loss Estimation Methodology, HAZUS99 Technical Manual. Report prepared for the Federal Emergency Management Agency, Washington D.C.

- Natural Earthquake Hazards Reduction Program (NEHRP), (1992). “Guidelines for the Seismic Rehabilitation of Buildings”, Technical Report FEMA 178, Washington.

- Ottazzi, Yep, Blondet, Villa-Garcia and Ginocchio (1989). “Ensayos de Simulacion Sismica de Viviendas de Adobe”, Report of Pntificia Universidad del Peru Departemento de Ingenieria, Report No. D1-89-01, Peru

- Paulay, T. and Priestley, MJN., (1992). “Seismic Design of Reinforced Concrete and Masonry Buildings”, John Wiley and Sons, New York

- Porro, B. and Schraft, A., (1989). “Investigation of Insured Earthquake Damage”. Natural Hazards 2, pp. 173-184.

- Rubinstein, R.Y. (1981). “Simulation and the Monte Carlo Method”, Wiley, 278 pages.

- Sharif, I., Meisl, C.S. and Elwood, K.J. (2007). “Assessment of ASCE 41 Height-to-Thickness Ratio Limits for URM Walls”, Earthquake Spectra 23(4), 893-908.

- Shinozuka, M., Feng, M.Q., Lee, J. and Naganuma, T., (2000). "Statistical Analysis of Fragility Curves", Journal of Engineering Mechanics ASCE 126(12): 1224-1231.

- Simsir, C., (2004). "Influence of Diaphragm Flexibility on the Out-of-Plane Dynamic Response of Unreinforced Masonry Walls", Ph.D. Dissertation, Department of Civil and Environmental Engineering, University of Illinois at Urbana-Champaign.

- Spence, R. and D'Ayala, D., (1999). "Damage Assessment and Analysis of the 1997 Umbria-Marche Earthquakes", Structural Engineering International, 9(3).

- Sucuoğlu, H, Anderson, JG., Zeng, Y., (2003). "Predicting Intensity and Damage Distribution during the 1995 Dinar, Turkey, Earthquake with Generated Strong Motion Accelerograms", Bulletin of the Seismological Society of America, 93(3): 1267-1279.

- Sucuoğlu, H. and Erberik, MA., (1997). "Performance Evaluation of a Three-Storey URM Building During 1992 Erzincan Earthquake", Earthquake Engineering and Structural Dynamics, 26: 319-336.

- Sucuoğlu, H., Yakut, A., Erberik, M.A., (2006). "Seismic Assessment of Buildings Stock in Fatih: Evaluation of First Stage Report", Middle East Technical University, Ankara.

- Trifunac, M.D. and Brady, A. G., (1975). "A Study on the Duration of Strong Earthquake Ground Motion", Bull. Seis. Soc. Am., V.65, pp.581-626.

- TS-2510, (1977). "Design and Construction Methods for Masonry", Turkish Standards Institute, Ankara, Turkey

- TS-705, (1979). "Standard Test Method for Solid Bricks and Vertically Perforated Bricks", Turkish Standards Institute, Ankara, Turkey

- Turkish Ministry of Public Works and Settlement, (1975). "Specification for Structures to be Built in Disaster Areas", TEC-75, Ankara, Turkey.

- Turkish Ministry of Public Works and Settlement, (1998). “Specification for Structures to be Built in Disaster Areas”, TEC-98, Ankara, Turkey.

- Turkish Ministry of Public Works and Settlement, (2007). “Specification for Structures to be Built in Disaster Areas”, TEC-07, Ankara, Turkey.

- Turkish Standards TS EN 771-1, (2005). “Specification for Masonry Units Part I: Clay Masonry Units”, Turkish Standards Institute, Ankara, Turkey.

- Turkish Standards TS EN 771-2, (2001). “Specification for Masonry Units Part I: Calcium Silicate Masonry Units”, Turkish Standards Institute, Ankara, Turkey.

- Turkish Standards TS-2514, (1997). “Adobe Blocks and Construction Methods. Turkish Standards Institute”, Ankara, Turkey.

- Turkish Standards TS406, (1988). “Concrete Blocks and Bricks for Walls”, Turkish Standards Institute, Ankara, Turkey.

- Turnsek, V. and Cacovic, F., (1970). “Some experimental results on the strength of brick masonry walls”, Proceedings of the 2nd International Brick Masonry Conference, Stoke-on-Trent.

- Valluzzi, M.R., Cardani, G., Binda L. and Modena, C., (2004). ”Seismic Vulnerability Methods for Masonry Buildings in Historical Centers: Validation and Application for Prediction Analyses and Intervention Proposals”, Proceedings of the 13th World Conference on Earthquake Engineering, Vancouver, Paper No: 2765.

- Wasti, ST., Erberik, MA., Sucuoğlu, H., Kaur, C., (1998). “Studies on Strengthening of Rural Structures Damaged in the 1995 Dinar Earthquake”, Proceedings of the Eleventh European Conference on Earthquake Engineering, CNIT, Paris la Defense, France.

- Wen, YK., Ellingwood, BR., Bracci., J., (2004). “Vulnerability Function Framework for Consequence-Based Engineering”, Mid-America Earthquake Center, CD Release 04-04.

- Wyss, G.D. and Jorgensen, K.H., (1998). “A User’s Guide to LHS: Sandia’s Latin Hypercube Sampling Software”, Technical Report SAND98–0210, Risk Assessment and Systems Modeling Department, Sandia National Laboratories, Albuquerque, NM.

- Yılmaz, N. and Uran, T, (2010). “8 March 2010 Elazığ Earthquakes”, Earthquake Department, Disaster and Emergency Management Presidency, Ankara.

- Zor, E., Sandvol, E., Xie, J., Türkelli, N., Mitchell, B., Gasanov, A. H., and Yetirmishli, G., (2007). “Crustal Attenuation within the Turkish Plateau and Surrounding Regions”, Bull. Seism. Soc. Am. 97, 151 -161.

APPENDIX A

PLAN GEOMETRY OF GENERATED MASONRY BUILDING MODELS

A.1. R1-W1 MODEL

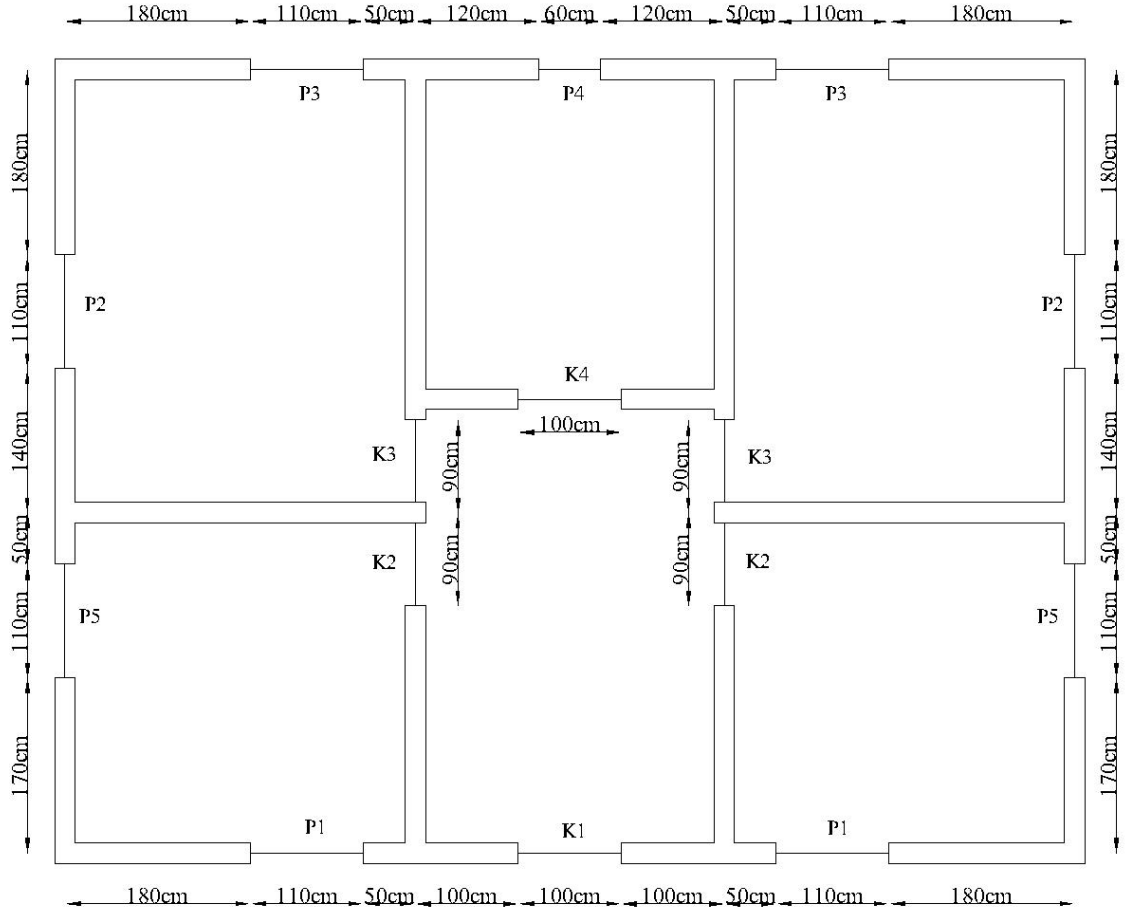

Figure A.1. 1. Plan geometry of the masonry building model of R1W1 subclass.

A.1. R1-W2 MODEL

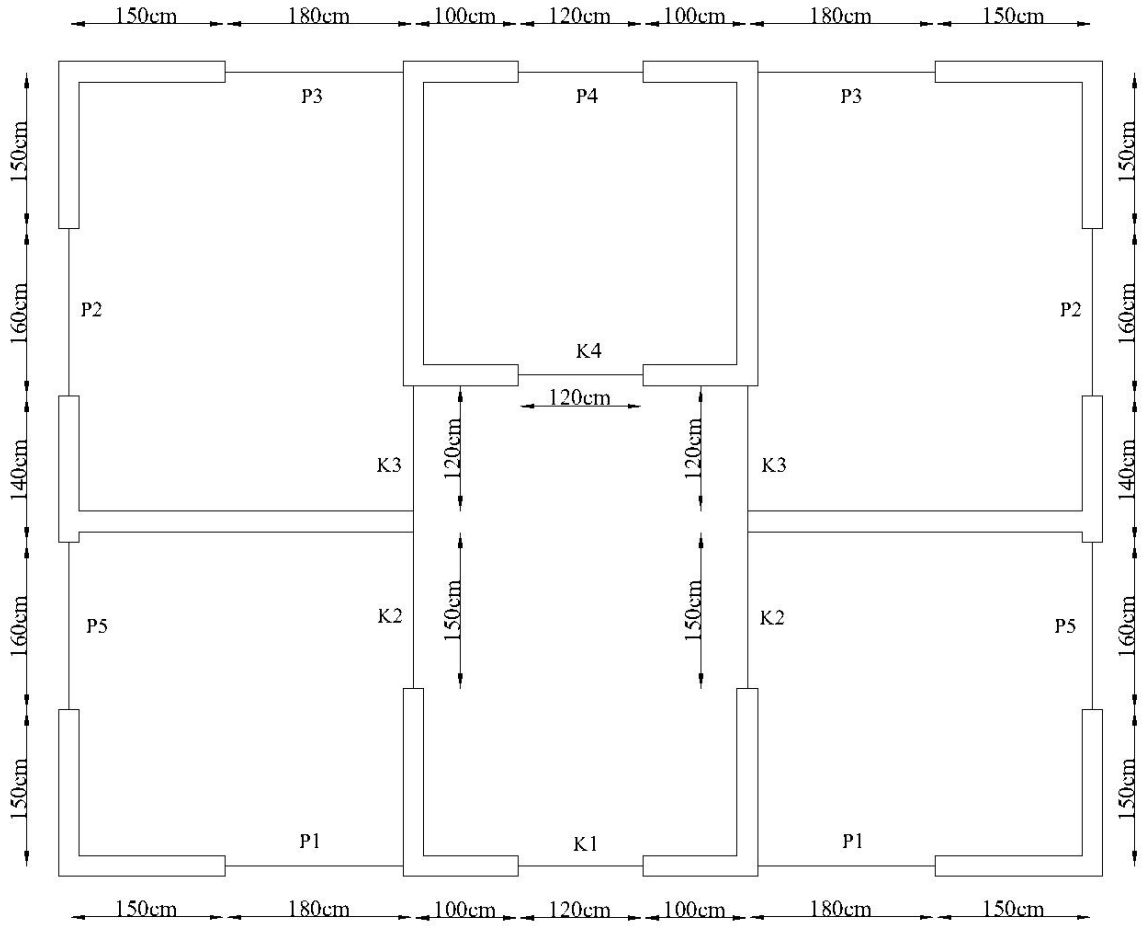

Figure A.1. 2. Plan geometry of the masonry building model of R1W2 subclass.

A.1. R1-W3 MODEL

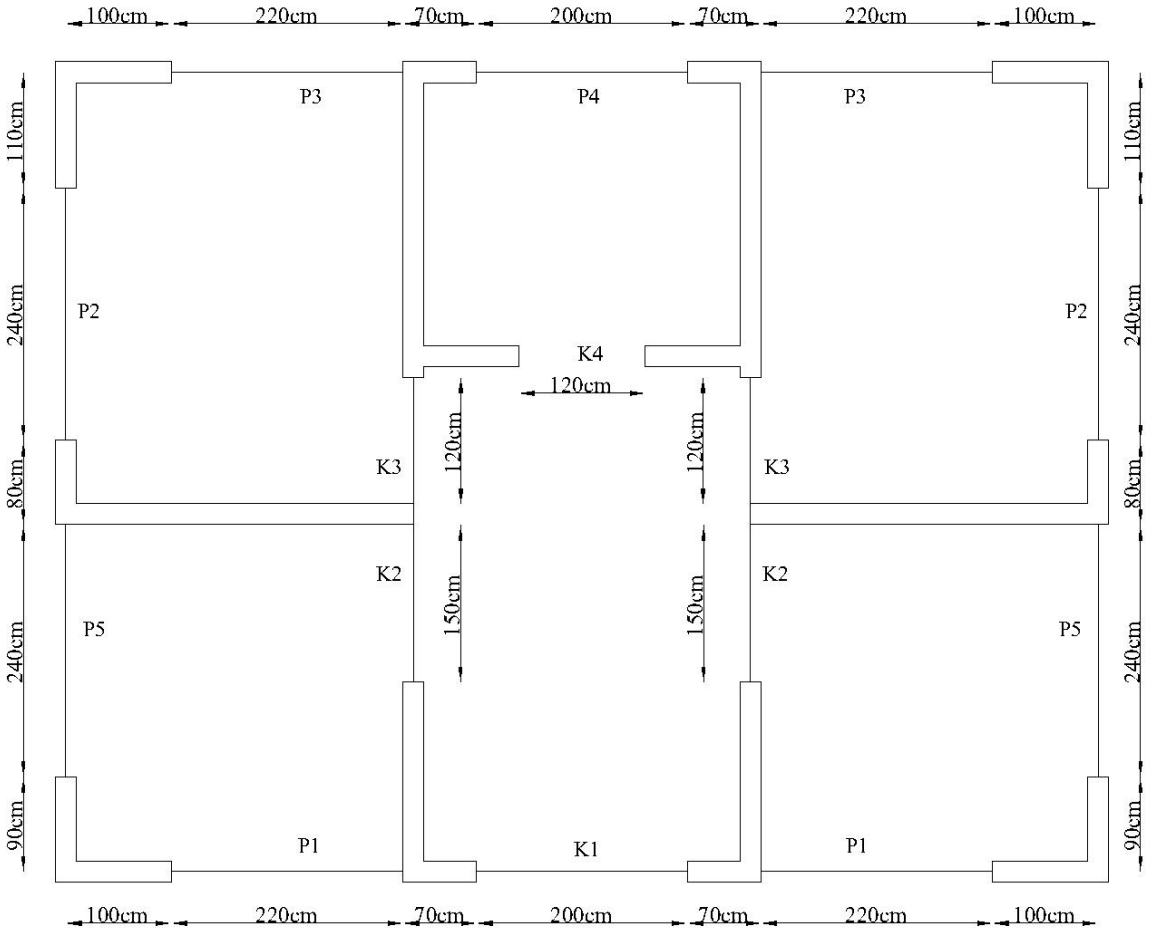

Figure A.1. 3. Plan geometry of the masonry building model of R1W3 subclass.

A.1. R2-W1 MODEL

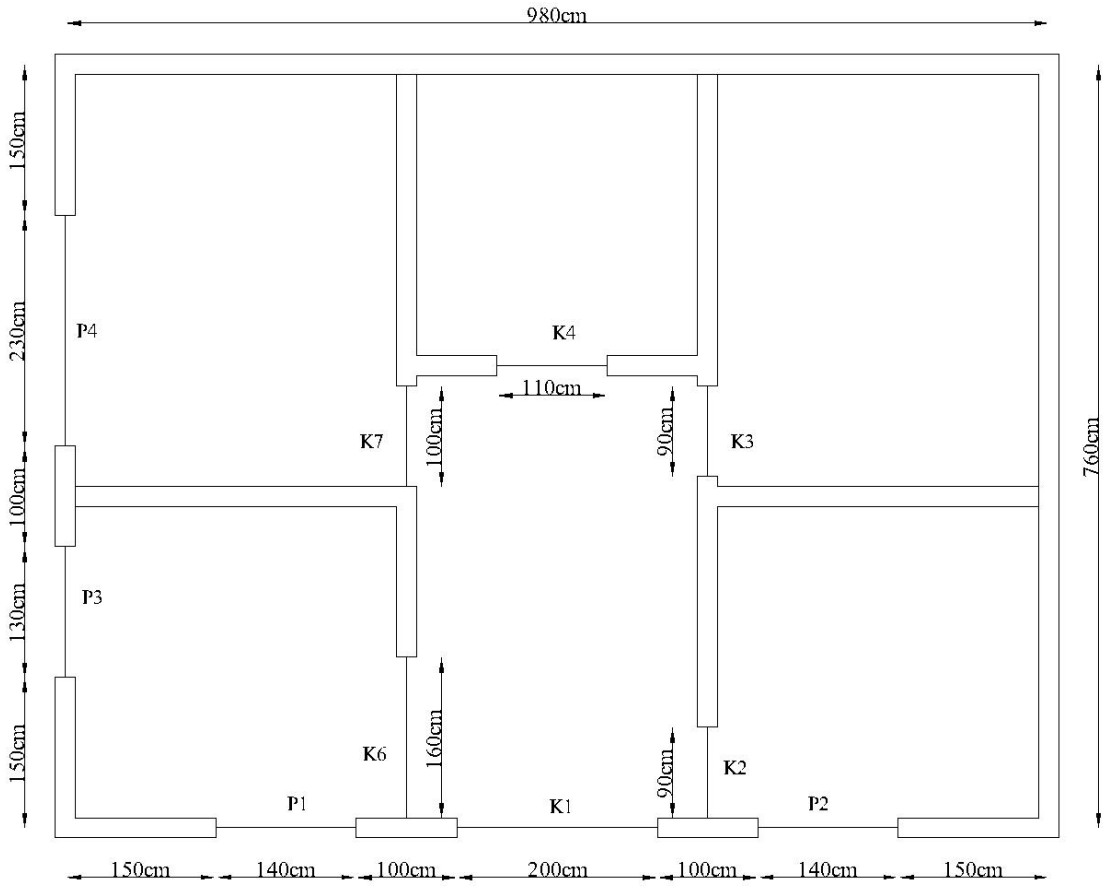

Figure A.1. 4. Plan geometry of the masonry building model of R2W1 subclass.

A.1. R2-W2 MODEL

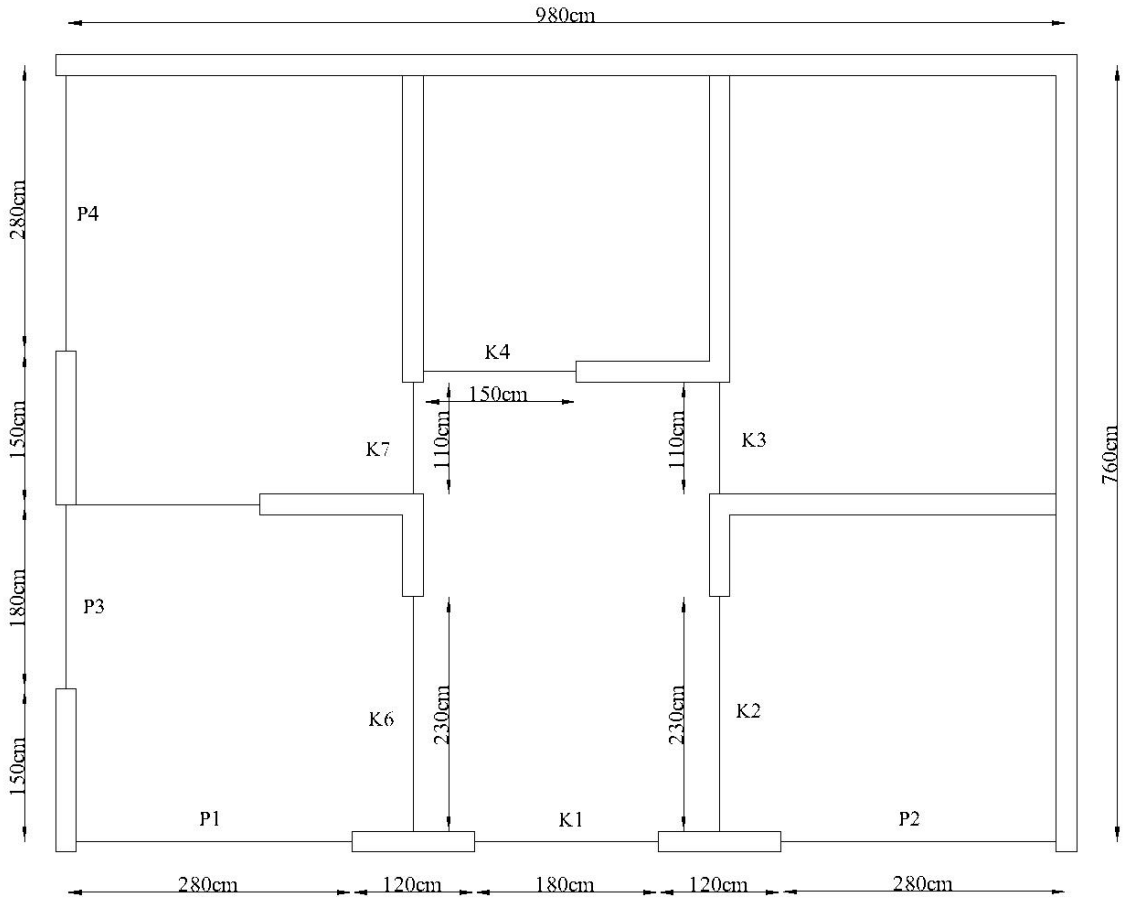

Figure A.1. 5. Plan geometry of the masonry building model of R2W2 subclass.

A.1. R2-W3 MODEL

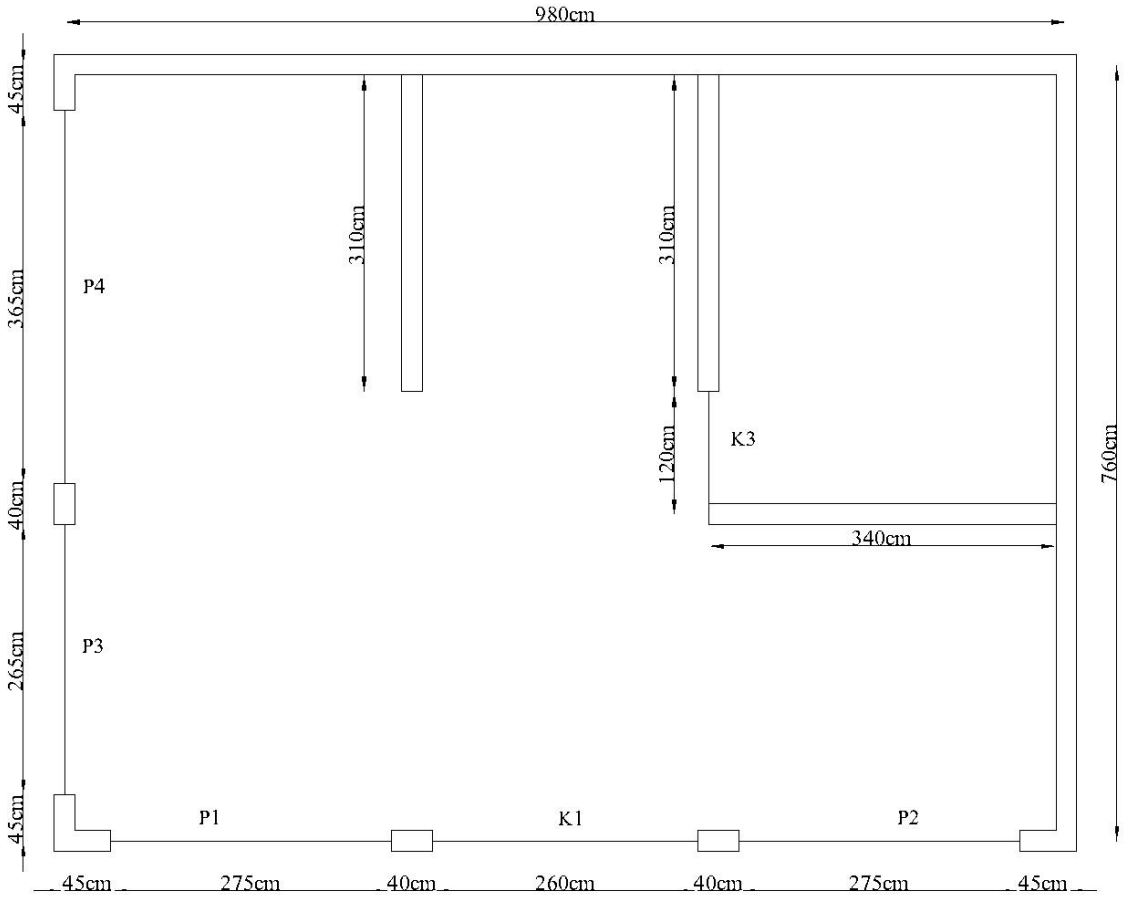

Figure A.1. 6. Plan geometry of the masonry building model of R2W3 subclass.

APPENDIX B

DAMAGE EVALUATION FORM

T.C.
İSTANBUL BÜYÜKŞEHİR BELEDİYE BAŞKANLIĞI
EMLAK VE İSTİMLAK DAİRE BAŞKANLIĞI
YERLEŞMELER VE KENTSEL DÖNÜŞÜM MÜDÜRLÜĞÜ
FATİH İLÇESİ YAPI DEĞERLENDİRME FORMU
YIĞMA - KARMA

Plan geometrisi

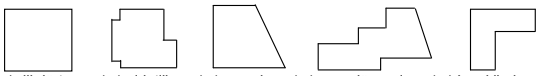

( ) dikdörtgen ( ) girintili ( ) yamuk ( ) aşırı düzensiz ( ) L şeklinde

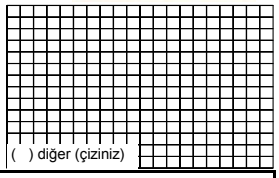

( ) diğer (çiziniz)

FORM 1 KİMLİK BİLGİLERİ

İNCELEME YAPAN KİŞİ / TARİH	
MAHALLE / SOKAK	
KAPI NO / ADA PARSEL	
BİNA KİMLİK KODU	
BİNANIN YAŞI	
COĞRAFİ KOORDİNATLAR (GPS) (E / N)	

FORM 2 BİNA BİLGİLERİ

SERBEST KAT ADEDİ	TOPLAM ( )
BODRUM KAT	YOK ( ) VAR ( ) BELİRLENEMEDİ ( )
TAŞIYICI DUVAR TİPİ	KERPİÇ ( ) BRİKET ( ) DELİKLİ FABRİKA TUĞLASI ( ) HARMAN TUĞLASI ( ) TAŞ ( ) KARMA ( ) BELİRLENEMEDİ ( )
PLAN GENİŞLİĞİ (ÖN CEPHE)	.....m
BOŞLUK MİKTARI (ÖN CEPHE)	.....m
PLAN GENİŞLİĞİ (YAN CEPHE)	.....m
BOŞLUK MİKTARI (YAN CEPHE)	.....m
DUVAR BOŞLUK DÜZENİ	DÜZENLİ ( ) AZ DÜZENLİ ( ) DÜZENSİZ ( )
DÖŞEME TİPİ	BETONARME ( ) AHŞAP ( ) BELİRLENEMEDİ ( )
YAPI NİZAMI	AYRIK ( ) BİTİŞİK ( ) KÖŞEDE BİTİŞİK ( )
ZAYIF / YUMUŞAK KAT	YOK ( ) VAR ( )
BİTİŞİK BİNALAR İLE YÜKSEKLİK FARKI	YOK ( ) VAR ( )
BİTİŞİK BİNALARLA DÖŞEME SEVİYELERİ	AYNI ( ) FARKLI ( )
ÇATI GEOMETRİSİ	DÜZ - TERAS ( ) OTURTMA ( )
BİNANIN GÖRÜNEN KALİTESİ	İYİ ( ) ORTA ( ) KÖTÜ ( )
ARSANIN EĞİMİ	DÜZ ( ) AZ EĞİMLİ ( ) DİK ( )

FORM 3 PLANLAMA BİLGİLERİ

BİNA FONKSİYONU						
ZEMİN KAT						
ASMA KAT						
NORMAL KATLAR						
BİNA KULLANIMI						
		DOLU	BOŞ		DOLU	BOŞ
	KONUT SAYISI			KÜÇÜK SANAYİ		
	TİCARET SAYISI			BÜYÜK SANAYİ		
KOMŞU KULLANIMLAR	ÖN BAHÇE VAR ( ) YOK ( )			ARKA BAHÇE VAR ( ) YOK ( )		
YANGIN MERDİVENİ	VAR ( )			YOK ( )		

Figure B. 1. The form used to gather information about masonry buildings during the sidewalk survey of Fatih